

An effective description of dark matter and dark energy in the mildly non-linear regime

Matthew Lewandowski^{1,2,3}, Azadeh Maleknejad⁴, Leonardo Senatore^{1,2}

¹ *Stanford Institute for Theoretical Physics,
Stanford University, Stanford, CA 94306*

² *Kavli Institute for Particle Astrophysics and Cosmology,
Physics Department and SLAC, Menlo Park, CA 94025*

³ *Institut de Physique Théorique, Université Paris Saclay,
CEA, CNRS, 91191 Gif-sur-Yvette, France*

⁴ *School of Physics, Institute for Research in Fundamental Sciences (IPM),
P. Code. 19538-33511, Tehran, Iran*

Abstract

In the next few years, we are going to probe the low-redshift universe with unprecedented accuracy. Among the various fruits that this will bear, it will greatly improve our knowledge of the dynamics of dark energy, though for this there is a strong theoretical preference for a cosmological constant. We assume that dark energy is described by the so-called Effective Field Theory of Dark Energy, which assumes that dark energy is the Goldstone boson of time translations. Such a formalism makes it easy to ensure that our signatures are consistent with well-established principles of physics. Since most of the information resides at high wavenumbers, it is important to be able to make predictions at the highest wavenumber that is possible. The Effective Field Theory of Large-Scale Structure (EFTofLSS) is a theoretical framework that has allowed us to make accurate predictions in the mildly non-linear regime. In this paper, we derive the non-linear equations that extend the EFTofLSS to include the effect of dark energy both on the matter fields and on the biased tracers. For the specific case of clustering quintessence, we then perturbatively solve to cubic order the resulting non-linear equations and construct the one-loop power spectrum of the total density contrast.

Contents

1	Introduction	3
2	Review of EFTs of Dark Energy and Large-Scale Structure	6
2.1	Effective Field Theory of Dark Energy	6
2.1.1	Background equations	8
2.1.2	Perturbations in the dark-energy sector	8
2.2	Effective Field Theory of Large-Scale Structure	9
3	EFTofLSS with DE: clustering quintessence example	13
3.1	Linear equations	14
3.2	Non-linear equations	16
4	Solution for $c_s^2 \rightarrow 0$: clustering quintessence	19
4.1	Linear perturbations	20
4.2	Non-linear perturbations	22
4.2.1	Second-order perturbations	23
4.2.2	Third-order perturbations	23
4.2.3	Counterterms	24
4.3	Power spectrum	28
5	Biased tracers	29
6	Results	31
7	Conclusions	33
A	Details regarding δK	36
A.1	Review of the ADM formalism	36
A.2	Computation of δK_u	37
B	Linear equations	39
B.1	Linear solution of π with $\bar{m}_1^3 = 0$	41
B.1.1	π during matter domination	43

B.2 Linear solution of π , including \bar{m}_1^3	44
C The density and velocity Green's functions	45
D Non-linear evolution with smooth dark energy	47

1 Introduction

One of the most unexpected discoveries of modern cosmology is the observation of the accelerated expansion of the Universe in 1998. It had been first observed by supernovae Ia (SnIa) surveys [1, 2, 3] and then it was confirmed by other observations including large-scale structure (LSS) [4, 5], cosmic microwave background (CMB) [6, 7] and baryon acoustic oscillations (BAO) [8, 9] that about 70% of the Universe today is made of an unknown component called dark energy (DE). Concerning the background evolution, current observations restrict the value of the equation-of-state of DE to be very close to -1 at low redshifts, while present constraints on the time evolution of w and DE energy density at higher redshifts are still very weak [7]. Even less constrained is the behavior of the fluctuations in DE.

Contrary to the case of inflation, it is *relatively* easy to make progress in our observational knowledge of dark energy with respect to the one of inflation. In fact, phenomena that left significant signatures in the early universe have already been exposed to being probed by the CMB. This has provided very accurate measurements in the last three decades of the universe at the recombination epoch, significantly constraining all processes that affected that epoch (including the initial conditions for the fluctuations). It is expected that the CMB will make further progress in the measurement of the polarization, but most luckily the largest gain in information will be associated to measurements of large-scale structure *through* the CMB. Since dark energy is mainly important at low redshifts, where our knowledge is much less accurate than at higher redshifts,¹ in the next few years our improvement has the chance to be quite spectacular. In fact, a number of upcoming probes, both through CMB and Large-Scale Structure surveys, will improve our knowledge of the low-redshift universe. Among them are the space missions Euclid [10] and Wide Field Infrared Survey Telescope (WFIRST) [11] as well as ground-based experiments such as the Dark Energy Spectroscopic Instrument (DESI), the Large Synoptic Survey Telescope (LSST), the Ground-Based Stage IV BAO Experiment (BigBOSS) and the Hobby-Eberly Telescope Dark Energy Experiment (HETDEX). Also, CMB probes will keep measuring with greater and greater accuracy the LSS through the induced lensing on the CMB (see for example [12, 13]). For some exhaustive reviews on the subject see [14], [15] and the references within.

Let us now pass to the theoretical side. By a very very large amount, an amount that it is difficult to overstate, the current preferred model for dark energy is a cosmological constant. In fact, the cosmological constant is already part of our laws of physics. We just do not know its

¹Though there can be constraints originating from the behavior of dark energy at high redshift, which is, however, model dependent [7]. Of course, when this is the case, the high redshift measurements provide a very strong constraint.

size. Historically, it has been extremely difficult to tame the large quantum corrections that affect its size, and that are expected to make it huge. However, a beautiful possible explanation of its smallness was provided by Weinberg in 1987 [16], based on anthropic reasoning. Weinberg reflected that if the cosmological constant were to be very large, then it would dominate the energy density of the universe before any structure such as planets could have formed. In such a universe, there would be no observers to measure a large value of a cosmological constant. Therefore, Weinberg inferred that if we live in a multiverse where the cosmological constant can take several different values, our observed value of the cosmological constant must be below an upper bound so that structures could have formed. Furthermore, he argued that, given that it is famously hard to make the cosmological constant small, the observed value will most likely be close to the upper bound given by the requirement of structure formation. Subsequently, the landscape of string theory and the inflationary paradigm have provided a natural theoretical framework of this anthropic explanation.

Weinberg’s line of reasoning predicted that our universe should be currently accelerating with w close to -1 , driven by a non-fluctuating component which is a cosmological constant with a certain value. Within the uncertainties of this theoretical argument, these predictions were matched by the observations made one decade later and the subsequent ones.

So, if Weinberg’s explanation is so compelling, why do we not declare dark energy to be a cosmological constant? While many authors would agree in doing this, including at least one of the authors of this paper, it is true that in the next few years we are going to make such a tremendous observational progress that it is worth giving a further look at the problem, both observationally and theoretically. Of course, while we do this, we have the chance of making discoveries even greater than the one of the cosmological constant.

A quite general approach is to assume that the current acceleration of the universe is associated to the presence of a new light degree of freedom, called DE. It should be stressed that this hypothesis does not necessarily imply that the universe is accelerating, nor offers automatically an explanation of the smallness of the cosmological constant. However, it is conceivable, at least as a matter of principle, that the presence of this degree of freedom is associated to the acceleration of the universe, and since we are going to test this hypothesis with unprecedented precision, then it is worth studying this hypothesis.

We will parametrize the generic signatures of DE by assuming that this light degree of freedom is associated to the breaking of time translations, which is quite a general phenomenon in an FRW universe. In this case, the new degree of freedom is the Goldstone boson of time translations, whose action can be constructed without specific knowledge of the dynamics that leads to the onset of the background cosmology. This approach to describe dark energy is called ‘The Effective Field Theory of Dark Energy’ (EFTofDE) and was originally developed in [17]. Then, it was further developed and applied to describe Inflation in [18] and then further developed in the context of dark energy (where the name effective field theory of dark energy was actually introduced, and the research program on the phenomenology of dark energy more systematically initiated) in [19, 20, 21] and a large subsequent literature (see for example, [22, 23, 24, 25, 26, 27, 28, 29]).

This approach to describe dark energy has the advantage of being very general. Maybe even more important is the fact that the signatures derive from a Lagrangian. This simple fact guarantees

us that the system respects our generally accepted principle of physics, such as locality, causality, unitarity, etc.² This is the main difference between using a formalism such as the EFTofDE, versus some more phenomenological approaches, that parametrize the equation of state, $\delta P/\delta\rho$, the difference between the gravitational potentials, $\Phi - \Psi$, and the modifications of the Poisson equation, in some general form. The latter approach runs the uncontrollable risk of including regimes that are incompatible with the currently accepted principles of physics.

Observationally, since the number of modes is dominated by the shortest wavenumbers, most of the information about dark energy (and pretty much everything else), will be stored at those wavenumbers where the non-linearities of the LSS will be sizable. This makes it important to be able to describe the mildly non-linear regime both for dark matter and dark energy.

In the last few years, remarkable progress has occurred in our capability to describe the quasi-linear clustering of large-scale structures in the absence of dark energy, through the introduction of the so-called Effective Field Theory of Large-Scale Structure (EFTofLSS) [31, 32, 33, 34]. The availability of a satisfactory analytical treatment for large-scale structure has been delayed for about three decades because of the difficulty in dealing with the strong non-linearities at short distances that affect long wavelength perturbations. Since short distance fluctuations are not under perturbative control, it appeared that it was naively impossible to parametrize their effect at long distances. Instead, in the EFTofLSS, such an effect is accurately accounted for by the inclusion of suitable counterterms, that, after the related coupling constants are fitted to observations, can correctly include the effect of short distance fluctuations at long distances. In recent years, a large activity has occurred in this small field, see for example [31, 32, 33, 34, 35, 36, 37, 38, 39, 40, 41, 42, 43, 44, 45, 46, 47, 48, 49, 50, 51, 52, 53, 54, 55, 56, 57, 58, 59, 60, 61, 62]. This community, as we review later, has been able to satisfactorily show that the clustering of large-scale structures can be reproduced with great accuracy both for dark matter, galaxies, and in redshift space up to relatively high wavenumbers.

The purpose of this paper will be to develop a formalism that allows us to treat the mildly non-linear dynamics of large-scale structure in the presence of dark energy. We will achieve this by extending the EFTofLSS to include the presence of an additional species, dark energy, whose dynamics is described by the EFTofDE. For simplicity, we will focus on some specific choices of parameters of the EFTofDE, which amounts to studying the so-called clustering quintessence, though our methods are straightforwardly extendable to other choices of parameters, that allow one, for example, to describe the so-called Horndeski models³ and other models of modified gravity. After formulating the set of coupled non-linear equations, including the relevant counterterms, we will compute the power spectrum of the total density at one-loop order. Throughout the paper, we will use the notation $\partial^2 = \sum_{i=1}^3 \partial_i \partial_i$, $\dot{F} = dF/dt$ and $F' = dF/da$.

²Not all values of the parameters of the EFTofDE are allowed by these same principles, as for example, some values can lead to non-analyticity of the S -matrix or to superluminal propagation [30]. For a discussion about some of the constraints on the parameters of the EFTofDE imposed by these issues, see [28] and [29].

³Horndeski models are the most generic scalar-tensor theories, universally coupled to gravity, with second-order equations of motion.

2 Review of EFTs of Dark Energy and Large-Scale Structure

2.1 Effective Field Theory of Dark Energy

In this subsection, we review the effective field theory of dark energy developed in [17], which was applied to inflation in [18] and further developed for dark energy in [20]. The basic idea is that we would like to describe the most general low-energy theory of fluctuations around a time-dependent background solution, which necessarily spontaneously breaks time diffeomorphisms by providing a preferred time slicing of space-time. In the context of inflation, such a scenario is highly motivated because inflation must end and be smoothly connected to a hot big bang phase. The time slicing in this case is usually, but not necessarily, achieved by the evolution of a scalar field $\bar{\phi}(t)$ which acts as the clock for the system. Because of the new field $\phi(\vec{x}, t)$, the system now has, in addition to gravitational degrees of freedom, an additional scalar degree of freedom $\delta\phi(\vec{x}, t) = \phi(\vec{x}, t) - \bar{\phi}(t)$ which describes the fluctuations around the background solution. Although time diffeomorphisms $t \rightarrow t + \xi^0(\vec{x}, t)$ are not realized linearly on $\delta\phi$, they are realized non-linearly, through $\delta\phi \rightarrow \delta\phi - \dot{\bar{\phi}}\xi^0$, because the original theory was invariant.

Unitary gauge is the one in which we choose the time coordinate such that $\delta\phi(\vec{x}, t) = 0$ on the constant time surfaces, and the scalar degree of freedom appears in the metric. One then has a theory of three degrees of freedom, the two standard ones from the metric and the new scalar which in unitary gauge appears in the metric as well. To build the most general theory in this gauge, we write all of the operators in terms of the metric that are invariant under the remaining time-dependent spatial diffeomorphisms $x^i \rightarrow x^i + \xi^i(\vec{x}, t)$, but that do not have to be invariant under time diffeomorphisms. The new scalar degree of freedom can then be introduced by performing a broken time diffeomorphism on this action via the Stückelberg trick: $t \rightarrow \tilde{t} = t + \xi^0(\vec{x}, t)$. Then we make the replacement $\xi^0(x(\tilde{x})) \rightarrow -\tilde{\pi}(\tilde{x})$, where π is the Goldstone boson that non-linearly realizes the time diffeomorphism symmetry, which is restored if π transforms like $\pi(\vec{x}, t) \rightarrow \pi(\vec{x}, t) - \xi^0(\vec{x}, t)$.

The situation is similar for dark energy where we consider a general Friedmann-Robertson-Walker (FRW) background close to de Sitter. We know that the universe is close to Λ CDM, which has a constant cosmological constant Λ and is fully diffeomorphism invariant, so it makes sense to describe deviations from Λ CDM by assuming that time diffeomorphisms are spontaneously broken. As in the inflationary case, in this case there will be a Goldstone mode related to this symmetry breaking. The main new ingredient with respect to inflation is that this theory is coupled to matter. To get the most general theory, we write the actions for the metric and matter in unitary gauge, and we allow the inclusion of operators that break time diffeomorphism invariance, but are invariant under time-dependent spatial diffeomorphisms. This allows the inclusion in the action of n_μ , the unit normal to equal time hypersurfaces, and covariant derivatives of n_μ . This implies that the gravitational action, S_G , can depend on gauge invariant operators like the cosmological constant and contractions of the Riemann tensor, and can also depend on operators which break time diffeomorphisms, like a time-dependent cosmological constant (and other time-dependent couplings), g^{00} (or any other 4-dimensional tensor with upper 0 indices), and K_{ij} (the extrinsic curvature of equal-time slices). For a more complete discussion of the fields which break time diffeomorphisms, see Section 2.1.2 and

Appendix A. Thus, the gravitational action has the following form [17, 18, 20]

$$S_G = \int d^4x \sqrt{-g} F_G (R_{\mu\nu\rho\sigma}, g^{00}, K_{ij}, \nabla_\mu; t) . \quad (2.1)$$

The matter action, S_M , can also in principle depend on all of the aforementioned fields and the matter fields, χ_a , coupled in such a way that allows operators which break time diffeomorphisms. Thus, the generic form is (see [63] for example)

$$S_M = \int d^4x \sqrt{-g} F_M (R_{\mu\nu\rho\sigma}, g^{00}, K_{ij}, \nabla_\mu, \chi_a; t) , \quad (2.2)$$

with the same rule that for any covariant object, it is allowed to appear with an upper 0 index. For example, one can generically have couplings like $(g^{00})^2 \chi_a^2$ and $\partial^0 \chi_a \partial^0 \chi_a$ in F_M . From the unitary gauge action, one can introduce π , the Goldstone mode related to the broken time diffeomorphisms, in the standard way using the Stückelberg trick.

In this work, where we concentrate on correctly joining the EFT of dark matter and the EFT of dark energy, we choose a simplified setup for illustration purposes. We assume the existence of a frame, called the Jordan frame, where each matter species is minimally coupled to the same metric. In addition to simplifying our computations below, this assumption also ensures that the weak equivalence principle (WEP) holds (since all matter follows geodesics of the same metric). This is not a necessary assumption, and our results can be extended to WEP violating theories, but experiments strongly constrain the amount of WEP violation (see for example [64]). Then, the action in the Jordan frame in unitary gauge reads

$$S = S_G[g_{\mu\nu}] + S_M[g_{\mu\nu}, \chi_a], \quad (2.3)$$

where S_G is as in Eq. (2.1), but S_M is fully diffeomorphism invariant. Thus, when the Goldstone mode π is introduced, there is no direct coupling between π and the matter sector. More specifically, we will consider the example

$$S_G = \int d^4x \sqrt{-g} \left[\frac{M_{\text{Pl}}^2}{2} f(t) R - \Lambda(t) - c(t) g_{\text{u}}^{00} \right] + S_{DE}^{(2)}, \quad (2.4)$$

where $S_{DE}^{(2)}$ only contains terms quadratic and higher in the perturbations, so that the other operators shown are the only ones containing linear perturbations. In this paper, for convenience, we choose the following form for $S_{DE}^{(2)}$

$$S_{DE}^{(2)} = \int d^4x \sqrt{-g} \left[\frac{M_2^4(t)}{2} (\delta g_{\text{u}}^{00})^2 - \frac{\bar{m}_1^3(t)}{2} \delta g_{\text{u}}^{00} \delta K_{\text{u}} \right], \quad (2.5)$$

and in fact we will take $f(t) = 1$ for simplicity. In the above equation, $\delta g_{\text{u}}^{00} = 1 + g_{\text{u}}^{00}$ and δK_{u} is the variation of the trace of the extrinsic curvature [17, 65, 20] (for which we present a detailed computation to second order in Appendix A). The two functions $c(t)$ and $\Lambda(t)$ are chosen to fix the background equations, i.e. to eliminate the tadpole terms, and $f(t)$, $M_2^4(t)$ and $\bar{m}_1^3(t)$ encode the different theories of fluctuations in this particular setup. The “u” subscript on the operators that break time diffeomorphisms emphasize the fact that they are presented in unitary gauge, where the new scalar degree of freedom is contained in the metric. Later in 2.1.2, by means of the Stückelberg trick, we restore the diffeomorphism and re-introduce the scalar field fluctuations. In this paper, we will study the linear equations for both of the operators $(\delta g_{\text{u}}^{00})^2$ and $\delta g_{\text{u}}^{00} \delta K_{\text{u}}$, which we present in Appendix B, and we will study the non-linear system with $\bar{m}_1^3 = 0$ in the rest of the text.

2.1.1 Background equations

The matter in our theory is cold dark matter (CDM), and so its background equations are described by a time dependent energy density $\bar{\rho}_m(t)$ and a pressure $\bar{p}_m(t)$. Then, the zeroth order Einstein equations (Friedman equations) for the background FRW metric are

$$c(t) = -\dot{H}M_{\text{Pl}}^2 - \frac{1}{2}(\bar{\rho}_m + \bar{p}_m) \quad (2.6)$$

$$\Lambda(t) = (\dot{H} + 3H^2)M_{\text{Pl}}^2 - \frac{1}{2}(\bar{\rho}_m - \bar{p}_m) . \quad (2.7)$$

Instead of using $c(t)$ and $\Lambda(t)$ to describe the background, it is useful to change to two new functions $\bar{\rho}_D(t)$ and $\bar{p}_D(t)$ such that

$$c(t) = \frac{1}{2}(\bar{\rho}_D + \bar{p}_D) , \quad (2.8)$$

$$\Lambda(t) = \frac{1}{2}(\bar{\rho}_D - \bar{p}_D) , \quad (2.9)$$

after which Eq. (2.6) and Eq. (2.7) become

$$-2\dot{H}M_{\text{Pl}}^2 = \bar{\rho}_m + \bar{p}_m + \bar{\rho}_D + \bar{p}_D \quad (2.10)$$

$$3H^2M_{\text{Pl}}^2 = \bar{\rho}_m + \bar{\rho}_D . \quad (2.11)$$

These are the Friedman equations in a much more recognizable form, written in terms of the background dark-energy energy density $\bar{\rho}_D(t)$ and pressure $\bar{p}_D(t)$. In order to describe normal cold dark matter, we assume the background continuity equation $\dot{\bar{\rho}}_m + 3H(\bar{\rho}_m + \bar{p}_m) = 0$. For the rest of this paper, we will take $\bar{p}_m = 0$ because we are describing CDM. Thus we have

$$\bar{\rho}_m = \rho_{m,0} \left(\frac{a}{a_0} \right)^{-3} . \quad (2.12)$$

Hereafter, the subscript 0 denotes the present time value. Then, taking the time derivative of Eq. (2.11), we find that $\dot{\bar{\rho}}_D + 3H(\bar{\rho}_D + \bar{p}_D) = 0$. In this work, for simplicity, we consider a dark-energy component whose background is described by a constant equation of state $\bar{p}_D = w\bar{\rho}_D$. This gives a background solution

$$\bar{\rho}_D = \rho_{D,0} \left(\frac{a}{a_0} \right)^{-3(1+w)} . \quad (2.13)$$

It is also useful to write the Friedman equation as

$$\frac{H^2}{H_0^2} = \Omega_{m,0} \left(\frac{a}{a_0} \right)^{-3} + \Omega_{D,0} \left(\frac{a}{a_0} \right)^{-3(1+w)} , \quad (2.14)$$

where $\Omega_{m,0} \equiv \frac{\rho_{m,0}}{\rho_{m,0} + \rho_{D,0}}$ and $\Omega_{D,0} = \frac{\rho_{D,0}}{\rho_{m,0} + \rho_{D,0}}$ are the current day energy density fractions of CDM and dark energy, respectively.

2.1.2 Perturbations in the dark-energy sector

With the action in unitary gauge, it is useful to introduce the Goldstone mode π using the Stückelberg trick. In order to do that, we perform a time diffeomorphism $x^0 \rightarrow x^0 + \xi^0(\vec{x}, t)$ and $x^i \rightarrow x^i$ on the

action Eq. (2.3). Under a general diffeomorphism $x^\mu \rightarrow \tilde{x}^\mu(x)$, the metric changes in the standard way

$$\tilde{g}^{\mu\nu}(\tilde{x}(x)) = \frac{\partial \tilde{x}^\mu}{\partial x^\sigma} \frac{\partial \tilde{x}^\nu}{\partial x^\rho} g^{\sigma\rho}(x) , \quad (2.15)$$

which means that, following [18], after changing variables of integration in the action, replacing $\xi^0(x(\tilde{x})) \rightarrow -\tilde{\pi}(\tilde{x})$, and then dropping all of the tildes, we should make the replacements

$$g^{\mu\nu}(x) \rightarrow P^\mu{}_\rho P^\nu{}_\sigma g^{\rho\sigma}(x) \quad g_{\mu\nu}(x) \rightarrow P^{-1\rho}{}_\mu P^{-1\sigma}{}_\nu g_{\rho\sigma}(x) , \quad (2.16)$$

in the action, where the transformation matrices are given by

$$P^\mu{}_\rho = \begin{pmatrix} 1 + \dot{\pi} & \partial_i \pi \\ 0 & 1 \end{pmatrix}_{\mu\rho} \quad P^{-1\rho}{}_\mu = \begin{pmatrix} \frac{1}{1+\dot{\pi}} & -\frac{\partial_i \pi}{1+\dot{\pi}} \\ 0 & 1 \end{pmatrix}_{\rho\mu} , \quad (2.17)$$

and all of the π fields are evaluated at the point x . The arguments of the time dependent coefficients in the action, like $f(t)$, $c(t)$, $\Lambda(t)$, $M_2^4(t)$, and $\bar{m}_1^3(t)$, shift like

$$c(t) \rightarrow c(t + \pi) = c(t) + \dot{c}(t)\pi + \frac{1}{2}\ddot{c}(t)\pi^2 + \dots . \quad (2.18)$$

Finally, the replacement rule for derivatives is

$$\partial_\mu \rightarrow P^{-1\rho}{}_\mu \partial_\rho . \quad (2.19)$$

Some specific examples that we will need are

$$g_{\text{u}}^{00} \rightarrow P^0{}_\mu P^0{}_\nu g^{\mu\nu} = g^{00} + 2g^{0\mu} \partial_\mu \pi + g^{\mu\nu} \partial_\mu \pi \partial_\nu \pi \quad (2.20)$$

$$g_{\text{u}}^{0i} \rightarrow P^0{}_\mu P^i{}_\nu g^{\mu\nu} = g^{0i} + g^{i\mu} \partial_\mu \pi \quad (2.21)$$

$$g_{\text{u}}^{ij} \rightarrow g^{ij} \quad (2.22)$$

$$\delta K_{\text{u}} \rightarrow \delta K_g - a^{-2} \partial^2 \pi - 3\dot{H}\pi , \quad (2.23)$$

where δK_g depends only on the metric. The first three expressions above are fully expanded in terms of π , but the metrics appearing can still be expanded in perturbations. In the last line, we have only presented our expression for δK_{u} to linear order because these are the most important terms. In Appendix A, we present a detailed computation of δK_{u} , including a discussion of higher order terms, and thus extend the computations done in [17, 65, 20].

2.2 Effective Field Theory of Large-Scale Structure

We now review the other main ingredient of our study, The Effective Field Theory of Large-Scale Structure,⁴ which describes the dynamics of collisionless dark matter on large scales in the Λ CDM universe. The EFTofLSS community has studied the dark matter density two-point function [32, 34, 36, 52, 53], three-point function [40, 41], four-point function [55, 56], the dark matter momentum power spectrum [34, 53], the displacement field [41], and the vorticity slope [36, 66]. Additionally, baryonic effects on the matter correlation functions have been described within the EFTofLSS in [44].

⁴Formerly known as the Effective Field Theory of Large Scale Structures.

The extension of the EFTofLSS to describe biased tracers has been performed in [43], and predictions have been compared to data for the power spectrum and bispectrum (including all mixed correlation functions between matter and halos) in [47, 61]. The EFTofLSS was used to describe redshift-space distortions in [43], and predictions have been compared to numerical data for matter power spectra in [58]. Methods to measure the parameters of the EFTofLSS in small numerical simulations have been developed in [32, 67, 68, 69, 60]. The IR-resummation was implemented and compared to numerical data of dark matter clustering in [34], extended to halos in [43] and compared to halo datasets in [47], recently extended to dark matter in redshift space and compared to simulated datasets in [43, 58], and finally extended to halos in redshift space in [62]. The signature of primordial non-Gaussianity on large-scale structure observables [47, 49, 57, 58] has also been recently included. Recently, fast implementations of the predictions of the EFTofLSS, which allows us to efficiently explore their dependence on various cosmological parameters, have been developed in [59], with public codes available at the following website⁵ (including the Mathematica notebook used in this paper).

In the rest of this section, we briefly review some of the results and findings of the EFTofLSS in Λ CDM. The relevant long wavelength degrees of freedom are the overdensity $\delta_m(\vec{x}, t) \equiv (\rho_m(\vec{x}, t) - \bar{\rho}_m(t))/\bar{\rho}_m(t)$ and the velocity divergence $\theta_m(\vec{x}, t) \equiv \partial_i v_m^i(\vec{x}, t)$.⁶ After integrating out the effects of short scale (UV) physics below some non-linear wavenumber scale k_{NL} , the equations for the long wavelength fields take the form

$$\dot{\delta}_m + \frac{1}{a} \partial_i ((1 + \delta_m) v_m^i) = 0 \quad (2.24)$$

$$\partial_i \dot{v}_m^i + H \partial_i v_m^i + \frac{1}{a} \partial_i (v_m^j \partial_j v_m^i) + \frac{1}{a} \partial^2 \Phi = -\frac{1}{a} \partial_i \left(\frac{1}{\rho_m} \partial_j \tau^{ij} \right)_s \quad (2.25)$$

$$a^{-2} \partial^2 \Phi = \frac{3}{2} \frac{\Omega_{m,0} \mathcal{H}_0^2 a_0}{a^3} \delta_m . \quad (2.26)$$

The effects of UV physics on long distances are encoded in the effective stress tensor $\left(\frac{1}{\rho_m} \partial_j \tau^{ij} \right)_s$, which depends on short modes. Since we cannot describe the short modes exactly, we expand the stress tensor in powers and derivatives of the long wavelength fields, and we include all operators, called counterterms, that are consistent with the equivalence principle. As has been discussed [42, 36, 38], the EFTofLSS is non-local in time. This means that, after taking the expectation value over the short modes in the background of the long modes, the effective stress tensor can be written as an integral over some unknown kernel of time of an expansion in powers and derivatives of $\partial_i \partial_j \Phi$ and $\partial_i v_m^j$, evaluated along the fluid line element. The lowest order terms in this expansion are

$$\begin{aligned} - \left(\frac{1}{\rho_m} \partial_j \tau^{ij} \right)_s (a, \vec{x}) = & \int da' \left[\kappa^{(1)}(a, a') \partial^i \partial^2 \Phi(a', \vec{x}_{\text{fl}}(\vec{x}; a, a')) \right. \\ & + \kappa^{(2)}(a, a') \frac{1}{H} \partial^i \partial_j v_m^j(a', \vec{x}_{\text{fl}}(\vec{x}; a, a')) \\ & \left. + \kappa^{(\text{stoch.})}(a, a') \partial^i \bar{\Delta}_{\text{stoch.}}(a', \vec{x}_{\text{fl}}(\vec{x}; a, a')) + \dots \right], \quad (2.27) \end{aligned}$$

⁵<http://web.stanford.edu/~senatore/>

⁶Vorticity is generated in the EFTofLSS at a high order, but it can be ignored for the one-loop discussion that we present here [36].

where the various $\kappa(a, a')$ are the kernels encoding UV physics, $\bar{\Delta}_{\text{stoch.}}$ is the stochastic counterterm not proportional to the long wavelength fields (which we will ignore in this paper, but is explained in more detail below), the fluid line element \bar{x}_{fl} is defined implicitly as [36]

$$\bar{x}_{\text{fl}}(\bar{x}; a, a') = \bar{x} - \int_{a'}^a da'' \frac{d\tau}{da}(a'') \bar{v}_m(a'', \bar{x}_{\text{fl}}(\bar{x}; a, a'')) , \quad (2.28)$$

and τ is conformal time. The terms associated with the past trajectory, i.e. expanding in \bar{x}_{fl} , appear at higher orders in the expansion, and we ignore them in this study. As discussed in [36], the non-locality in time can be written such that the counterterms appear as local-in-time. For example, using the Poisson equation Eq. (2.26) and the fact that the linear solution is $\delta_m^{(1)}(a, \bar{x}) = D(a)\delta_m^{(1)}(a_i, \bar{x})/D(a_i)$, we can write

$$\int da' \kappa^{(1)}(a, a') \partial^i \partial^2 \Phi^{(1)}(a', \bar{x}) = \left(\int da' \tilde{\kappa}^{(1)}(a, a') \frac{D(a')}{D(a)} \right) \partial^i \delta_m^{(1)}(a, \bar{x}) , \quad (2.29)$$

where $\kappa^{(1)}$ and $\tilde{\kappa}^{(1)}$ are related by the factors in the Poisson equation. We can then define the local-in-time speed-of-sound parameters by symbolically performing the a' integral, thus leaving us with an unknown function of one variable a . In fact, as a function of the fields, Eq. (2.29) is the generic form for a counterterm at one loop, since the term proportional to $\kappa^{(2)}$ in Eq. (2.27) can be written as proportional to $\partial^i \delta_m^{(1)}$ by using Eq. (2.24), where the integrand involves some rescaled $\tilde{\kappa}^{(2)}$ as in Eq. (2.29). Putting this all together gives us the final expression for the stress tensor at this order

$$- \left(\frac{1}{\rho_m} \partial_j \tau^{ij} \right)_s (a, \bar{x}) \sim \left(\int da' K(a, a') \frac{D(a')}{D(a)} \right) \partial^i \delta_m^{(1)}(a, \bar{x}) , \quad (2.30)$$

where we neglect a factor of $e^{i\vec{k} \cdot (\bar{x}_{\text{fl}} - \bar{x})} \simeq 1$ at the order that we work, and $K = \tilde{\kappa}^{(1)} + \tilde{\kappa}^{(2)}$. In Fourier space, using the conventions $F(\bar{x}) = \int \frac{d^3 k}{(2\pi)^3} e^{-i\vec{k} \cdot \bar{x}} F(\vec{k})$, and switching to the scale factor a as the time variable, we finally have

$$a \mathcal{H} \delta_m(a, \vec{k})' + \theta_m(a, \vec{k}) = - \int \frac{d^3 q}{(2\pi)^3} \alpha(\vec{q}, \vec{k} - \vec{q}) \theta_m(a, \vec{q}) \delta_m(a, \vec{k} - \vec{q}) \quad (2.31)$$

$$a \mathcal{H} \theta_m(a, \vec{k})' + \mathcal{H} \theta_m(a, \vec{k}) + \frac{3}{2} \frac{\Omega_{m,0} \mathcal{H}_0^2 a_0}{a} \delta_m(a, \vec{k}) = 9 (2\pi)^2 c_{s,m}^2(a) H(a)^2 \frac{k^2}{k_{\text{NL}}^2} \delta_m(a, \vec{k}) - \int \frac{d^3 q}{(2\pi)^3} \beta(\vec{q}, \vec{k} - \vec{q}) \theta_m(a, \vec{k} - \vec{q}) \theta_m(a, \vec{q}) \quad (2.32)$$

where

$$\alpha(\vec{q}_1, \vec{q}_2) = 1 + \frac{\vec{q}_1 \cdot \vec{q}_2}{q_1^2} \quad (2.33)$$

$$\beta(\vec{q}_1, \vec{q}_2) = \frac{|\vec{q}_1 + \vec{q}_2|^2 \vec{q}_1 \cdot \vec{q}_2}{2q_1^2 q_2^2} , \quad (2.34)$$

$\mathcal{H} = aH$, and we have included the one-loop counterterm, proportional to $(k/k_{\text{NL}})^2$. The effective field theory is a controlled expansion in k/k_{NL} , and is valid for $k/k_{\text{NL}} \ll 1$. For $k/k_{\text{NL}} \ll 1$, observables can be computed to arbitrary precision, apart from non-perturbative effects, by including more and more loops and counterterms. On the right hand side of Eq. (2.32), we should also include

a stochastic counterterm $\frac{k^2}{k_{\text{NL}}^2} \Delta_{\text{stoch.}}(\vec{k})$. This field does not correlate with the matter fields, but it does correlate with itself like

$$\langle \Delta_{\text{stoch.}}(\vec{k}) \Delta_{\text{stoch.}}(\vec{k}') \rangle = \frac{(2\pi)^3}{k_{\text{NL}}^3} \delta(\vec{k} + \vec{k}'), \quad (2.35)$$

and so contributes a term like k^4/k_{NL}^4 to the power spectrum. This term is negligible in a one-loop computation, so we ignore it for now.

We then seek a perturbative solution to Eq. (2.31) and Eq. (2.32) in the form $\delta_m = \delta_m^{(1)} + \delta_m^{(2)} + \delta_m^{(3)} + \delta_m^{(ct)} + \dots$, where $\delta_m^{(n)}$ is sourced by n powers of the linear solution $\delta_m^{(1)}$, i.e. $\delta_m^{(n)} \sim [\delta_m^{(1)}]^n$, and $\delta_m^{(ct)}$ is the same order as $\delta_m^{(3)}$. The linear solution that grows fastest with time is called the growth factor $D(a)$, so that $\delta_m^{(1)}(a, \vec{x}) = D(a)\delta_m^{(1)}(a_i, \vec{x})/D(a_i)$, and is given by

$$D(a) = \frac{5}{2} \mathcal{H}_0^2 \Omega_{m,0} \frac{\mathcal{H}(a)a_0}{a} \int_0^a \frac{d\tilde{a}}{\mathcal{H}(\tilde{a})^3}. \quad (2.36)$$

The linear power spectrum is defined by

$$\langle \delta_m^{(1)}(a, \vec{k}) \delta_m^{(1)}(a, \vec{k}') \rangle = (2\pi)^3 \delta(\vec{k} + \vec{k}') \left(\frac{D(a)}{D(a_i)} \right)^2 P_{11}(a_i, k), \quad (2.37)$$

and the initial power spectrum defined at some initial time a_i is taken from CAMB [70], for example. Then, to solve for the higher order fields, we can use the Green's function for the system Eq. (2.31) and Eq. (2.32). We will use this method later in the paper, but for now we present an approximate solution called the EdS approximation, which is exact in the matter era, but in general relies on $(\Omega_{m,0} \mathcal{H}_0^2 a_0 / (a \mathcal{H}^2)) / (a D' / D)^2$ being close to unity. This ratio is one at early times and is 1.15 at $a = 1$ [32], but is close to one for most of the time evolution.

The one-loop power spectra are defined by

$$2 \langle \delta^{(1)}(a, \vec{k}) \delta^{(3)}(a, \vec{k}') \rangle = (2\pi)^3 \delta(\vec{k} + \vec{k}') \left(\frac{D(a)}{D(a_i)} \right)^4 P_{13}(a_i, k) \quad (2.38)$$

$$\langle \delta^{(2)}(a, \vec{k}) \delta^{(2)}(a, \vec{k}') \rangle = (2\pi)^3 \delta(\vec{k} + \vec{k}') \left(\frac{D(a)}{D(a_i)} \right)^4 P_{22}(a_i, k) \quad (2.39)$$

$$2 \langle \delta^{(1)}(a, \vec{k}) \delta^{(ct)}(a, \vec{k}') \rangle = (2\pi)^3 \delta(\vec{k} + \vec{k}') P_{13}^{ct}(a, k), \quad (2.40)$$

and P_{13} and P_{22} are the standard one-loop expressions for dark matter.⁷ The counterterm power

⁷The standard expressions for the loop integrals are

$$P_{22}(a_i, k) = \frac{k^3}{392\pi^2} \int_0^{\Lambda/k} dr \int_{-1}^1 dx \frac{(-10rx^2 + 3r + 7x)^2}{(r^2 - 2rx + 1)^2} P_{11}(a_i, kr) P_{11}(a_i, k\sqrt{r^2 - 2rx + 1})$$

$$P_{13}(a_i, k) = \frac{k^3}{1008\pi^2} P_{11}(a_i, k) \int_0^{\Lambda/k} dr \left(\frac{3}{r^3} (r^2 - 1)^3 (7r^2 + 2) \log \left| \frac{1+r}{1-r} \right| - 42r^4 + 100r^2 + \frac{12}{r^2} - 158 \right) P_{11}(a_i, kr). \quad (2.41)$$

The above loop integrals are cut off (or smoothed over) at a scale $\Lambda > k_{\text{NL}}$ because the theory is not under perturbative control at such high momenta. As is thoroughly discussed in previous work [32, 36], the speed of sound parameters, like c_m^2 , depend on Λ in such a way as to cancel the final dependence of any physical observable on Λ .

spectrum is given by

$$P_{13}^{ct}(a, k) = -2 (2\pi) \bar{c}_m^2(a) \frac{k^2}{k_{\text{NL}}^2} \left(\frac{D(a)}{D(a_i)} \right)^2 P_{11}(a_i, k) , \quad (2.42)$$

where we have redefined the speed of sound parameter for convenience.⁸

3 EFTofLSS with DE: clustering quintessence example

In this section, in order to provide an explicit computation, we consider the following action for the dark-energy degree of freedom

$$\int d^4x \sqrt{-g} \left[\frac{M_{\text{Pl}}^2}{2} R - \Lambda(t) - c(t) g_{\text{u}}^{00} + \frac{M_2^4(t)}{2} (\delta g_{\text{u}}^{00})^2 \right] . \quad (3.1)$$

This is coupled to the dark-matter field through gravity in the following way

$$\dot{\delta}_m + \frac{1}{a} \partial_i ((1 + \delta_m) v_m^i) = 0 \quad (3.2)$$

$$\partial_i \dot{v}_m^i + H \partial_i v_m^i + \frac{1}{a} \partial_i (v_m^j \partial_j v_m^i) + \frac{1}{a} \partial^2 \Phi = -\frac{1}{a} \partial_i \left(\frac{1}{\rho_m} \partial_j \tau^{ij} \right)_s + \frac{1}{a} \partial_i \gamma_s^i , \quad (3.3)$$

where γ_s^i is the effective force which accounts for the fact that the two species can exchange momentum [44]. Furthermore, we will consider this system in the non-relativistic limit (i.e. on sub-horizon scales where gravitational non-linearities are most important), and when the dark-energy has a small speed of sound (which we discuss in more detail below). This scenario is equivalent to the clustering quintessence model studied in [19, 71, 72]. We will also extend (and make a slight correction to) the computation in [72] to include the third-order density fluctuation and counterterm operators, thus treating the dark matter sector as provided by the EFTofLSS. One can see also [73, 74, 75] for other approaches to non-linear clustering quintessence, which differ from our approach in the treatment

⁸In the power spectrum, the relevant parameter is the following integral:

$$\bar{c}_m^2(a) = \int^a da' G(a, a') \frac{D(a')}{D(a)} 9 H(a')^2 c_{s,m}^2(a') , \quad (2.43)$$

where G is the retarded Green's function for the linear equation

$$\begin{aligned} -a^2 \mathcal{H}^2 G'' - (2a \mathcal{H}^2 + a^2 \mathcal{H} \mathcal{H}') G' + \frac{3\mathcal{H}_0^2 a_0 \Omega_m}{2a} G &= \delta_D^{(1)}(a - \bar{a}) , \\ G(a, a) = 0 , \quad \partial_a G(a, \bar{a})|_{a=\bar{a}} &= \frac{1}{\bar{a}^2 \mathcal{H}(\bar{a})^2} . \end{aligned} \quad (2.44)$$

In order to estimate the numerical size of the integration over the Green's function, we approximate the integral in (2.43) with the corresponding EdS form and choose $c_{s,m}^2 \propto a^4$ as an example. This gives

$$\bar{c}_m^2(a_0) \simeq c_{s,m}^2(a_0) . \quad (2.45)$$

and explains the factor of 9 that is present in the definition of $c_{s,m}^2$ in Eq. (2.32).

of UV modes.⁹ In this paper, we work in a spatially flat FRW background in the Newtonian gauge and ignore tensor fluctuations of the metric. This means that we can write the metric as¹⁰

$$ds^2 = -(1 + 2\Phi)dt^2 + a(t)^2(1 - 2\Psi)\delta_{ij}dx^i dx^j . \quad (3.4)$$

3.1 Linear equations

Using Eq. (2.20), we see that the kinetic part of the action for π is

$$S_{\text{kin.}} = \int d^4x \sqrt{-g} \left((c(t) + 2M_2^4(t)) \dot{\pi}^2 - c(t) a^{-2} \partial^2 \pi \right) , \quad (3.5)$$

from which we can read off the speed of sound of π fluctuations to be

$$c_s^2 = \frac{c(t)}{c(t) + 2M_2^4(t)} . \quad (3.6)$$

As discussed in [17], there is a range of parameters for which the effective field theory is unstable. In order to prevent the presence of ghosts, we should assume $c(t) + 2M_2^4(t) > 0$. The presence of ghost fields is dangerous because the vacuum is unstable against the spontaneous production of positive energy matter particles and negative energy π particles. Then, notice that it is possible to have $c(t) \equiv \bar{\rho}_D(t)(1 + w)/2 < 0$ and still satisfy the no-ghost condition. From Eq. (3.6) we see that this makes $c_s^2 < 0$, which seems to signal that the system has a gradient instability. However, as shown in [17], higher derivative terms in the action like $(\partial^2 \pi)^2$ stabilize the system at short scales, where the dispersion relation becomes $\omega^2 \approx k^4/M_2^2$ and the system behaves like the Ghost Condensate [76]. The main point, though, is that on cosmological scales these higher order terms are highly suppressed unless $|1 + w|\Omega_D \lesssim 10^{-34}$ [17, 19], which means that for any values of w distinguishable from the cosmological constant, the system only behaves like the Ghost Condensate on very short scales which are irrelevant for cosmology. Taking this short scale stabilization into account, there is no problem with $w < -1$, but in that case one needs $-c_s^2 \lesssim 10^{-30}$ in order to make the remaining gradient instability timescale longer than H^{-1} . The bottom line is that for $w > -1$, any value of $c_s^2 \leq 1$ is allowed, but $c_s^2 \rightarrow 0$ as $w \rightarrow -1$, and for $w < -1$ we must have $-c_s^2 \lesssim 10^{-30}$. As a final point also noted in [17, 18], $|c_s^2| \ll 1$ is technically natural, i.e. is not significantly renormalized by

⁹ In particular, references [73, 74, 75] claim to apply some resummation schemes for the infrared modes below the non-linear scale, but ignore contaminations from non-linear modes. This is radically different from our approach: while references [73, 74, 75] attempt to provide a more accurate solution to the equations of a perfect pressureless fluid coupled to dark energy, here we are rather changing the equations of motion for the fluid. Therefore, there is a major difference already at the level of the equations to be solved. We change the equations because we need to include counterterms to consistently describe the effect of non-linear modes at long distances. The requirement of these terms has by now been quite well established by the literature on the EFTofLSS, and therefore we consider it inconsistent to not include these terms. Therefore, we do not find the need to perform an explicit comparison with the results of [73, 74, 75]. In fact, in this paper we are treating the modes below the non-linear scale perturbatively (i.e. no resummation). Readers interested in these resummation schemes [73, 74, 75] may find it interesting to apply them within the EFTofLSS with DE, and see if they can improve the results. However, this goes beyond the scope of the present paper.

¹⁰From the constraint equation Eq. (B.11), we see that $\Phi = \Psi$ for our study. We will usually keep track of the fields separately, but in the end we will always set $\Phi = \Psi$.

higher order operators, because $c_s^2 = 0$ is protected by the shift symmetry in the Ghost Condensate theory. We will explicitly verify this in Section 3.2 when we consider non-linear terms.

For clustering quintessence, we are interested in the limit $c_s^2 \rightarrow 0$. Then, assuming that c_s^2 is constant for simplicity, and keeping in mind that $2c(t) = \bar{\rho}_D(t)(1+w)$, we have

$$M_2^4(t) \approx \frac{\bar{\rho}_D(t)(1+w)}{4c_s^2} . \quad (3.7)$$

Thus, in the $c_s^2 \rightarrow 0$ limit, the full linear equation for π Eq. (B.6) becomes (see for example [19, 71, 21])

$$\ddot{\pi} - \dot{\Phi} + \frac{\partial_t M_2^4}{M_2^4} (\dot{\pi} - \dot{\Phi}) + 3H(\dot{\pi} - \dot{\Phi}) - c_s^2 a^{-2} \partial^2 \pi = 0 , \quad (3.8)$$

or

$$\frac{1}{a^3 M_2^4} \frac{d}{dt} \{ a^3 M_2^4 (\dot{\pi} - \dot{\Phi}) \} = c_s^2 a^{-2} \partial^2 \pi . \quad (3.9)$$

Without solving this equation, we can immediately find an important property of the solution, namely that $\dot{\pi} - \dot{\Phi} \sim c_s^2 \partial^2 \Phi / H^2$. To see this, write $\pi = \pi_0 + c_s^2 \pi_{c_s}$, plug this into Eq. (3.9), and expand in powers of c_s^2 . We obtain $\dot{\pi}_0 = \dot{\Phi}$ and

$$\frac{1}{a^3 M_2^4} \frac{d}{dt} \{ a^3 M_2^4 \dot{\pi}_{c_s} \} = a^{-2} \partial^2 \pi_0 \sim a^{-2} H^{-1} \partial^2 \Phi , \quad (3.10)$$

where we have taken time derivatives to be of order H . This gives $\pi_{c_s} \sim \partial^2 \Phi / H$, and shows that $\dot{\pi} - \dot{\Phi} \sim c_s^2 \partial^2 \Phi / H^2$. We will often use this scaling, along with $\pi \sim \Phi / H$, to estimate the sizes of various contributions and determine the non-relativistic limit in the rest of this paper. For example, $\partial_i \pi \sim \partial_i \Phi / H \sim v^i$, where $v \sim 10^{-5} k / H$ is the characteristic velocity of the large-scale modes. Thus, in any equation for $\partial^2 \pi \sim \theta$, the non-relativistic limit means that we ignore terms like $\partial_i \pi \partial_i \pi \sim v^2$ but keep terms like $\partial^2 \pi \partial^2 \pi \sim \theta^2$.

In $c_s^2 \rightarrow 0$ limit, the Poisson equation Eq. (B.7) becomes (see for example [19, 71, 20])

$$a^{-2} \partial^2 \Psi = \frac{3}{2} \frac{\Omega_{m,0} \mathcal{H}_0^2 a_0}{a^3} \left(\delta_m + \frac{4M_2^4}{\bar{\rho}_m} (\dot{\pi} - \dot{\Phi}) \right) , \quad (3.11)$$

where we have used that $\bar{\rho}_m / (2M_{\text{pl}}^2) = 3\Omega_{m,0} \mathcal{H}_0^2 a_0 / (2a^3)$.¹¹ In this paper, we are interested in computing correlation functions of the adiabatic mode, i.e. the one that sources the gravitational potential and is defined by $\delta_A = 2M_{\text{pl}}^2 a^{-2} \partial^2 \Psi / \bar{\rho}_m$. In this case, using Eq. (3.11), we have

$$\delta_A = \delta_m + \frac{4a^3 M_2^4}{a_0^3 \bar{\rho}_{m,0}} (\dot{\pi} - \dot{\Phi}) . \quad (3.13)$$

Now we are in a position to derive the relevant equations for δ_A . Looking back at the equation of motion Eq. (3.9) we see that, for $c_s^2 \rightarrow 0$, we can ignore the right hand side and obtain $\dot{\pi} - \dot{\Phi} \propto$

¹¹To make a connection to a fluid picture of quintessence, it may be useful to use the Poisson equation to define the overdensity of quintessence, δ_D . If we write $2M_{\text{pl}}^2 a^{-2} \partial^2 \Psi = \sum_i \bar{\rho}_i \delta_i$, then this gives

$$\delta_D = \frac{1+w}{c_s^2} (\dot{\pi} - \dot{\Phi}) , \quad (3.12)$$

to linear order and in the non-relativistic limit.

$(a^3 M_2^4)^{-1}$, which is decaying because $M_2^4 \propto a^{-3(1+w)}$ and $w \approx -1$. Thus, after this mode decays away, we have $\dot{\pi} - \Phi = 0$, and in particular, that $\partial_i \dot{\pi} - \partial_i \Phi = 0$. Using the Euler equation Eq. (2.25) for dark matter to linear order, this gives $\frac{d}{dt} [a(v_m^i + a^{-1} \partial_i \pi)] = 0$, or

$$-a^{-1} \partial_i \pi = v_m^i \quad \text{and} \quad -a^{-1} \partial^2 \pi = \theta_m, \quad (3.14)$$

on the growing adiabatic mode. This means that the two species follow the same geodesics, i.e. that they are comoving.

Next, take the time derivative of the definition of δ_A to get

$$\dot{\delta}_A = \dot{\delta}_m + \frac{4}{a_0^3 \bar{\rho}_{m,0}} \frac{d}{dt} \{a^3 M_2^4 (\dot{\pi} - \Phi)\} \quad (3.15)$$

$$= -\frac{1}{a} \theta_m + \frac{4 a^3 M_2^4}{a_0^3 \bar{\rho}_{m,0}} c_s^2 a^{-2} \partial^2 \pi = -\frac{1}{a} C(a) \theta_m, \quad (3.16)$$

where

$$C(a) = 1 + \frac{4 a^3 M_2^4 c_s^2}{a_0^3 \bar{\rho}_{m,0}} = 1 + (1+w) \frac{\Omega_{D,0}}{\Omega_{m,0}} \left(\frac{a}{a_0}\right)^{-3w}, \quad (3.17)$$

and we have used the linear dark-matter continuity equation Eq. (2.24), the equation of motion for π Eq. (3.9), and the fact that the two species are comoving. Although the term proportional to c_s^2 in Eq. (3.8) is not needed to find the relation Eq. (3.14), it is needed to find the continuity equation Eq. (3.16) because there is a term proportional to $1/c_s^2$ in the definition of δ_A . Thus, writing $v_A^i \equiv v_m^i = -a^{-1} \partial_i \pi$ for the common velocity, we are led to the standard linear equations for the adiabatic mode in clustering quintessence [72]

$$\dot{\delta}_A + \frac{1}{a} C(a) \theta_A = 0 \quad (3.18)$$

$$\dot{\theta}_A + H \theta_A + \frac{3}{2} \frac{\Omega_{m,0} \mathcal{H}_0^2 a_0}{a^2} \delta_A = 0. \quad (3.19)$$

From the combination of the above equations, we can find a single second order differential equation for δ_A which we will solve in Section 4.1. Note that we do not need to know the solution of π to determine δ_A . In fact, having the solution for δ_A and therefore Φ , we can solve the linear field equation for π , as shown in Appendix B.1.

3.2 Non-linear equations

There are two main non-linear effects to consider: the non-linear effects on the dynamics of π , and the effects of the non-linear definition of δ_A in terms of π . We can discuss the former by considering the action for π Eq. (3.1) and using the linear solution to estimate the scale $k_{\text{NL},D}$ when the dark-energy sector will become non-linear. The leading non-linear interaction term in the action in the $c_s^2 \rightarrow 0$ limit is $M_2^4 \dot{\pi} (\partial \pi)^2$, and the leading quadratic term is $M_2^4 \dot{\pi}^2$. Using $\dot{\pi} \sim \Phi \sim H v/k$ and $\partial \pi \sim v$, we have

$$\frac{M_2^4 \dot{\pi} (\partial \pi)^2}{M_2^4 \dot{\pi}^2} \Big|_{k_{\text{NL},D}} \sim \frac{k v}{H} \Big|_{k_{\text{NL},D}}, \quad (3.20)$$

which becomes order one at the same scale as dark matter, so we have that the scales are comparable, $k_{\text{NL},D} \approx k_{\text{NL}}$. This was to be expected, since dark energy and dark matter have the same velocity, so

that when dark matter becomes non-linear, so does dark energy. We can also verify that $|c_s^2| \ll 1$ is not a fine tuning, i.e. that it is not significantly renormalized by higher order terms. The coefficient of the $(\partial\pi)^2$ term is protected by the shift symmetry present for $w = -1$, so we should look for a renormalization of the $M_2^4 \dot{\pi}^2$ term. This can come from the $M_2^4 \dot{\pi}(\partial\pi)^2$ term, changing the coefficient from M_2^4 to something of the order $M_2^4 (1 + \langle \delta_A(x)\delta_A(x) \rangle_{k_{\text{NL}}})$, which is at most an order one change and so cannot significantly change the speed of sound away from the $|c_s^2| \ll 1$ value.

Next, we move on to consider the non-linear corrections to Eq. (3.18) and Eq. (3.19), which depend on the non-linear definition of δ_A , and for this we will have to look at the equations for motion. As we saw in the last section, the equation of motion forces $\dot{\pi} - \Phi \propto c_s^2$ so that the dark-energy contribution to δ_A , given by $c_s^{-2}(\dot{\pi} - \Phi)$ in Eq. (3.13), scales like c_s^0 , which is good because we do not expect any terms to blow up in the $c_s^2 \rightarrow 0$ limit that we are considering. To see that this is true at all orders in perturbations, start with the general form of the equation of motion for π

$$\nabla^\mu \frac{\delta \mathcal{L}}{\delta \partial_\mu \pi} = \frac{\delta \mathcal{L}}{\delta \pi}, \quad (3.21)$$

where \mathcal{L} is the Lagrange density for the action Eq. (3.1), after introducing π with the Stückelberg trick. The coefficients $\Lambda(t + \pi)$, $c(t + \pi)$, and $M_2^4(t + \pi)$ depend only on powers of π , while δg_{u}^{00} contains derivatives of π . Thus, we have

$$\frac{\delta \mathcal{L}}{\delta \partial_\mu \pi} = \frac{\delta \delta g_{\text{u}}^{00}}{\delta \partial_\mu \pi} \frac{\delta \mathcal{L}}{\delta \delta g_{\text{u}}^{00}} = \frac{\delta \delta g_{\text{u}}^{00}}{\delta \partial_\mu \pi} (-c + M_2^4 \delta g_{\text{u}}^{00}) \quad (3.22)$$

$$\frac{\delta \mathcal{L}}{\delta \pi} = \frac{\delta(c - \Lambda)}{\delta \pi} - \frac{\delta c}{\delta \pi} \delta g_{\text{u}}^{00} + \frac{1}{2} \frac{\delta M_2^4}{\delta \pi} (\delta g_{\text{u}}^{00})^2, \quad (3.23)$$

which gives the full equation of motion as

$$\frac{1}{\sqrt{-g}} \partial_\mu \left(\sqrt{-g} \frac{\delta \delta g_{\text{u}}^{00}}{\delta \partial_\mu \pi} (-c + M_2^4 \delta g_{\text{u}}^{00}) \right) = \frac{\delta(c - \Lambda)}{\delta \pi} - \frac{\delta c}{\delta \pi} \delta g_{\text{u}}^{00} + \frac{1}{2} \frac{\delta M_2^4}{\delta \pi} (\delta g_{\text{u}}^{00})^2. \quad (3.24)$$

We will solve Eq. (3.24) perturbatively (for example writing $\delta g_{\text{u}}^{00} = \delta g_{\text{u}}^{00(1)} + \delta g_{\text{u}}^{00(2)} + \dots$) so in the $c_s^2 \rightarrow 0$ limit, the linear equation of motion is

$$a^{-3} \partial_0 \left(a^3 M_2^4(t) \delta g_{\text{u}}^{00(1)} \right) \propto c_s^0, \quad (3.25)$$

which means that $\delta g_{\text{u}}^{00(1)} \propto c_s^2$ when evaluated on the linear solution, as we found earlier. Now, if we continue to expand the equation of motion to higher orders, we will always get

$$a^{-3} \partial_0 \left(a^3 M_2^4(t) \delta g_{\text{u}}^{00(n)} \right) \propto c_s^0, \quad (3.26)$$

because any time that a factor of M_2^4 shows up on the right hand side, it will be multiplied by a lower order δg_{u}^{00} , which, because we are solving iteratively, is proportional to c_s^2 . Thus, we find that the equations of motion force $\delta g_{\text{u}}^{00} \propto c_s^2$ at all orders. Indeed, we expected this result, since $M_2^4 (\delta g_{\text{u}}^{00})^2$ provides the kinetic term for the action in the limit $c_s^2 \rightarrow 0$, and so was not expected to blow up.

The reason that this is important is because this is the combination, $M_2^4 \delta g_{\text{u}}^{00}$, that shows up in δ_A , which is given by the (00) component of the stress tensor, up to relativistic corrections, as

$$\delta_A = \delta_m - \frac{2a^{-3}}{\bar{\rho}_m} \frac{\delta \sqrt{-g} \mathcal{L}}{\delta g^{00}}, \quad (3.27)$$

which in the $c_s^2 \rightarrow 0$ limit becomes

$$\delta_A \rightarrow \delta_m - \frac{2}{\bar{\rho}_m} \frac{\sqrt{-g}}{a^3} \left(\frac{\delta \delta g_u^{00}}{\delta g^{00}} (-c + M_2^4 \delta g_u^{00}) - \frac{1}{2} g_{00} (c - \Lambda) \right) - \frac{\bar{\rho}_D}{\bar{\rho}_m} , \quad (3.28)$$

and is now guaranteed to have a good limit for $c_s^2 \rightarrow 0$, as expected (note that terms like $M_2^4 (\delta g_u^{00})^2$ are negligible because they are proportional to c_s^2).

From here, it is easy to see that the two species remain comoving (apart from possible counterterms, which we will discuss later) in the $c_s^2 \rightarrow 0$ limit even at higher orders. We know that $\delta g_u^{00} \propto c_s^2$, so in particular, we have $\partial_i \delta g_u^{00} = 0$ for $c_s^2 \rightarrow 0$, which means that, up to relativistic corrections,

$$0 = \partial_i \left(\dot{\pi} - \Phi - \frac{1}{2} a^{-2} (\partial\pi)^2 \right) \quad (3.29)$$

$$= \frac{d}{dt} (a v_m^i + \partial_i \pi) + v_m^j \partial_j v_m^i - a^{-2} \partial_j \pi \partial_j \partial_i \pi . \quad (3.30)$$

Any higher order corrections to Eq. (3.30) are relativistic, so in fact this equation is solved by setting $\partial_i \pi = -a v_m^i$ at all orders. Since the velocity is the same, this means that the velocity of the adiabatic mode follows the same Euler equation as the dark-matter field, up to counterterm contributions (which we discuss later).

Now we move on to compute the non-linear corrections to the continuity equation Eq. (3.18). For that, we take the time derivative of the definition of δ_A in Eq. (3.28). In general, there are many terms contributing to δ_A , even at linear level, but we are only interested in the non-relativistic limit. In that limit, we use the linear equations to see that the only non-relativistic term is $M_2^4 \delta g_u^{00} \propto H^{-2} \partial^2 \Phi$ (the rest are proportional to $\dot{\pi}$, π , $\dot{\Phi}$, Φ , etc.), so Eq. (3.28) simplifies to¹²

$$\delta_A = \delta_m - \frac{2}{\bar{\rho}_m} M_2^4 \delta g_u^{00} . \quad (3.32)$$

The equation of motion Eq. (3.24) also simplifies greatly in the non-relativistic limit

$$- \frac{2}{a^3} \partial_t (a^3 M_2^4 \delta g_u^{00}) = -2a^{-2} \partial_i (\partial_i \pi (-c + M_2^4 \delta g_u^{00})) , \quad (3.33)$$

and so we see that the non-linear corrections in the non-relativistic limit enter through δg_u^{00} . Now, taking the time derivative of δ_A in Eq. (3.32)

$$\dot{\delta}_A = \dot{\delta}_m - \frac{2}{\bar{\rho}_{m,0}} \partial_t (a^3 M_2^4 \delta g_u^{00}) \quad (3.34)$$

$$= \dot{\delta}_m - \frac{2}{\bar{\rho}_m} a^{-2} \partial_i (\partial_i \pi (-c + M_2^4 \delta g_u^{00})) \quad (3.35)$$

$$= -\frac{1}{a} \theta_m - \frac{1}{a} \partial_i (\delta_m v_m^i) \quad (3.36)$$

$$+ \frac{2c a^{-2}}{\bar{\rho}_m} \partial^2 \pi - \frac{2}{\bar{\rho}_m} a^{-2} \partial_i (M_2^4 \delta g_u^{00} \partial_i \pi) \quad (3.37)$$

$$= -\frac{1}{a} C(a) \theta_A - \frac{1}{a} \partial_i (\delta_A v_A^i) , \quad (3.38)$$

¹²In the fluid picture, following Eq. (3.12), the non-linear equations lead to a definition of the quintessence overdensity

$$\delta_D = \frac{1+w}{c_s^2} \left(\dot{\pi} - \Phi - \frac{1}{2} a^{-2} (\partial\pi)^2 \right) . \quad (3.31)$$

where we used the non-linear Euler equation for δ_m Eq. (3.3) and the fact that the two species are comoving $\theta_m = -a^{-1}\partial^2\pi \equiv \theta_A$. This, combined with the non-linear Euler equation for the velocity, gives the system at quadratic order for clustering quintessence [72] (apart from counterterms, which we consider in Section 4.2.3)

$$\dot{\delta}_A + \frac{1}{a}C(a)\theta_A = -\frac{1}{a}\partial_i(\delta_A v_A^i) \quad (3.39)$$

$$\dot{\theta}_A + H\theta_A + \frac{3}{2}\frac{\Omega_{m,0}\mathcal{H}_0^2 a_0}{a^2}\delta_A = -\frac{1}{a}\partial_i(v_A^j\partial_j v_A^i) . \quad (3.40)$$

4 Solution for $c_s^2 \rightarrow 0$: clustering quintessence

Up to now, we found the explicit form of the non-linear equations for the adiabatic mode in the presence of clustering quintessence. In this section, we solve these equations up to third order and obtain the density power spectrum up to one-loop order, and we include the one-loop counterterm to correctly describe the dark matter contribution. In this section, we extend (and make a slight correction to) the computation done in [72], by including $\delta_A^{(3)}$, and most importantly, the effects of UV physics through $\delta_A^{(ct)}$. For the one-loop computation that we present in this paper, we find it easier to use the exact perturbative time dependence (i.e. Green's functions), rather than the approximate $\delta^{(n)} \sim D^n$ which is sometimes employed.

From now on, for simplicity, we use δ instead of δ_A and it is more convenient to write the continuity and Euler equations in terms of the rescaled θ which is defined as

$$\Theta \equiv -\frac{C}{\mathcal{H}f_+}\theta, \quad (4.1)$$

where f_{\pm} are the linear growth rate, $f_{\pm} = \frac{d\ln D_{\pm}}{d\ln a}$. Our perturbative expansion for $\delta_{\vec{k}}$ and $\Theta_{\vec{k}}$ (switching notation to $\delta_{\vec{k}}$ instead of $\delta(\vec{k})$ for the Fourier transform) can be written

$$\delta_{\vec{k}}(a) = \sum_{n=1}^{\infty} \delta_{\vec{k}}^{(n)}(a) + \delta_{\vec{k}}^{(ct)}(a) \quad \text{and} \quad \Theta_{\vec{k}}(a) = \sum_{n=1}^{\infty} \Theta_{\vec{k}}^{(n)}(a) + \Theta_{\vec{k}}^{(ct)}(a), \quad (4.2)$$

where $\delta^{(n)}$ are the n -th order solutions in the absence of counterterms, and $\delta^{(ct)}$ is the field sourced by the effective stress tensor and effective force. First, we will ignore the stress tensor, then in Section 4.2.3 we compute the counterterm contribution.

In terms of the above and in Fourier space, equations Eq. (3.39) and Eq. (3.40) read as

$$a\delta'_{\vec{k}} - f_+\Theta_{\vec{k}} = \frac{(2\pi)^3 f_+}{C} \iint \frac{d^3 q_1}{(2\pi)^3} \frac{d^3 q_2}{(2\pi)^3} \delta_D(\vec{k} - \vec{q}_1 - \vec{q}_2) \alpha(\vec{q}_1, \vec{q}_2) \Theta_{\vec{q}_1} \delta_{\vec{q}_2}, \quad (4.3)$$

$$a\Theta'_{\vec{k}} - f_+\Theta_{\vec{k}} - \frac{f_-}{f_+}(\Theta_{\vec{k}} - \delta_{\vec{k}}) = \frac{(2\pi)^3 f_+}{C} \iint \frac{d^3 q_1}{(2\pi)^3} \frac{d^3 q_2}{(2\pi)^3} \delta_D(\vec{k} - \vec{q}_1 - \vec{q}_2) \beta(\vec{q}_1, \vec{q}_2) \Theta_{\vec{q}_1} \Theta_{\vec{q}_2},$$

such that the continuity and Euler equations at the n -th order respectively are

$$a\delta_{\vec{k}}^{(n)'} - f_+ \Theta_{\vec{k}}^{(n)} = \frac{f_+}{C} \sum_{m=1}^{n-1} \int \frac{d^3q}{(2\pi)^3} \alpha(\vec{q}, \vec{k} - \vec{q}) \Theta_{\vec{q}}^{(m)} \delta_{\vec{k}-\vec{q}}^{(n-m)}, \quad (4.4)$$

$$a\Theta_{\vec{k}}^{(n)'} - f_+ \Theta_{\vec{k}}^{(n)} - \frac{f_-}{f_+} (\Theta_{\vec{k}}^{(n)} - \delta_{\vec{k}}^{(n)}) = \frac{f_+}{C} \sum_{m=1}^{n-1} \int \frac{d^3q}{(2\pi)^3} \beta(\vec{q}, \vec{k} - \vec{q}) \Theta_{\vec{q}}^{(m)} \Theta_{\vec{k}-\vec{q}}^{(n-m)}, \quad (4.5)$$

and α and β are given in Eq. (2.33) and Eq. (2.34). In order to determine the density correlation up to one-loop order (without counterterms), we need to determine $\delta_{\vec{k}}^{(1)}$, $\delta_{\vec{k}}^{(2)}$ and $\delta_{\vec{k}}^{(3)}$.

4.1 Linear perturbations

At first order in perturbations, Eq. (4.4) and Eq. (4.5) imply that

$$\delta_{\vec{k}}^{(1)}(a) = \frac{D(a)}{D(a_i)} \delta_{\vec{k}}^{\text{in}} \quad \text{and} \quad \Theta_{\vec{k}}^{(1)}(a) = \delta_{\vec{k}}^{(1)}(a). \quad (4.6)$$

where $\delta_{\vec{k}}^{\text{in}} \equiv \delta_{\vec{k}}(a_i)$ is the initial value of $\delta_{\vec{k}}$ on which we will comment later. The growth function $D(a)$ is given by the following equation

$$\frac{d^2}{d \ln a^2} \left(\frac{D}{H} \right) + \left(2 + 3 \frac{d \ln H}{d \ln a} - \frac{d \ln C}{d \ln a} \right) \frac{d}{d \ln a} \left(\frac{D}{H} \right) = 0, \quad (4.7)$$

where $C(a)$ is

$$C(a) \equiv \left(1 + (1+w) \frac{\Omega_{D,0}}{\Omega_{m,0}} a^{-3w} \right). \quad (4.8)$$

The equation Eq. (4.7) has two solutions, one growing mode [72]

$$D_+(a) = \frac{5}{2} \int_0^a C(\tilde{a}) \Omega_m(\tilde{a}) \frac{H(a)}{H(\tilde{a})} d\tilde{a}, \quad (4.9)$$

and a decaying mode which is

$$D_-(a) = \frac{H(a)}{H_0 \Omega_{m,0}^{1/2}}, \quad (4.10)$$

where H_0 is the current value of the Hubble parameter. We find it convenient to define the time dependent energy density ratios

$$\Omega_m(a) \equiv \Omega_{m,0} \frac{H_0^2}{H(a)^2} \left(\frac{a}{a_0} \right)^{-3}, \quad \Omega_D(a) \equiv \Omega_{D,0} \frac{H_0^2}{H(a)^2} \left(\frac{a}{a_0} \right)^{-3(1+w)}. \quad (4.11)$$

The linear growth indices $f_{\pm} \equiv \frac{d \ln D_{\pm}}{d \ln a}$ are given as

$$f_+(a) = \left(\frac{5}{2} \frac{a}{D_+(a)} - \frac{3}{2} \Omega_m(a) \right) C(a), \quad (4.12)$$

and

$$f_-(a) = -\frac{3}{2} \Omega_m(a) C(a). \quad (4.13)$$

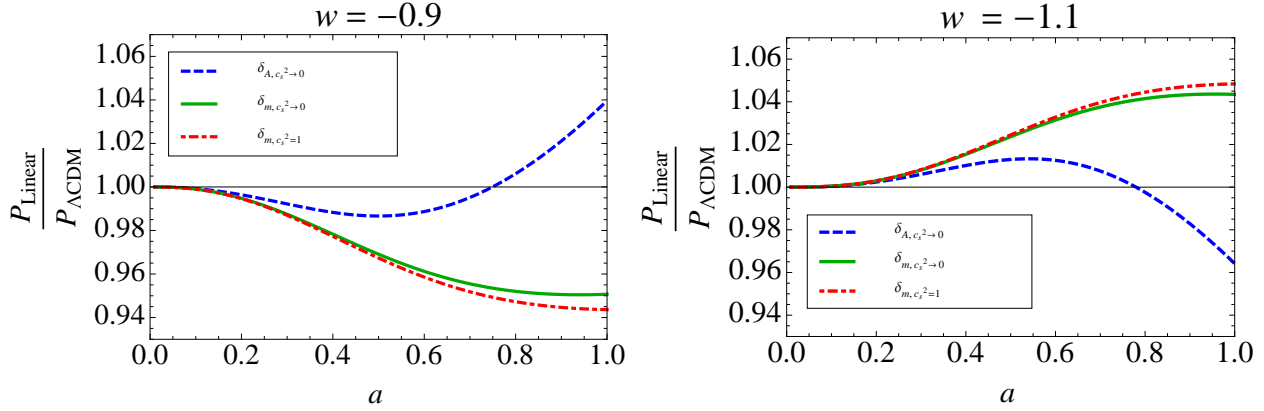


Figure 1: In these plots, we compare various linear power spectra to the linear power spectrum in Λ CDM. The dashed (blue) and solid (green) lines correspond to the power spectrum of δ_A and δ_m in the clustering quintessence model respectively. The dot-dashed (red) line represents the power spectrum of δ_m in w CDM (smooth dark energy, described in Appendix D). In the left panel, $w = -0.9$ and in the right panel $w = -1.1$. As we see, the power spectrum in the clustering and w CDM models are almost the same for redshifts $a < 0.3$, while they start to diverge as we approach the present time. Interestingly, $\delta_{m, c_s^2 \rightarrow 0}$ in the clustering case remains close to its corresponding quantity in the smooth case, $\delta_{m, c_s^2 = 1}$. This means that the effect of the clustering quintessence *on matter* is small. However, the total density contrast, $\delta_{A, c_s^2 \rightarrow 0}$ in the clustering case is noticeably different from δ_m in the clustering and smooth dark energy.

During the matter era where $\frac{\Omega_D(a)}{\Omega_m(a)}$ is negligible and $C(a) \simeq 1$, the growth functions are approximately equal to their corresponding value in the exact Λ CDM model

$$D_+(a) \simeq a \quad \text{and} \quad D_-(a) \simeq a^{-\frac{3}{2}}, \quad (4.14)$$

and in the same limit, the growth indices are reduced to $f_+ \simeq 1$ and $f_- \simeq -\frac{3}{2}$. However, as we approach the dark energy era, the linear solutions deviate from Λ CDM and depending on the sign of $(1+w)$, they have different behaviors. In Figure 1, we show the linear behavior of the power spectra of $\delta_{A, c_s^2 \rightarrow 0}$ (the adiabatic mode in clustering quintessence), $\delta_{m, c_s^2 \rightarrow 0}$ (the matter field in clustering quintessence), and $\delta_{m, c_s^2 = 1}$ (the matter field in the presence of smooth dark energy, described in Appendix D) compared to Λ CDM. We see that $\delta_{m, c_s^2 = 1}$ is very close to $\delta_{m, c_s^2 \rightarrow 0}$, which means that clustering quintessence fluctuations have only a small effect on the matter power spectrum (the overall deviation from Λ CDM is due to the different background expansion, which is the dominant effect of non-clustering quintessence). The dominant effect of clustering quintessence fluctuations is the way that they change the adiabatic power spectrum, which is an effect of order $1+w$ compared to the smooth case at $a = 1$ (note that $\delta_{A, c_s^2 = 1} \approx \delta_{m, c_s^2 = 1}$).

Before going any further, let us take a brief moment to comment on the initial conditions. During matter domination at sufficiently early times, the linear equations are valid, and we have $\delta_m(a, \vec{k}) = \frac{a}{a_i} \delta_m(a_i, \vec{k})$, where a_i is the time at which we set the initial conditions. Using the linear

continuity equations for δ_m and the adiabatic mode δ , we have that $\delta'_m = \delta'/C(a)$ which gives¹³ [19]

$$\delta_{\vec{k}}^{\text{in}} = \left(1 + \frac{1+w}{1-3w} \frac{\Omega_{D,0}}{\Omega_{m,0}} \left(\frac{a_i}{a_0} \right)^{-3w} \right) \delta_m^{(1)}(a_i, \vec{k}). \quad (4.15)$$

The initial power spectrum for $\delta_m^{(1)}$ can be gotten from CAMB, but we must keep in mind two subtleties. The first is that the above expression is only valid in the matter era, so we must set the initial conditions at a time early enough so that we are in the matter era. For this, we want $\Omega_{D,0}a^{-3(1+w)}/(\Omega_{m,0}a^{-3}) \ll 1$, or more specifically, $D_+(a)/a \approx 1$. For example, with $w = -0.9$, at $a = 0.167$, $\Omega_{D,0}a^{-3(1+w)}/(\Omega_{m,0}a^{-3}) = 0.021$, and $D_+(a)/a = 0.996$, which is well within the matter era. On the other hand, we need to be at a late enough time such that the linear growth rate D_+ accurately describes the growth of structure. At early times, when the effects of radiation are still present, our equations are incomplete (see [77] for a discussion of radiation effects in the bispectrum). Because of this, we choose to implement the initial conditions at $a = 0.167$. Here, the difference between the linear evolution from $a = 0.167$ to $a = a_0$ with CAMB and the linear evolution with D_+^2 of the power spectrum is 0.2%, well within our computational precision. Alternatively, and specifically for more general dark-matter actions, one could use one of the recently developed linear codes for the EFT of dark energy [25, 29, 78, 79].

4.2 Non-linear perturbations

In this subsection, we present the solutions for the higher order fields $\delta^{(2)}$ and $\delta^{(3)}$, and for the counterterm contribution $\delta^{(ct)}$. The non-linear continuity and Euler equations can be solved perturbatively in terms of four Green's functions. In particular, one can write $\delta_{\vec{k}}^{(n)}(a)$ and $\Theta_{\vec{k}}^{(n)}(a)$ at any perturbative order as

$$\delta_{\vec{k}}^{(n)} = \int_0^a d\tilde{a} \left(G_1^\delta(a, \tilde{a}) S_1^{(n)}(\tilde{a}, \vec{k}) + G_2^\delta(a, \tilde{a}) S_2^{(n)}(\tilde{a}, \vec{k}) \right), \quad (4.16)$$

$$\Theta_{\vec{k}}^{(n)} = \int_0^a d\tilde{a} \left(G_1^\Theta(a, \tilde{a}) S_1^{(n)}(\tilde{a}, \vec{k}) + G_2^\Theta(a, \tilde{a}) S_2^{(n)}(\tilde{a}, \vec{k}) \right), \quad (4.17)$$

where G_1^δ, G_2^δ are the density Green's functions, G_1^Θ, G_2^Θ are velocity Green's functions and $S_1^{(n)}(\tilde{a}, \vec{k})$ and $S_2^{(n)}(\tilde{a}, \vec{k})$ are the source terms of the continuity and Euler equations at the n -th order respectively. Here we only report the final solutions and we present the details of the calculations and the explicit form of the source terms in Appendix C.

Having the formal solutions Eq. (4.16) and Eq. (4.17), we can find the solutions of δ and Θ at any perturbative order. Since we are interested in the one-loop power spectrum, next, we calculate the second and third order perturbations.

¹³As an alternative approach, we solve the linear π equations during matter era directly in Appendix B and read δ in terms of δ_m in Eq. (B.35).

4.2.1 Second-order perturbations

At second order in the perturbations, using the linear solution in Eq. (4.6) along with the expression for the second-order source term in Eq. (C.3), we find the source terms

$$S_1^{(2)}(a, \vec{k}) = \frac{f_+(a)D_+^2(a)}{C(a)D_+^2(a_i)} \int \frac{d^3q}{(2\pi)^3} \alpha_s(\vec{q}, \vec{k} - \vec{q}) \delta_{\vec{q}}^{\text{in}} \delta_{\vec{k}-\vec{q}}^{\text{in}}, \quad (4.18)$$

$$S_2^{(2)}(a, \vec{k}) = \frac{f_+(a)D_+^2(a)}{C(a)D_+(a_i)} \int \frac{d^3q}{(2\pi)^3} \beta(\vec{q}, \vec{k} - \vec{q}) \delta_{\vec{q}}^{\text{in}} \delta_{\vec{k}-\vec{q}}^{\text{in}}, \quad (4.19)$$

where $\alpha_s(\vec{q}_1, \vec{q}_2) = \frac{1}{2}(\alpha(\vec{q}_1, \vec{q}_2) + \alpha(\vec{q}_2, \vec{q}_1))$, and α and β are given in Eq. (2.33) and Eq. (2.34). After plugging the above in the solutions Eq. (4.16) and Eq. (4.17), we have¹⁴

$$\delta_{\vec{k}}^{(2)}(a) = \int \frac{d^3q}{(2\pi)^3} \left(\alpha_s(\vec{q}, \vec{k} - \vec{q}) \mathcal{G}_1^\delta(a) + \beta(\vec{q}, \vec{k} - \vec{q}) \mathcal{G}_2^\delta(a) \right) \delta_{\vec{q}}^{\text{in}} \delta_{\vec{k}-\vec{q}}^{\text{in}}, \quad (4.20)$$

$$\Theta_{\vec{k}}^{(2)}(a) = \int \frac{d^3q}{(2\pi)^3} \left(\alpha_s(\vec{q}, \vec{k} - \vec{q}) \mathcal{G}_1^\Theta(a) + \beta(\vec{q}, \vec{k} - \vec{q}) \mathcal{G}_2^\Theta(a) \right) \delta_{\vec{q}}^{\text{in}} \delta_{\vec{k}-\vec{q}}^{\text{in}}. \quad (4.21)$$

where \mathcal{G}_1^δ , \mathcal{G}_2^δ , \mathcal{G}_1^Θ and \mathcal{G}_2^Θ are four functions of time given as

$$\mathcal{G}_\sigma^\delta(a) = \int_0^1 \frac{f_+(\tilde{a})D_+^2(\tilde{a})}{C(\tilde{a})D_+^2(a_i)} G_\sigma^\delta(a, \tilde{a}) d\tilde{a}, \quad (4.22)$$

$$\mathcal{G}_\sigma^\Theta(a) = \int_0^1 \frac{f_+(\tilde{a})D_+^2(\tilde{a})}{C(\tilde{a})D_+^2(a_i)} G_\sigma^\Theta(a, \tilde{a}) d\tilde{a}, \quad (4.23)$$

for $\sigma = 1, 2$. Notice that, because the Green's functions depend only on time, the momentum and time integrals separate. This means that at all orders in perturbation theory, each loop can be written as a sum over terms which are a product of a function of momentum times a function of time, which greatly reduces computational time. Deep inside the matter era, where we can neglect the effect of dark energy, the above time functions are simply $\mathcal{G}_1^\delta(a) \simeq \frac{5}{7} \left(\frac{D_+(a)}{D_+(a_i)} \right)^2$, $\mathcal{G}_2^\delta(a) \simeq \frac{2}{7} \left(\frac{D_+(a)}{D_+(a_i)} \right)^2$, $\mathcal{G}_1^\Theta(a) \simeq \frac{3}{7} \left(\frac{D_+(a)}{D_+(a_i)} \right)^2$ and $\mathcal{G}_2^\Theta(a) \simeq \frac{4}{7} \left(\frac{D_+(a)}{D_+(a_i)} \right)^2$.

4.2.2 Third-order perturbations

The third-order source terms (derived in Eq. (C.22)) are

$$S_1^{(3)}(a, \vec{k}) = \frac{f_+(a)D_+(a)}{C(a)D_+(a_i)} \iint \frac{d^3p}{(2\pi)^3} \frac{d^3q}{(2\pi)^3} \left(\alpha^\sigma(\vec{k}, \vec{p}, \vec{q}) \mathcal{G}_\sigma^\delta(a) + \gamma^\sigma(\vec{k}, \vec{p}, \vec{q}) \mathcal{G}_\sigma^\Theta(a) \right) \delta_{\vec{k}-\vec{p}}^{\text{in}} \delta_{\vec{p}-\vec{q}}^{\text{in}} \delta_{\vec{q}}^{\text{in}},$$

$$S_2^{(3)}(a, \vec{k}) = \frac{f_+(a)D_+(a)}{C(a)D_+(a_i)} \iint \frac{d^3p}{(2\pi)^3} \frac{d^3q}{(2\pi)^3} \beta^\sigma(\vec{k}, \vec{p}, \vec{q}) \mathcal{G}_\sigma^\Theta(a) \delta_{\vec{k}-\vec{p}}^{\text{in}} \delta_{\vec{p}-\vec{q}}^{\text{in}} \delta_{\vec{q}}^{\text{in}}, \quad (4.24)$$

¹⁴Our expressions for the second order fields differ from the analogous expressions in [72]. In fact, one can quickly check that the solutions Eq. (73) and Eq. (74) of [72] are not related by the equation of motion Eq. (71) in that paper. Inside of the parentheses of Eq. (74) of [72], the coefficient of $(2\alpha_s - 2\beta)/5$ should be $e^{\bar{\eta}-\eta} \partial_\eta D_-(\eta)/D_-(\bar{\eta})$. Then, the boundary conditions of the Green's functions should be set without changing the relative coefficients of the terms inside of the parentheses.

where again $\sigma = 1, 2$ and summation over upper and lower indices is assumed. Note that here, $\{\alpha^\sigma, \beta^\sigma, \gamma^\sigma\}$ are six functions of momenta made of the standard functions from dark-matter perturbation theory $\alpha(\vec{k}_1, \vec{k}_2)$ and $\beta(\vec{k}_1, \vec{k}_2)$ which we present in Eq. (C.14) - Eq. (C.19).

From the combination of Eq. (4.16) and Eq. (4.24), we find $\delta_{\vec{k}}^{(3)}$ and $\Theta_{\vec{k}}^{(3)}$ as

$$\delta_{\vec{k}}^{(3)}(a) = \iint \frac{d^3p}{(2\pi)^3} \frac{d^3q}{(2\pi)^3} \left(\alpha^\sigma(\vec{k}, \vec{p}, \vec{q}) \mathcal{U}_\sigma^\delta(a) + \beta^\sigma(\vec{k}, \vec{p}, \vec{q}) \mathcal{V}_{\sigma 2}^\delta(a) \right. \\ \left. + \gamma^\sigma(\vec{k}, \vec{p}, \vec{q}) \mathcal{V}_{\sigma 1}^\delta(a) \right) \delta_{\vec{k}-\vec{p}}^{\text{in}} \delta_{\vec{p}-\vec{q}}^{\text{in}} \delta_{\vec{q}}^{\text{in}}, \quad (4.25)$$

$$\Theta_{\vec{k}}^{(3)}(a) = \iint \frac{d^3p}{(2\pi)^3} \frac{d^3q}{(2\pi)^3} \left(\alpha^\sigma(\vec{k}, \vec{p}, \vec{q}) \mathcal{U}_\sigma^\Theta(a) + \beta^\sigma(\vec{k}, \vec{p}, \vec{q}) \mathcal{V}_{\sigma 2}^\Theta(a) \right. \\ \left. + \gamma^\sigma(\vec{k}, \vec{p}, \vec{q}) \mathcal{V}_{\sigma 1}^\Theta(a) \right) \delta_{\vec{k}-\vec{p}}^{\text{in}} \delta_{\vec{p}-\vec{q}}^{\text{in}} \delta_{\vec{q}}^{\text{in}}, \quad (4.26)$$

where $\mathcal{U}_\sigma^\delta(a)$, $\mathcal{V}_{\sigma\bar{\sigma}}^\delta(a)$, $\mathcal{U}_\sigma^\Theta(a)$ and $\mathcal{V}_{\sigma\bar{\sigma}}^\Theta(a)$ are functions of time given as

$$\mathcal{U}_\sigma^\delta(a) = \int_0^1 \frac{f_+(\tilde{a}) D_+(\tilde{a})}{C(\tilde{a}) D_+(a_i)} \mathcal{G}_\sigma^\delta(\tilde{a}) G_1^\delta(a, \tilde{a}) d\tilde{a}, \quad (4.27)$$

$$\mathcal{U}_\sigma^\Theta(a) = \int_0^1 \frac{f_+(\tilde{a}) D_+(\tilde{a})}{C(\tilde{a}) D_+(a_i)} \mathcal{G}_\sigma^\Theta(\tilde{a}) G_1^\Theta(a, \tilde{a}) d\tilde{a}, \quad (4.28)$$

$$\mathcal{V}_{\sigma\bar{\sigma}}^\delta(a) = \int_0^1 \frac{f_+(\tilde{a}) D_+(\tilde{a})}{C(\tilde{a}) D_+(a_i)} \mathcal{G}_\sigma^\Theta(\tilde{a}) G_{\bar{\sigma}}^\delta(a, \tilde{a}) d\tilde{a}, \quad (4.29)$$

$$\mathcal{V}_{\sigma\bar{\sigma}}^\Theta(a) = \int_0^1 \frac{f_+(\tilde{a}) D_+(\tilde{a})}{C(\tilde{a}) D_+(a_i)} \mathcal{G}_\sigma^\Theta(\tilde{a}) G_{\bar{\sigma}}^\Theta(a, \tilde{a}) d\tilde{a}. \quad (4.30)$$

During the matter era when dark energy is negligible, the above time functions are proportional to $D_+^3(a)$. Some examples are $\mathcal{U}_1^\delta(a) \simeq \frac{5}{18} \left(\frac{D_+(a)}{D_+(a_i)}\right)^3$, $\mathcal{U}_2^\delta(a) \simeq \frac{1}{9} \left(\frac{D_+(a)}{D_+(a_i)}\right)^3$, $\mathcal{U}_1^\Theta(a) \simeq \frac{5}{42} \left(\frac{D_+(a)}{D_+(a_i)}\right)^3$, $\mathcal{U}_2^\Theta(a) \simeq \frac{1}{21} \left(\frac{D_+(a)}{D_+(a_i)}\right)^3$, $\mathcal{V}_{11}^\delta(a) \simeq \frac{1}{6} \left(\frac{D_+(a)}{D_+(a_i)}\right)^3$, and $\mathcal{V}_{12}^\delta(a) \simeq \frac{1}{21} \left(\frac{D_+(a)}{D_+(a_i)}\right)^3$.

4.2.3 Counterterms

Our approach to dealing with the counterterms will be to first work in the basis of δ_m and π , and then find the contribution to the δ_A equations. First, let us consider the response of dark matter to gravitational non-linearities; we will have to include an explicit counterterm to describe how the UV physics of dark-energy affects the large scale dark-matter field. In general, the expansion of the dark-matter stress tensor and force term will take a form analogous to the two fluid case in [44]

$$-\left(\frac{1}{\rho_m} \partial_j \tau^{ij}\right)_s(a, \vec{x}) + \gamma_s^i(a, \vec{x}) = \quad (4.31) \\ \int da' \left[\kappa^{(1)}(a, a') \partial^i \partial^2 \Phi(a', \vec{x}_\text{fl}(\vec{x}; a, a')) + \kappa^{(2)}(a, a') \frac{1}{H} \partial^i \partial_j v_m^j(a', \vec{x}_\text{fl}(\vec{x}; a, a')) \right. \\ \left. + \kappa_1^{(\text{stoch.})}(a, a') \bar{\Delta}_{\text{stoch.}}^i(a', \vec{x}_\text{fl}(\vec{x}; a, a')) \dots \right].$$

Notice that we do not include a direct coupling like $\partial^i \partial_j \partial^j \pi \sim \partial^i \partial_j v_D^j$ because the two species interact only through gravity, which means that when gravity is turned off, dark matter should not

feel a response from dark energy. As discussed in [44], the relative velocity, $v_{\text{rel}}^i \equiv v_m^i - \partial^i \pi$, can appear with no derivatives. For the case that we study in this paper, the species are comoving, so $v_{\text{rel}}^i = 0$. The stochastic term $\bar{\Delta}_{\text{stoch.}}^i$ is now different from the pure dark matter case considered in Section 2.2 because of the effective force $\gamma_s^i(a, \vec{x})$. In the dark-matter only case, the stochastic contribution to the power spectrum goes like k^4 because of momentum conservation. However, in the case of two species which can exchange momentum, momentum is not conserved separately in each species, so the contribution to the power spectrum can go like k^2 . In particular, we expect the stochastic part of γ_s^i to be Poisson-like so that in momentum space we can have

$$\langle \Delta_{\text{stoch.}}^i(\vec{k}) \Delta_{\text{stoch.}}^j(\vec{k}') \rangle = \frac{(2\pi)^3}{k_{\text{NL}}^3} \delta(\vec{k} + \vec{k}') C^{(1)} \delta^{ij} + \dots, \quad (4.32)$$

where $C^{(1)}$ is expected to be an order one number, and \dots stands for terms higher order in k/k_{NL} . To get the contribution to the power spectrum, we contract the above with $k_i k_j$, and so we have a k^2 contribution. However, as discussed in [44], this is expected to be subleading with respect to the counterterm contribution $k^2 P(k)$, so we will not study these operators in this paper.¹⁵

Thus, evaluating the counterterms Eq. (4.31) on the linear solutions and performing the a' integral as usual, we are led to the following counterterm on the right-hand side of the Euler equation for dark matter Eq. (2.32):

$$9(2\pi) H(a)^2 \frac{k^2}{k_{\text{NL}}^2} \left(c_{s,\delta}^2(a) \delta_{\vec{k}}(a) + c_{s,v_m}^2(a) \frac{1}{H} \theta_{m,\vec{k}}(a) \right), \quad (4.33)$$

which after using the linear equations of motion, and the fact that the species are comoving at linear order, becomes

$$9(2\pi) H(a)^2 \frac{k^2}{k_{\text{NL}}^2} \left(c_{s,\delta}^2(a) \delta_{\vec{k}}^{(1)}(a) - c_{s,v_m}^2(a) \frac{a^2}{C(a)} \delta_{\vec{k}}^{(1)}(a)' \right) \quad (4.34)$$

$$= 9(2\pi) H(a)^2 \frac{k^2}{k_{\text{NL}}^2} c_{A,m}^2(a) \delta_{\vec{k}}^{(1)}(a). \quad (4.35)$$

where $c_{A,m}^2(a) = \left(c_{s,\delta}^2(a) - c_{s,v_m}^2(a) \frac{a^2 D'_+(a)}{D_+(a) C(a)} \right)$. As the name suggests, $c_{A,m}^2$ is the contribution to the speed of sound of the adiabatic mode from the matter sector.

Next, we move on to the dark-energy sector.¹⁶ Although it is perfectly consistent to have $|c_s^2| \ll \bar{c}_m^2$ (which must be true if $w < -1$), we can also consider the case that $c_s^2 \approx \bar{c}_m^2$ and perturbatively find the effects of a small but non-zero c_s^2 . When $c_s^2 \neq 0$, the two species are not

¹⁵ Stochastic terms can also be included in the Lagrangian for the dark-energy degree of freedom by coupling π to a dissipative sector through terms like $\mathcal{O} \delta g_u^{00}$, where \mathcal{O} is some composite operator of the dissipative sector [80]. However, as in the dark-matter sector, we expect these effects to be small for the one-loop computation that we perform, so we ignore them in this work.

¹⁶ In the dark-energy sector, it is worth checking that the quantum unitarity cutoff for the dark-energy action can be near or above the non-linear scale for dark matter, k_{NL} . In the small c_s^2 limit, the EFT for dark-energy will eventually become strongly coupled, bringing the cutoff down to smaller momentum. Thus, we need to make sure that a cutoff near k_{NL} and a small c_s^2 are not contradictory assumptions. From [18, 81], we know that the cutoff for the dark-energy sector is $\Lambda_U^4 \simeq 16\pi^2 M_2^4 c_s^7$. In the small c_s^2 limit, we have that $M_2^4 \approx \bar{\rho}_D(1+w)/(4c_s^2)$, and at the current time we have $\bar{\rho}_D \approx 3H^2 M_{\text{pl}}^2$, so we can write the cutoff as

comoving, and one would expect to have to solve the full system for both degrees of freedom δ_m and π , even at linear level. However, we can get away with solving for just the adiabatic mode δ by considering this new feature perturbatively. We start with the following equations for $\delta^{(ct)}$ sourced by $\delta^{(1)}$ in Fourier space (we suppress the \vec{k} argument because it is the same on all fields)

$$\mathcal{H}\delta^{(ct)'} + \frac{1}{a}\theta_m^{(ct)} + \frac{1}{a}(1+w)\frac{\Omega_{D,0}}{\Omega_{m,0}}\left(\frac{a}{a_0}\right)^{-3w}a^{-1}k^2\pi^{(ct)} = 0 \quad (4.38)$$

$$a\mathcal{H}\theta_m^{(ct)'} + \mathcal{H}\theta_m^{(ct)} - k^2\Phi^{(ct)} = 9(2\pi)H(a)^2\frac{k^2}{k_{\text{NL}}^2}c_{A,m}^2(a)\delta^{(1)} \quad (4.39)$$

$$\mathcal{H}\frac{d}{da}\left(a^3M_2^4\left(\mathcal{H}\pi^{(ct)'} - \Phi^{(ct)}\right)\right) = -c_s^2a^3M_2^4a^{-2}k^2\pi^{(1)}, \quad (4.40)$$

where we have left off some relativistic terms proportional to c_s^2 in Eq. (4.38). Since we will need an explicit form for $-k^2\pi^{(ct)}$ to plug into Eq. (4.38), we integrate Eq. (4.40) with respect to a one time and take ∂^2 to obtain¹⁷

$$-\mathcal{H}k^2\pi^{(ct)'} + k^2\Phi^{(ct)} = \frac{c_s^2}{a^3M_2^4}\int^a d\tilde{a}\frac{\tilde{a}^3M_2^4(\tilde{a})}{\mathcal{H}(\tilde{a})}\tilde{a}^{-2}k^4\pi^{(1)}(\tilde{a}) \quad (4.42)$$

$$= 9(2\pi)H^2(a)c_s^2f_1(a)\frac{k^2}{k_{\text{NL},D}^2}\delta^{(1)}(a), \quad (4.43)$$

where we have written the correction in terms of the non-linear scale in the dark-matter sector $k_{\text{NL},D}$, which in general could be different from the non-linear scale for dark matter k_{NL} , but as shown in Eq. (3.20) it is expected to be comparable. However, for the rest of this paper, we will assume $k_{\text{NL},D} = k_{\text{NL}}$ for simplicity. Next, add Eq. (4.43) to Eq. (4.39) and integrate the result with

$\Lambda_U^4 = 12\pi^2H^2M_{\text{Pl}}^2(1+w)c_s^5$. Now, imposing that $\Lambda_U \gtrsim \alpha c_s k_{\text{NL}}$, we find that

$$|c_s| \gtrsim \frac{\alpha^4}{12\pi^2|1+w|}\left(\frac{k_{\text{NL}}}{H}\right)^4\left(\frac{H}{M_{\text{Pl}}}\right)^2, \quad (4.36)$$

or in terms of the dark matter speed of sound $\bar{c}_m^2 \sim H^2/k_{\text{NL}}^2$ we have

$$|c_s| \gtrsim \frac{\alpha^4}{12\pi^2|1+w|}\frac{1}{\bar{c}_m^4}\left(\frac{H}{M_{\text{Pl}}}\right)^2. \quad (4.37)$$

Using $\bar{c}_m \sim 10^{-3}$ and $H/M_{\text{Pl}} \sim 10^{-60}$ today, the above constraint becomes $|c_s| \gtrsim \alpha^4 10^{-110}/|1+w|$. If c_s^2 does not satisfy this, then the effective field theory would not be valid for computing at the non-linear scale. Taking a hypothetical value of $c_s^2 \sim \bar{c}_m^2$, we see that the unitarity cutoff Λ_U will be much higher than k_{NL} . This does not mean, however, that the non-linear scale determined by gravitational non-linearities in the dark-energy sector, $k_{\text{NL},D}$, will be so high: Λ_U is the scale at which quantum fluctuations make the system strongly coupled, and $k_{\text{NL},D}$ is the scale at which the non-linear couplings in the classical equations of motion become important.

¹⁷Here, we have used the linear equations $a^{-1}k^2\pi^{(1)} = \theta_m^{(1)} = -a\mathcal{H}\delta^{(1)'} / C(a)$, and defined

$$f_1(a) = \frac{-k_{\text{NL},D}^2}{9(2\pi)H^2(a)}\frac{1}{a^3M_2^4(a)}\int^a d\tilde{a}\frac{\tilde{a}^3M_2^4(\tilde{a})}{C(\tilde{a})}\frac{D'_+(\tilde{a})}{D_+(\tilde{a})}. \quad (4.41)$$

respect to a to obtain¹⁸

$$a\theta_m^{(ct)} - k^2\pi^{(ct)} = -9(2\pi)H(a)c_1^2(a)\frac{k^2}{k_{\text{NL}}^2}\delta^{(1)}(a), \quad (4.45)$$

which gives the deviation of the dark energy from the dark-matter trajectories. In a sense, this generates an isocurvature mode, as the two species no longer move together. Next, use Eq. (4.45) to replace $-k^2\pi^{(ct)}$ in Eq. (4.38), then take the time derivative of that and use Eq. (4.39) to replace $\mathcal{H}\partial_a(a\theta_m^{(ct)})$ to finally obtain¹⁹

$$-\mathcal{H}(a)\frac{d}{da}\left(\frac{a^2\mathcal{H}(a)}{C(a)}\frac{d\delta^{(ct)}}{da}\right) + \frac{3}{2}\frac{\Omega_{m,0}\mathcal{H}_0^2a_0}{a}\delta^{(ct)} = 9(2\pi)H(a)^2c_A^2(a)\frac{k^2}{k_{\text{NL}}^2}\delta^{(1)}. \quad (4.48)$$

Notice that the linear differential operator on the left-hand side is indeed the same as the one for the adiabatic mode in Eq. (4.7). Analogous to Eq. (2.43), we can use the Green's function of Eq. (4.48) to define the speed of sound $\bar{c}_A^2(a)$ that enters the power spectrum²⁰

$$\delta_k^{(ct)}(a) = -(2\pi)\bar{c}_A^2(a)\frac{k^2}{k_{\text{NL}}^2}\frac{D_+(a)}{D_+(a_i)}\delta_k^{\text{in}}. \quad (4.51)$$

Thus, we see that at one-loop, both c_s^2 and $c_{A,m}^2$ contribute to the power spectrum with the same functional dependence. Thus, even if c_s^2 is comparable to $c_{A,m}^2$, the effect is automatically included in \bar{c}_A^2 .

Of course, in this discussion we have neglected the initial isocurvature mode, which however is expected to be extremely small. In any case, its inclusion in the formalism and the calculations is straightforward, as it is identical to including the initial isocurvature mode for baryons (which is larger), as done in [44].

¹⁸We have defined

$$c_1^2(a) = \frac{-1}{H(a)}\int^a d\tilde{a}\frac{H(\tilde{a})^2}{\mathcal{H}(\tilde{a})}(c_{A,m}^2(\tilde{a}) + c_s^2f_1(\tilde{a}))\frac{D_+(\tilde{a})}{D_+(a)}. \quad (4.44)$$

¹⁹Again, we make some definitions

$$c_A^2(a) = c_{A,m}^2(a) + (1+w)\frac{\Omega_{D,0}}{\Omega_{m,0}}\left(\frac{a}{a_0}\right)^{-3w}c_{A,2}^2(a) \quad (4.46)$$

$$c_{A,2}^2(a) = \mathcal{H}(a)(H(a)^2D_+(a)a^{-3w})^{-1}\frac{d}{da}\left(\frac{H(a)a^{-3w}c_1^2(a)D_+(a)}{C(a)}\right). \quad (4.47)$$

²⁰Analogous to Eq. (2.43), we define

$$\bar{c}_A^2(a) = \int^a d\tilde{a}G_+(a,\tilde{a})\frac{D_+(\tilde{a})}{D_+(a)}9H(\tilde{a})^2c_A^2(\tilde{a}), \quad (4.49)$$

where G_+ is the retarded Green's function for the linear equation

$$\begin{aligned} -\mathcal{H}(a)\frac{d}{da}\left(\frac{a^2\mathcal{H}(a)}{C(a)}\frac{dG_+(a,\tilde{a})}{da}\right) + \frac{3}{2}\frac{\Omega_{m,0}\mathcal{H}_0^2a_0}{a}G_+(a,\tilde{a}) &= \delta_D^{(1)}(a-\tilde{a}), \\ G_+(a,a) = 0, \quad \partial_a G_+(a,\tilde{a})|_{a=\tilde{a}} &= \frac{C(\tilde{a})}{\tilde{a}^2\mathcal{H}(\tilde{a})^2}. \end{aligned} \quad (4.50)$$

4.3 Power spectrum

Up to now, we worked out the total density up to third order, including the counterterm contribution. Now, we use this result to determine the adiabatic power spectrum in the presence of the dark energy up to one-loop order. The equal-time power spectrum is defined in terms of the density variance as

$$\langle \delta_{\vec{k}}(a) \delta_{\vec{k}'}(a) \rangle = (2\pi)^3 \delta_D(\vec{k} + \vec{k}') P(a, k) . \quad (4.52)$$

Using the perturbative expansion of the field in Eq. (4.2), and assuming Gaussian initial conditions,²¹ we can write

$$P(a, k) = P_{11}(a, k) + P_{22}(a, k) + P_{13}(a, k) + P_{13}^{ct}(a, k) + \dots \quad (4.53)$$

where the various contributions are given by

$$\langle \delta_{\vec{k}}^{(1)}(a) \delta_{\vec{k}'}^{(1)}(a) \rangle' = P_{11}(a, k) \quad (4.54)$$

$$\langle \delta_{\vec{k}}^{(2)}(a) \delta_{\vec{k}'}^{(2)}(a) \rangle' = P_{22}(a, k) \quad (4.55)$$

$$2 \langle \delta_{\vec{k}}^{(1)}(a) \delta_{\vec{k}'}^{(3)}(a) \rangle' = P_{13}(a, k) \quad (4.56)$$

$$2 \langle \delta_{\vec{k}}^{(1)}(a) \delta_{\vec{k}'}^{(ct)}(a) \rangle' = P_{13}^{ct}(a, k) , \quad (4.57)$$

and $\langle \dots \rangle'$ means that we have removed a factor of $(2\pi)^3 \delta_D(\vec{k} + \vec{k}')$ from the expectation value. In particular, on the initial conditions, this means that $\langle \delta_{\vec{k}}^{\text{in}} \delta_{\vec{k}'}^{\text{in}} \rangle' = P_{\vec{k}}^{\text{in}}$.

Then, using the linear solution Eq. (4.6), the second-order solution Eq. (4.20), the third-order solution Eq. (4.25), and the counterterm solution Eq. (4.51), we have the following expressions for the power spectrum contributions

$$P_{11}(a, k) = \frac{D_+^2(a)}{D_+^2(a_i)} P_{\vec{k}}^{\text{in}}, \quad (4.58)$$

$$P_{22}(a, k) = 2 \int \frac{d^3 q}{(2\pi)^3} \left(\alpha_s(\vec{q}, \vec{k} - \vec{q}) \mathcal{G}_1^\delta(a) + \beta(\vec{q}, \vec{k} - \vec{q}) \mathcal{G}_2^\delta(a) \right)^2 P_{\vec{k}-\vec{q}}^{\text{in}} P_{\vec{q}}^{\text{in}}, \quad (4.59)$$

$$P_{13}(a, k) = 4 \frac{D_+(a)}{D_+(a_i)} P_{\vec{k}}^{\text{in}} \int \frac{d^3 q}{(2\pi)^3} \left(\alpha^\sigma(\vec{k}, \vec{k} + \vec{q}, \vec{k}) \mathcal{U}_\sigma^\delta(a) + \beta^\sigma(\vec{k}, \vec{k} + \vec{q}, \vec{k}) \mathcal{V}_{\sigma 2}^\delta(a) \right. \\ \left. + \gamma^\sigma(\vec{k}, \vec{k} + \vec{q}, \vec{k}) \mathcal{V}_{\sigma 1}^\delta(a) \right) P_{\vec{q}}^{\text{in}}, \quad (4.60)$$

$$P_{13}^{ct}(a, k) = -2 (2\pi) \bar{c}_A^2(a) \frac{k^2}{k_{\text{NL}}^2} \left(\frac{D_+(a)}{D_+(a_i)} \right)^2 P_{\vec{k}}^{\text{in}} . \quad (4.61)$$

We can also write the one-loop contributions in a more compact form. P_{22} can be written as

$$P_{22}(a, k) = 2 \left(\mathcal{A}^{\sigma\bar{\sigma}}(k) \mathcal{G}_\sigma^\delta(a) \mathcal{G}_{\bar{\sigma}}^\delta(a) \right), \quad (4.62)$$

²¹Here, we restrict to Gaussian initial conditions, although it is straightforward to extend to non-Gaussian initial conditions [47, 49, 57].

where the symmetric momentum matrix $\mathcal{A}^{\sigma\bar{\sigma}}(k)$ is given as

$$\mathcal{A}^{11}(k) = \int \frac{d^3q}{(2\pi)^3} \left(\alpha_s(\vec{q}, \vec{k} - \vec{q}) \right)^2 P_{\vec{k}-\vec{q}}^{\text{in}} P_{\vec{q}}^{\text{in}}, \quad (4.63)$$

$$\mathcal{A}^{22}(k) = \int \frac{d^3q}{(2\pi)^3} \left(\beta(\vec{k} - \vec{q}, \vec{q}) \right)^2 P_{\vec{k}-\vec{q}}^{\text{in}} P_{\vec{q}}^{\text{in}}, \quad (4.64)$$

$$\mathcal{A}^{12}(k) = \mathcal{A}^{21}(k) = \int \frac{d^3q}{(2\pi)^3} \left(\alpha_s(\vec{k} - \vec{q}, \vec{q}) \beta(\vec{k} - \vec{q}, \vec{q}) \right) P_{\vec{k}-\vec{q}}^{\text{in}} P_{\vec{q}}^{\text{in}}. \quad (4.65)$$

Moreover, from Eq. (4.60), we can write P_{13} as

$$P_{13}(a, k) = 4 \frac{D_+(a)}{D_+(a_i)} \left(\mathcal{B}^{\sigma\bar{\sigma}}(k) \mathcal{V}_{\sigma\bar{\sigma}}^\delta(a) + \mathcal{C}^\sigma(k) \mathcal{U}_\sigma^\delta(a) \right), \quad (4.66)$$

where the momentum matrix $\mathcal{B}^{\sigma\bar{\sigma}}(k)$ is

$$\mathcal{B}^{11}(k) = P_{\vec{k}}^{\text{in}} \int \frac{d^3q}{(2\pi)^3} \alpha(\vec{k} + \vec{q}, -\vec{q}) \alpha_s(\vec{k}, \vec{q}) P_{\vec{q}}^{\text{in}}, \quad (4.67)$$

$$\mathcal{B}^{12}(k) = P_{\vec{k}}^{\text{in}} \int \frac{d^3q}{(2\pi)^3} 2\beta(-\vec{q}, \vec{k} + \vec{q}) \alpha_s(\vec{k}, \vec{q}) P_{\vec{q}}^{\text{in}}, \quad (4.68)$$

$$\mathcal{B}^{21}(k) = P_{\vec{k}}^{\text{in}} \int \frac{d^3q}{(2\pi)^3} \alpha(\vec{k} + \vec{q}, -\vec{q}) \beta(\vec{k}, \vec{q}) P_{\vec{q}}^{\text{in}}, \quad (4.69)$$

$$\mathcal{B}^{22}(k) = P_{\vec{k}}^{\text{in}} \int \frac{d^3q}{(2\pi)^3} 2\beta(-\vec{q}, \vec{k} + \vec{q}) \beta(\vec{k}, \vec{q}) P_{\vec{q}}^{\text{in}}, \quad (4.70)$$

and $\mathcal{C}^\sigma(k)$ is given as

$$\mathcal{C}^1(k) = P_{\vec{k}}^{\text{in}} \int \frac{d^3q}{(2\pi)^3} \alpha(-\vec{q}, \vec{k} + \vec{q}) \alpha_s(\vec{k}, \vec{q}) P_{\vec{q}}^{\text{in}}, \quad (4.71)$$

$$\mathcal{C}^2(k) = P_{\vec{k}}^{\text{in}} \int \frac{d^3q}{(2\pi)^3} \alpha(-\vec{q}, \vec{k} + \vec{q}) \beta(\vec{k}, \vec{q}) P_{\vec{q}}^{\text{in}}. \quad (4.72)$$

Thus, the final one-loop computation requires us to compute nine integrals over momentum and ten integrals over time.

5 Biased tracers

Up to now, we studied the total underlying density contrast δ_A , corresponding to the Newtonian potential Φ , and computed its power spectrum to one-loop level. Those are the quantities which are measured by weak lensing (WL) surveys [10].²² The other promising cosmological observation, complementary to WL, are large-scale structure surveys which observe the overdensity of collapsed objects, rather than the underlying density contrast. Therefore, for precision cosmology, it is important to relate observable properties of tracers (e.g. density of galaxies) to the initial conditions

²²In fact, the weak lensing and the integrated SachsWolfe (ISW) effect, are measuring the lensing potential, $(\Phi + \Psi)/2$. However since in our model we have $\Phi = \Psi$ (no anisotropic stress), the lensing and the Newtonian potentials are equal.

and underlying total matter distribution. In its most general form, biased tracers can be non-local and stochastic functions of the underlying dark matter density and velocity. Over the past few years, considerable progress has been made in this direction. In particular, the formulation of biased tracers in the EFTofLSS has been worked out in [42] (or equivalently, [45]) which generalized and completed the analysis of [82]. Recently, in [47], the predicted biased tracers in the EFTofLSS with two species, dark matter, and baryons, has been worked out, and, when restricted to dark matter only, compared to numerical simulation. Here, following [42, 47], we describe the bias expansion for the density of collapsed objects in the presence of clustering quintessence. In the case of the smooth dark energy with $c_s = 1$ (described in Appendix D), we expect the effect of dark energy perturbations is negligible and therefore its contribution to the bias is only through the expansion rate.²³

For the purpose of this work, we consider Gaussian and adiabatic initial conditions for the total density and neglect the perturbatively suppressed effect of baryons,²⁴ which can be straightforwardly included. Thus, in our setup, the final halo overdensity, δ_h , can only be a function of the tracers' trajectory as well as the local observables of the dark matter and dark energy. We expect that the contribution of the long wavelength perturbations of dark matter and dark energy is weighted by their density parameters which are

$$\Omega_m(t) = \Omega_{m,0}a(t)^{-3} \quad \text{and} \quad \Omega_D(t) = \Omega_{D,0}a(t)^{-3(1+w)}. \quad (5.1)$$

As a result, we expect that the effect of dark energy perturbations is negligible during the matter era while it can be important at low redshifts as the dark energy becomes dominant. At this point, for simplicity, we define ϕ which is the rescaled version of the Newtonian potential, Φ , so that

$$\partial^2\phi \equiv \delta_A. \quad (5.2)$$

In the presence of clustering dark energy, we have the following generalization to the overdensity of halos in Eulerian space

$$\begin{aligned} \delta_h(\vec{x}, t) \simeq & \int^t dt' H(t') \left(\bar{c}_{\partial^2\phi}(t, t') \frac{\partial^2\phi(\vec{x}_\text{fl}, t')}{H(t')^2} + \bar{c}_{\delta_D}(t, t') \Omega_D(t') \delta_D(\vec{x}_\text{fl}, t') \right. \\ & + \bar{c}_{\partial_i v^i}(t, t') \frac{\partial_i v_A^i(\vec{x}_\text{fl}, t')}{H(t')} + \bar{c}_{\partial_i v_{\text{rel}}^i}(t, t') \frac{\partial_i v_{\text{rel}}^i(\vec{x}_\text{fl}, t')}{H(t')} \\ & + \bar{c}_{\partial_i \partial_j \phi \partial^i \partial^j \phi}(t, t') \frac{\partial_i \partial_j \phi(\vec{x}_\text{fl}, t')}{H(t')^2} \frac{\partial^i \partial^j \phi(\vec{x}_\text{fl}, t')}{H(t')^2} + \dots \\ & + \bar{c}_{\epsilon_m}(t, t') \Omega_m(t') \epsilon_m(\vec{x}, t') + \bar{c}_{\epsilon_D}(t, t') \Omega_D(t') \epsilon_D(\vec{x}, t') \\ & + \left[\bar{c}_{\epsilon_m \partial^2\phi}(t, t') \Omega_m(t') \epsilon_m(\vec{x}_\text{fl}, t') + \bar{c}_{\epsilon_D \partial^2\phi}(t, t') \Omega_D(t') \epsilon_D(\vec{x}_\text{fl}, t') \right] \frac{\partial^2\phi(\vec{x}, t')}{H(t')^2} + \dots \\ & \left. + \bar{c}_{\partial^4\phi}(t, t') \frac{\partial_{x_\text{fl}}^2}{k_M^2} \frac{\partial^2\phi(\vec{x}, t')}{H(t')^2} + \dots \right), \end{aligned} \quad (5.3)$$

²³Deep inside the horizon, the divergence of the velocity grows with respect to δ_A . However, deep inside the horizon, it also oscillates rapidly compared to the time scale of formation of halos, which is Hubble. Therefore, we expect that its contribution will be highly suppressed as well.

²⁴It has been explicitly shown in [44] and [47] that the effect of baryons is perturbatively suppressed.

where k_M is the comoving wavenumber enclosing the mass of the halo, \vec{x}_fl is defined as

$$\vec{x}_\text{fl}(\vec{x}, \tau, \tau') = \vec{x} - \int_{\tau'}^{\tau} d\tau'' \vec{v}_A(\tau'', \vec{x}_\text{fl}(\vec{x}, \tau, \tau')), \quad (5.4)$$

and the operators which are labelled by ϵ are describing the stochastic effects. Note that in the above, we have included the possibility that the clustering depends independently on the dark energy (similar to what happens for baryons [47]). One therefore needs to work out what are the diffeomorphism invariant combinations that one can write out of π . At linear level, there are just two such combinations: $\dot{\pi} - \Phi$ and $\partial_i \pi$, which, unsurprisingly, are respectively equal to the (rest frame) overdensity δ_D and the velocity v_D^i (a similar construction can be carried on at higher order). However, as we discussed in Section 4.2.3, the isocurvature mode is very small, and is generated by the counterterms. In the absence of an initial isocurvature mode, the generated relative velocity is proportional to the gradient of δ_A , and so it is degenerate with terms we could have written just in terms of it. In fact, without the presence of initial isocurvature modes, it is unlikely that a non-degenerate term is ever generated.

The expression Eq. (5.3) allows us in principle to compute the correlation functions of tracers in the presence of dark energy. We leave the computation, and the inclusion of baryons and primordial non-Gaussianities, to future work.

6 Results

In this section, we present the results of our numerical computations.²⁵ All of our plots are done at $a = 1$ and we use the cosmological parameters $\Omega_{m,0} = 0.27$, $\Omega_{D,0} = 0.73$, $H_0 = 71$ km/s/Mpc, $\Delta_\zeta^2 = 2.42 \times 10^{-9}$ and $n_s = 0.963$. For comparison, we also include dark matter evolution in the presence of a smooth dark energy with $c_s^2 = 1$, typically called w CDM, which is a theory that provides a familiar and simple example against which to compare our results (see Appendix D). For notational convenience, we can write the various power spectra at $a = 1$ as

$$P^i[w, \bar{c}_i^2] = P_{11}^i[w] + P_{1-\text{loop}}^i[w] - 2(2\pi) \bar{c}_i^2 \left(\frac{k}{k_{\text{NL}}} \right)^2 P_{11}^i[w], \quad (6.1)$$

where i stands for Λ CDM, w CDM, or clustering quintessence (CQ). Furthermore, it is useful to parameterize the speed of sound of the adiabatic mode as

$$\bar{c}_A^2 = \bar{c}_m^2 \left(1 + \xi (1 + w) \frac{\Omega_{D,0}}{\Omega_{m,0}} \left(\frac{a}{a_0} \right)^{-3w} \right), \quad (6.2)$$

where \bar{c}_m^2 is the value of the speed of sound in Λ CDM ($w = -1$), and ξ encodes the deviation due to the extra species when $w \neq -1$. In general, we expect $\xi \sim \mathcal{O}(1)$ since we expect the effect to be of similar order as the ratio of the energy densities and proportional to $1 + w$. Although we do not discuss the time dependence in this paper, we include the time dependent factor in Eq. (6.2) so that the effect goes to zero at early times, as expected. Because we are not comparing to simulation data

²⁵The Mathematica notebook used for the computations in this section is available at <http://web.stanford.edu/~senatore/>

in this paper, and we would just like to stress the non-linear corrections, we choose a reasonable value of $\bar{c}_m^2 = 0.20 (k_{\text{NL}}/h\text{Mpc}^{-1})^2$ taken from a previous comparison to non-linear dark-matter data [58]. We would also like to note that while the plots in this section were made from our code with the exact $1 + w$ dependence in the growth factor and loops, we have also implemented in our code an approximate computation that expands to first order in $1 + w$. In the latter case, one does not have to rerun the computations of the loops and time dependent functions for each w . The trade-off is that one has to make about twice as many computations to start with, but then can freely explore different values of w , which overall saves computational time.

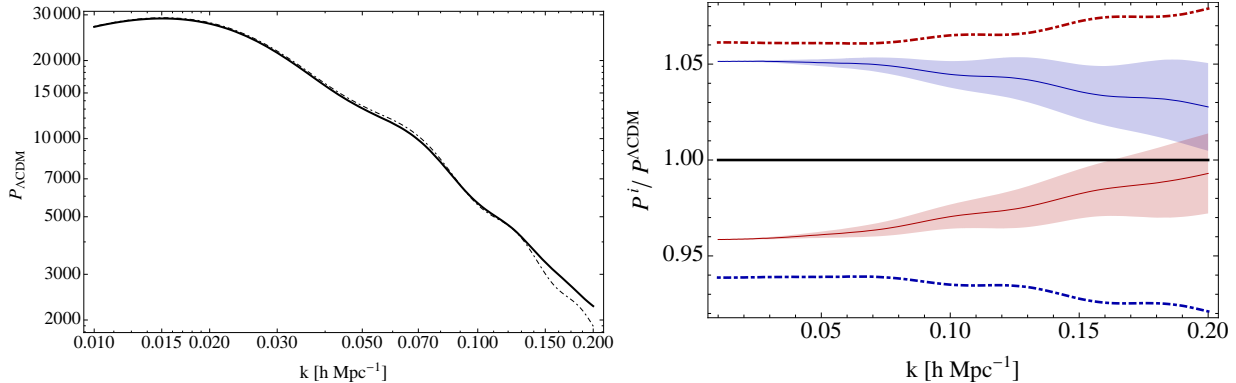


Figure 2: On the left-hand side, we show the linear (dot-dashed) and one-loop (solid) power spectra in Λ CDM (i.e. $w = -1$) for reference. On the right-hand side, we plot the one-loop computations compared with the one-loop Λ CDM power spectrum. The blue curves have $w = -0.9$, and the red curves have $w = -1.1$, the dot-dashed curves are the w CDM power spectra, the solid curves are clustering quintessence with $\xi = 0$ (defined in Eq. (6.2)), and the bands around them are $-1 \leq \xi \leq 1$. All curves have $\bar{c}_m^2 = 0.20 (k_{\text{NL}}/h\text{Mpc}^{-1})^2$.

In Figure 2, we compare clustering quintessence and w CDM to the Λ CDM power spectrum. Although w CDM with $w < -1$ *does not exist* as a consistent theory, we plot it for illustration purposes only. As expected, both clustering quintessence and w CDM are different from Λ CDM even at low k because of the different background evolution for $w \neq -1$. Also, the overall size of the corrections is of the expected order $1 + w$. In order to isolate the non-linear corrections in each model, we find it useful in Figure 3 to plot

$$R^i \equiv \frac{P^i}{P_{11}^i} . \quad (6.3)$$

From this plot, it is clear that the size of the corrections at low k , when compared to the relevant linear power spectra, all go to zero as expected. From Figure 2, we see that the non-linear corrections in clustering quintessence generically tend to make the power spectrum more like Λ CDM at higher values of k , while in w CDM the non-linear corrections continue to make the power spectrum different from Λ CDM. This explains the potentially confusing fact that, for example, the blue clustering quintessence curve is above 1 in Figure 2 but below 1 in Figure 3: in Figure 3, there is no information about the relative size of the Λ CDM and clustering quintessence power spectra, and the reason that the blue curve is below 1 in Figure 3 is the same as why it is decreasing in Figure 2. Then, in Figure

4, we examine the individual corrections, for which it is useful to write

$$P_{11}^i = P_{11}^{\Lambda\text{CDM}} + \Delta P_{11}^i \quad (6.4)$$

$$P_{1-\text{loop}}^i = P_{1-\text{loop}}^{\Lambda\text{CDM}} + \Delta P_{1-\text{loop}}^i. \quad (6.5)$$

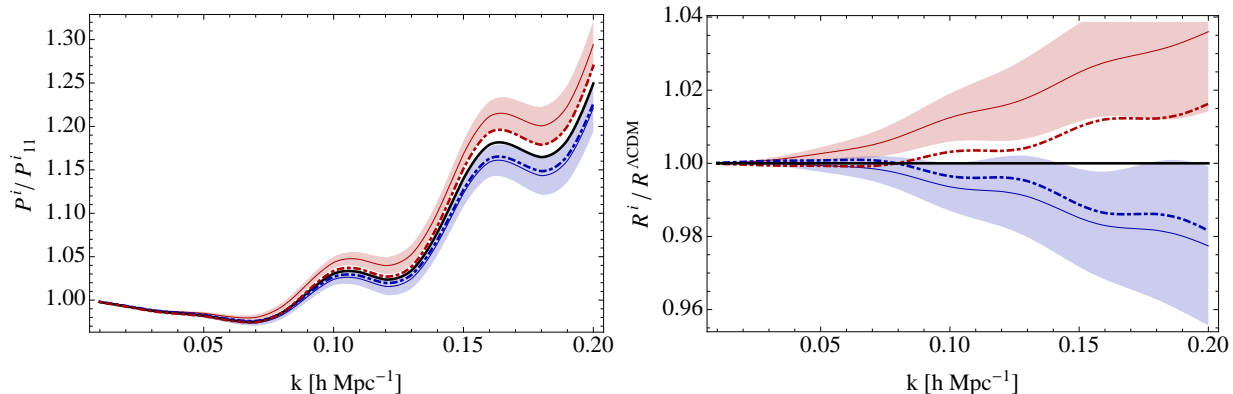


Figure 3: On the left-hand side, we show the size of the non-linear corrections for the various power spectra by plotting P^i/P_{11}^i , where i stands for ΛCDM , $w\text{CDM}$, or clustering quintessence. On the right-hand side, we compare the size of the non-linear corrections for the various power spectra to the size of the corrections in ΛCDM by plotting $\frac{P^i/P_{11}^i}{P^{\Lambda\text{CDM}}/P_{11}^{\Lambda\text{CDM}}}$. In both plots, the black curve is ΛCDM , blue curves have $w = -0.9$, the red curves have $w = -1.1$, the dot-dashed curves are the $w\text{CDM}$ power spectra, the solid curves are clustering quintessence with $\xi = 0$, and the bands around them are $-1 \leq \xi \leq 1$. All curves have $\bar{c}_m^2 = 0.20 (k_{\text{NL}}/h\text{Mpc}^{-1})^2$.

Finally, as an indication of the degeneracy between $w\text{CDM}$ and clustering quintessence in the adiabatic power spectrum, we present Figure 5, which shows that the two can be brought within 1% of each other by altering the values of w and \bar{c}_A^2 . Although we recognize this possibility, we do not investigate this degeneracy further, since it is out of the scope of this paper. We do note, however, that while there is a degeneracy in the adiabatic power spectrum, this will not be the case in other observables. For example, non-clustering $w\text{CDM}$ has $\delta_A \approx \delta_m$, but in clustering quintessence δ_A and δ_m are order $(1+w)$ different. Also, the physics is much different in the early universe because $w\text{CDM}$ is an extra relativistic species, while clustering quintessence is always non-relativistic.

7 Conclusions

The observational study of dark energy will make tremendous progress in the next few years thanks to the remarkable way we will be able to probe the Large-Scale structure of the universe either through galaxy surveys or through the CMB. Since most of the information is stored at high wavenumbers, it is important to have an accurate description of the mildly non-linear regime, which is amenable to a perturbative analysis. The Effective Field Theory of Large-Scale Structure provides the formalism to perform such analytic predictions in an accurate way. In the presence of dark energy, the clustering of LSS is affected both by the background cosmology and by the perturbations of dark energy. A very useful formalism to study the phenomenology of dark energy is the so-called Effective Field

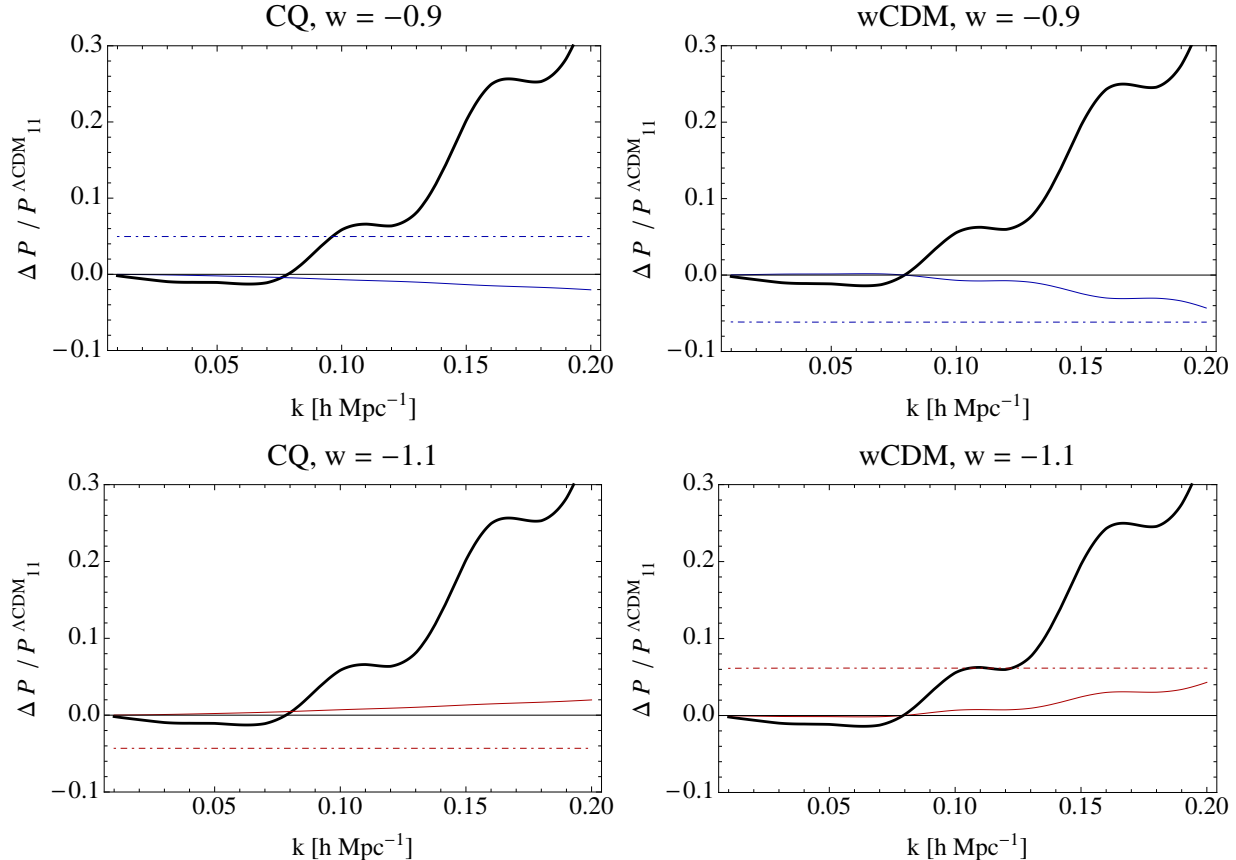


Figure 4: In these plots, we examine the various $1+w$ corrections to the power spectrum, which we decompose as $P_{11}^i = P_{11}^{\Lambda CDM} + \Delta P_{11}^i$ and $P_{1-loop}^i = P_{1-loop}^{\Lambda CDM} + \Delta P_{1-loop}^i$. All of the thick black curves are $P_{1-loop}^{\Lambda CDM}$, the dot-dashed curve is ΔP_{11}^i , the thin solid curve is ΔP_{1-loop}^i , the blue curves have $w = -0.9$, and the red curves have $w = -1.1$.

Theory of Dark Energy [17, 18, 19, 20, 21, 23], which assumes that dark energy is a system that spontaneously breaks time diffeomorphisms, and the fluctuating degree of freedom is the associated Goldstone boson. The advantage of using such a Lagrangian formalism to describe dark energy instead of a more general setup where one generically parametrizes some observational signatures is that the Lagrangian formulation makes it easy to ensure that our signatures originate from a system compatible with our well-established principles of physics: locality, causality, unitarity, etc.

In this paper, we have studied the dynamics of LSS in the presence of dark energy, with particular focus on the mildly non-linear regime. We formulated the set of non-linear equations for the system, including the relevant counterterms that account for the effect of short-distance physics at long distances, and that are modified in the presence of dark energy. We have also derived the equations that describe the clustering of biased tracers. Specializing for definiteness to the case of clustering quintessence, we have then perturbatively solved the equations of motion for dark matter and dark energy. This has allowed us to produce the one-loop power spectrum of the total density contrast. We have then discussed the different behaviors in the presence of smooth and clustering quintessence, for $w \gtrsim -1$, and for the linear and the non-linear solution. Finally, we have begun to discuss the

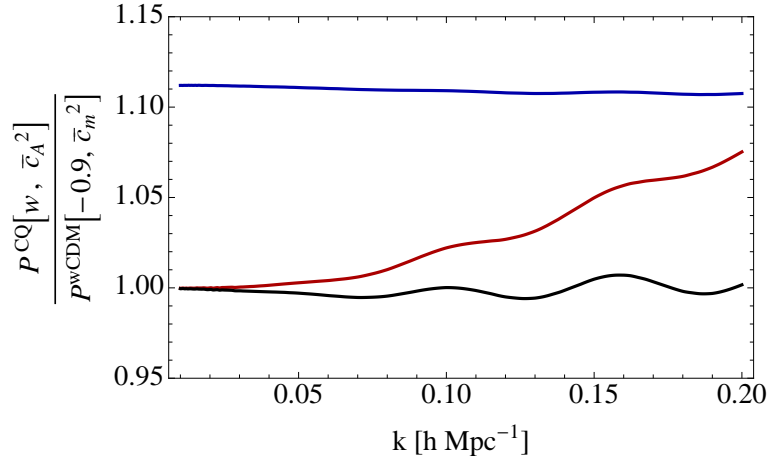


Figure 5: In this plot, we show how the adiabatic power spectrum in clustering quintessence can mimic the one from w CDM with different values of w and \bar{c}_A^2 . In this plot, for the power spectrum in clustering quintessence, we take the indicative values of $w = -0.9$ and $\bar{c}_m^2 = 0.20 (k_{\text{NL}}/h\text{Mpc}^{-1})^2$ and we vary the values of w and \bar{c}_A^2 in the clustering quintessence power spectrum. The blue curve has $w = -0.9$ and $\bar{c}_A^2 = \bar{c}_m^2$, the red curve has $w = -1.15$ and $\bar{c}_A^2 = \bar{c}_m^2$, and the black curve has $w = -1.15$ and $\bar{c}_A^2 = 1.9\bar{c}_m^2$.

effect on the predicted clustering of the modification of the numerical value of the counterterms that is expected in the presence of dark energy, and how these several effects can mimic each other.

There are several directions in which our work can be continued. One could perform calculations to higher order, to explore the k -reach of the theory. One can choose different parameters for the EFTofDE, effectively studying novel dark energy models: such an endeavor is already well developed at linear level [25, 78, 79], and it would be nice to construct it at the mildly-non-linear one. It would be interesting to study how much the unknown counterterms reduce the available information, and, in general, to perform numerical simulations of clustering quintessence to map out these counterterms in the case of dark energy. The EFTofLSS is in this case particularly useful because it should allow a more efficient implementation of the numerical simulations (see for example [67, 68, 69]), and also allows us to map out the very large parameter space using the Taylor expansion techniques of [59].

Acknowledgments

A.M. is grateful to the hospitality of Stanford University where this work was initiated and acknowledges partial support from Allameh Tabatabaai grant of Boniad Melli Nokhbegan Iran. L.S. is partially supported by DOE Early Career Award DE-FG02-12ER41854. M.L. is partially supported by a CEA Enhanced Eurotalents fellowship.

Appendices

A Details regarding δK

In this appendix, we review the details of the computation of δK_u and consider higher order terms, thus extending the computations done in [65] and [20].

A.1 Review of the ADM formalism

In this section, we mostly follow the notation and expressions in [83] and [84]. As a review of the formalism and notation, consider a space with coordinates x^μ and metric $g_{\mu\nu}$. Then consider a foliation of the space by space-like hypersurfaces Σ_t , where t labels the hypersurface. This foliation can be generated by a function $t(x^\mu)$ such that $t(x^\mu) = t_1$ defines the three-dimensional hypersurface Σ_{t_1} . The one-form dt is normal to the surface Σ_t , so we can define a unit normal whose components in the basis $\{dx^\mu\}$ are given by

$$n_\mu = -N \frac{\partial t}{\partial x^\mu}, \quad (\text{A.1})$$

where N is the lapse function and is given by

$$N = \frac{1}{\sqrt{-g^{\mu\nu} \partial_\mu t \partial_\nu t}}. \quad (\text{A.2})$$

Now, on each of the hypersurfaces, let y^i , for $i = 1, 2, 3$ be coordinates. Then, in order to use (t, y^i) as coordinates on the whole space, we first introduce a time-flow vector field defined by

$$t^\mu = \frac{\partial x^\mu}{\partial t}, \quad (\text{A.3})$$

which satisfies $t^\mu \partial_\mu t = 1$. This ensures that as we move in the direction of t^μ by an amount Δt away from surface Σ_{t_1} , we end up on the surface $\Sigma_{t_1 + \Delta t}$. We also have a set of three 4-vectors which are tangent to the hypersurfaces

$$e^\mu{}_i = \frac{\partial x^\mu}{\partial y^i}, \quad (\text{A.4})$$

and satisfy $e^\mu{}_i n_\mu = 0$ (this is also the transformation matrix used in pulling back the metric onto Σ_t , as we will see). In general, t^μ will not be parallel to n^μ , so we can define their relation as

$$t^\mu = N n^\mu + N^i e^\mu{}_i, \quad (\text{A.5})$$

and N^i is called the shift vector. We can imagine the original coordinates as a function of the new, adapted coordinates: $x^\mu(t, y^i)$, which means that the coordinate one forms are related by $dx^\mu = t^\mu dt + e^\mu{}_i dy^i$. The metric is then given by

$$ds^2 = g_{\mu\nu} dx^\mu dx^\nu = g_{\mu\nu} (t^\mu dt + e^\mu{}_i dy^i) (t^\nu dt + e^\nu{}_j dy^j) \quad (\text{A.6})$$

$$= -N^2 dt^2 + \hat{g}_{ij} (dy^i + N^i dt) (dy^j + N^j dt), \quad (\text{A.7})$$

where $\hat{g}_{ij} \equiv g_{\mu\nu} e^\mu{}_i e^\nu{}_j$ is the induced spatial metric (i.e. the metric $g_{\mu\nu}$ pulled back to the hypersurface). This is the standard ADM parametrization.

From Eq. (A.7), we can read off that $g_{00} = -N^2 + \hat{g}_{ij}N^iN^j$, $g_{0i} = \hat{g}_{ij}N^j$, and $g_{ij} = \hat{g}_{ij}$. Other important relationships between the ADM variables and the full inverse metric components $g^{\mu\nu}$ in the adapted coordinates are

$$\hat{g}_{ij} = g_{ij} \quad \hat{\nabla}_k \hat{g}_{ij} = 0 \quad (\text{A.8})$$

$$\sqrt{-g} = N\sqrt{\hat{g}} \quad N^2 = -\frac{1}{g^{00}} \quad (\text{A.9})$$

$$\hat{g}^{ij} \equiv (\hat{g}_{ij})^{-1} = g^{ij} - \frac{g^{0i}g^{0j}}{g^{00}} \quad N^i = -\frac{g^{0i}}{g^{00}}. \quad (\text{A.10})$$

To get the expression for \hat{g}^{ij} , we use the fact that $\hat{g}^{ij} \equiv (\hat{g}_{ij})^{-1}$, $g_{i\mu}g^{\mu\nu} = \delta_i^\nu$ (which implies $g_{0i} = -\frac{g_{ij}g^{0j}}{g^{00}}$) and $\hat{g}_{ij} = g_{ij}$, which gives

$$\hat{g}_{ik}\hat{g}^{ij} = g_{ik}g^{ij} + g_{0k}g^{0j} = \hat{g}_{ik}\left(g^{ij} - \frac{g^{0i}g^{0j}}{g^{00}}\right). \quad (\text{A.11})$$

Above, we have also introduced $\hat{\nabla}$, which is the spatial covariant derivative compatible with \hat{g}_{ij} , and is defined by $\hat{\nabla}_i \hat{T}_j = e^\mu{}_i e^\nu{}_j \nabla_\mu T_\nu$ where $\hat{T}_j = e^\nu{}_j T_\nu$.

A.2 Computation of δK_u

We start with the following expression for the extrinsic curvature K_{ij} (see [83] page 76)

$$K_{ij} = \frac{1}{2}e^\mu{}_i e^\nu{}_j \mathcal{L}_n g_{\mu\nu}, \quad (\text{A.12})$$

where \mathcal{L}_n is the Lie derivative in the direction of the unit normal n^μ . Then we make the following manipulations [84]

$$K_{ij} = \frac{1}{2N}e^\mu{}_i e^\nu{}_j (Nn^\sigma \nabla_\sigma g_{\mu\nu} + g_{\sigma\nu} N \nabla_\mu n^\sigma + g_{\mu\sigma} N \nabla_\nu n^\sigma) \quad (\text{A.13})$$

$$= \frac{1}{2N}e^\mu{}_i e^\nu{}_j (Nn^\sigma \nabla_\sigma g_{\mu\nu} + g_{\sigma\nu} \nabla_\mu (Nn^\sigma) + g_{\mu\sigma} \nabla_\nu (Nn^\sigma)) \quad (\text{A.14})$$

$$= \frac{1}{2N}e^\mu{}_i e^\nu{}_j (\mathcal{L}_t g_{\mu\nu} - \mathcal{L}_N g_{\mu\nu}), \quad (\text{A.15})$$

where we have used $e^\mu{}_i n_\mu = 0$, \mathcal{L}_t is the Lie derivative in the direction of t^μ , and \mathcal{L}_N is the Lie derivative in the direction $N^i e^\mu{}_i$. Then, we have

$$e^\mu{}_i e^\nu{}_j \mathcal{L}_N g_{\mu\nu} = e^\mu{}_i e^\nu{}_j (\nabla_\mu (g_{\nu\sigma} e^\sigma{}_i N^i) + \nabla_\nu (g_{\mu\sigma} e^\sigma{}_i N^i)) \quad (\text{A.16})$$

$$= \hat{\nabla}_i N_j + \hat{\nabla}_j N_i, \quad (\text{A.17})$$

where we have defined $N_i = \hat{g}_{ij}N^j$. Finally, in the (t, y^i) coordinates

$$e^\mu{}_i e^\nu{}_j \mathcal{L}_t g_{\mu\nu} = \partial_t \hat{g}_{ij}, \quad (\text{A.18})$$

which can be checked by expanding both sides and realizing that

$$e^\mu{}_i e^\nu{}_j g_{\sigma\nu} \partial_\mu t^\sigma = \frac{\partial x^\mu}{\partial y^i} e^\nu{}_j g_{\sigma\nu} \frac{\partial}{\partial x^\mu} \frac{\partial x^\sigma}{\partial t} = e^\nu{}_j g_{\sigma\nu} \frac{\partial}{\partial y^i} \frac{\partial x^\sigma}{\partial t} = e^\nu{}_j g_{\sigma\nu} \partial_t e^\sigma{}_i. \quad (\text{A.19})$$

This leads us to write

$$NK_{ij} = \frac{1}{2} \left(\partial_t \hat{g}_{ij} - \hat{\nabla}_i N_j - \hat{\nabla}_j N_i \right) \quad (\text{A.20})$$

in agreement with [84], so that

$$NK = N \hat{g}^{ij} K_{ij} = \frac{1}{2} \hat{g}^{ij} \partial_t \hat{g}_{ij} - \hat{\nabla}_i N^i. \quad (\text{A.21})$$

The background value of K is $3H$, so we have the trace of the perturbed extrinsic curvature as

$$\delta K = \frac{1}{N} \left(\frac{1}{2} \hat{g}^{ij} \partial_t \hat{g}_{ij} - \hat{\nabla}_i N^i \right) - 3H. \quad (\text{A.22})$$

From here, it is straightforward to introduce π . First of all, we will have $-3H \rightarrow -3H - 3\dot{H}\pi - \frac{3}{2}\ddot{H}\pi^2 + \dots$. Then we have

$$g_{\text{u}}^{00} \rightarrow g^{00} + 2g^{0\mu} \partial_\mu \pi + g^{\mu\nu} \partial_\mu \pi \partial_\nu \pi \quad (\text{A.23})$$

$$\hat{g}_{ij}^{\text{u}} = g_{ij}^{\text{u}} \rightarrow P^{-1\mu}{}_i P^{-1\nu}{}_j g_{\mu\nu} = g_{ij} + g_{00} \frac{\partial_i \pi \partial_j \pi}{1 + \dot{\pi}} \quad (\text{A.24})$$

$$g_{\text{u}}^{0i} \rightarrow P^0{}_\mu P^i{}_\nu g^{\mu\nu} = g^{ij} \partial_j \pi \quad (\text{A.25})$$

$$\sqrt{-g_{\text{u}}} \rightarrow \det P^{-1} \sqrt{-g} = (1 + \dot{\pi})^{-1} \sqrt{-g} \quad (\text{A.26})$$

$$g_{\text{u}}^{ij} \rightarrow g^{ij} \quad (\text{A.27})$$

$$\partial_0 \rightarrow \frac{1}{1 + \dot{\pi}} \partial_0, \quad \partial_i \rightarrow -\frac{\partial_i \pi}{1 + \dot{\pi}} \partial_0 + \partial_i, \quad (\text{A.28})$$

where, because we will need to derive the contribution to the Poisson equation, we have kept the full metric dependence, but have assumed that the metric is diagonal. We reproduce the transformation matrices here for convenience

$$P^\mu{}_\rho = \begin{pmatrix} 1 + \dot{\pi} & \partial_i \pi \\ 0 & 1 \end{pmatrix}_{\mu\rho}, \quad P^{-1\rho}{}_\mu = \begin{pmatrix} \frac{1}{1 + \dot{\pi}} & -\frac{\partial_i \pi}{1 + \dot{\pi}} \\ 0 & 1 \end{pmatrix}_{\rho\mu}. \quad (\text{A.29})$$

We will look at the two relevant terms individually. First consider

$$\frac{1}{2} \hat{g}_{\text{u}}^{ij} \partial_t \hat{g}_{ij}^{\text{u}} \rightarrow \frac{1}{2} \left(g^{ij} - \frac{g^{ik} g^{jl} \partial_k \pi \partial_l \pi}{g^{00} + 2g^{0\mu} \partial_\mu \pi + g^{\mu\nu} \partial_\mu \pi \partial_\nu \pi} \right) \frac{1}{1 + \dot{\pi}} \partial_t \left(g_{ij} + g_{00} \frac{\partial_i \pi \partial_j \pi}{1 + \dot{\pi}} \right). \quad (\text{A.30})$$

Next, consider

$$\hat{\nabla}_i N^i = \frac{1}{\sqrt{\hat{g}}} \partial_i \left(\sqrt{\hat{g}} N^i \right) = \partial_i N^i + N^i \partial_i \log \sqrt{\hat{g}}. \quad (\text{A.31})$$

The first term gives

$$\partial_i N_{\text{u}}^i \rightarrow \left(-\frac{\partial_i \pi}{1 + \dot{\pi}} \partial_0 + \partial_i \right) \left(\frac{-g^{ik} \partial_k \pi}{g^{00} + 2g^{0\mu} \partial_\mu \pi + g^{\mu\nu} \partial_\mu \pi \partial_\nu \pi} \right), \quad (\text{A.32})$$

and the second one

$$\begin{aligned} N_{\text{u}}^i \partial_i \log \sqrt{\hat{g}_{\text{u}}} &\rightarrow \left(\frac{-g^{ik} \partial_k \pi}{g^{00} + 2g^{0\mu} \partial_\mu \pi + g^{\mu\nu} \partial_\mu \pi \partial_\nu \pi} \right) \\ &\times \left(-\frac{\partial_i \pi}{1 + \dot{\pi}} \partial_0 + \partial_i \right) \log \left(\sqrt{-(g^{00} + 2g^{0\mu} \partial_\mu \pi + g^{\mu\nu} \partial_\mu \pi \partial_\nu \pi)} (1 + \dot{\pi})^{-1} \sqrt{-g} \right). \end{aligned} \quad (\text{A.33})$$

The metric perturbations are given by

$$g_{\mu\nu} = \begin{pmatrix} -(1+2\Phi) & 0 \\ 0 & a^2(1-2\Psi)\delta_{ij} \end{pmatrix}. \quad (\text{A.34})$$

Finally, putting this all together, we obtain, to second order in the perturbations,²⁶

$$\begin{aligned} \delta K_{\text{u}} \rightarrow & -3\dot{\Psi} - 3H\Phi - a^{-2}\partial^2\pi - 3\dot{H}\pi \\ & + a^{-2} \left((\partial^2\pi)(\dot{\pi} - \Phi - 2\Psi) + (\partial_i\pi)\partial_i \left(\frac{1}{2}H\pi + 2\dot{\pi} - 2\Phi + \Psi \right) \right) \\ & + \frac{9}{2}H\Phi^2 + 3\Phi\dot{\Psi} - 6\Psi\dot{\Psi} - \frac{3}{2}\ddot{H}\pi^2. \end{aligned} \quad (\text{A.35})$$

B Linear equations

In this appendix we will work out the linear equations that we will need in the rest of the paper. We are considering the action

$$\int d^4x \sqrt{-g} \left[\frac{M_{\text{Pl}}^2}{2} R - \Lambda(t) - c(t)g_{\text{u}}^{00} + \frac{M_2^4}{2} (\delta g_{\text{u}}^{00})^2 - \frac{\bar{m}_1^3}{2} \delta g_{\text{u}}^{00} \delta K_{\text{u}} \right]. \quad (\text{B.1})$$

For the equation of motion of π , we will include only the terms that are relevant for the linear equation of motion for π . This means that we have dropped all terms that do not involve a factor of π , and all terms that would contribute higher than first order in the equation of motion. First we consider

$$\begin{aligned} -\sqrt{-g} (c(t)g_{\text{u}}^{00} + \Lambda(t)) \approx & -a^3 (1 + \Phi - 3\Psi) \left\{ \Lambda - c + (\dot{\Lambda} - \dot{c})\pi + \frac{1}{2} (\ddot{\Lambda} - \ddot{c}) \pi^2 \right. \\ & \left. + 2c(\Phi - \dot{\pi}) + c(4\Phi\dot{\pi} - \dot{\pi}^2 + a^{-2}(\partial\pi)^2) + 2\dot{c}\pi(\Phi - \dot{\pi}) \right\}. \end{aligned} \quad (\text{B.2})$$

From this expression, we see that in order for the term linear in π to vanish, we must have that $\dot{\Lambda} + \dot{c} + 6Hc = 0$, which also means that $\ddot{\Lambda} + \ddot{c} + 6\dot{H}c + 6H\dot{c} = 0$. Using these two relations and $\dot{c} = -3H(1+w)c$, and letting $\pi \rightarrow \pi + \delta\pi$, we get that the change in the action due to this term is

$$\rightarrow 2a^3c(t) \left(-\dot{\pi} + 3Hw\dot{\pi} + a^{-2}\partial^2\pi + 3\dot{H}\pi + 3H(1-w)\Phi + \dot{\Phi} + 3\dot{\Psi} \right) \delta\pi. \quad (\text{B.3})$$

Next, we have

$$\sqrt{-g} \frac{M_2^4}{2} (\delta g_{\text{u}}^{00})^2 \rightarrow 4M_2^4 a^3 \left\{ \frac{\partial_t M_2^4}{M_2^4} (\Phi - \dot{\pi}) + 3H(\Phi - \dot{\pi}) + \dot{\Phi} - \dot{\pi} \right\} \delta\pi. \quad (\text{B.4})$$

And finally,

$$\begin{aligned} -\sqrt{-g} \frac{\bar{m}_1^3}{2} \delta g_{\text{u}}^{00} \delta K_{\text{u}} \approx & a^3 \bar{m}_1^3 (\dot{\pi} - \Phi) \left(-3\dot{\Psi} - 3H\Phi - a^{-2}\partial^2\pi - 3\dot{H}\pi \right) \\ \rightarrow & -\delta\pi \frac{d}{dt} \left\{ a^3 \bar{m}_1^3 \left(-3\dot{\Psi} - 3H\Phi - a^{-2}\partial^2\pi - 3\dot{H}\pi \right) \right\} \\ & - \delta\pi \left(a^3 \bar{m}_1^3 a^{-2} \partial^2 (\dot{\pi} - \Phi) + 3\dot{H} a^3 \bar{m}_1^3 (\dot{\pi} - \Phi) \right). \end{aligned} \quad (\text{B.5})$$

²⁶This formula differs from the one provided in [65] at second order. It also differs from one of the two expressions given in [20] at linear order.

Dividing by $a^3\delta\pi$, and adding the above contributions together gives the linear equation of motion

$$\begin{aligned}
& 2c \left(-\ddot{\pi} + 3Hw\dot{\pi} + a^{-2}\partial^2\pi + 3\dot{H}\pi + 3H(1-w)\Phi + \dot{\Phi} + 3\dot{\Psi} \right) \\
& - 4M_2^4 \left(\ddot{\pi} - \dot{\Phi} + \frac{\partial_t M_2^4}{M_2^4} (\dot{\pi} - \Phi) + 3H(\dot{\pi} - \Phi) \right) \\
& + (H\bar{m}_1^3 + \partial_t \bar{m}_1^3) a^{-2} \partial^2 \pi + \bar{m}_1^3 a^{-2} \partial^2 \Phi \\
& + 3a^{-3} \frac{d}{dt} \left\{ a^3 \bar{m}_1^3 (\dot{\Psi} + H\Phi) \right\} + 3\dot{H}\bar{m}_1^3 \Phi + 3a^{-3} \frac{d}{dt} \left(a^3 \bar{m}_1^3 \dot{H} \right) \pi = 0 . \tag{B.6}
\end{aligned}$$

In the limit $\bar{m}_1^3 \rightarrow 0$, the analogue of this equation is provided in synchronous gauge in [19], and for $\bar{m}_1^3 \neq 0$ it was provided in synchronous gauge in [25]. Reference [21] provides the linear equation of motion for π above and the Einstein equations below, in both Newtonian and synchronous gauges, for an even broader class of dark-energy Lagrangians than we consider in this work. For the Einstein equations at linear order, we take the expressions from [20], but relax the assumption of constant \bar{m}_1^3 and specialize to $\dot{f} = 0$. The equation for the (00) component is

$$\begin{aligned}
& 2M_{\text{Pl}}^2 (a^{-2} \partial^2 \Psi - 3H\dot{\Psi}) - 2c\dot{\pi} - (\dot{c} + \dot{\Lambda})\pi - 2\Lambda\Phi + 4M_2^4 (\Phi - \dot{\pi}) \\
& + \bar{m}_1^3 \left[3(\dot{\Psi} + H\Phi) + 3\dot{H}\pi + a^{-2} \partial^2 \pi + 3H(\Phi - \dot{\pi}) \right] = \delta T_{00} . \tag{B.7}
\end{aligned}$$

By using the background equations of motion $\dot{\Lambda} + \dot{c} + 6Hc = 0$, Eq. (2.8), Eq. (2.9), Eq. (2.11), and $\delta T_{00} = \delta\rho_m + 2\bar{\rho}_m\Phi$ we get

$$\begin{aligned}
& 2M_{\text{Pl}}^2 (a^{-2} \partial^2 \Psi - 3H(\dot{\Psi} + H\Phi)) + (\bar{\rho}_D + \bar{p}_D)(\Phi - \dot{\pi} + 3H\pi) + 4M_2^4 (\Phi - \dot{\pi}) \\
& + \bar{m}_1^3 \left[3(\dot{\Psi} + H\Phi) + 3\dot{H}\pi + a^{-2} \partial^2 \pi + 3H(\Phi - \dot{\pi}) \right] = \delta\rho_m . \tag{B.8}
\end{aligned}$$

The equation for the (ij) trace component is

$$\begin{aligned}
& 2M_{\text{Pl}}^2 \left(\ddot{\Psi} + H\dot{\Phi} + 3H\dot{\Psi} + (3H^2 + 2\dot{H})(\Phi + \Psi) + \partial^2(\Phi - \Psi)/(3a^2) \right) \\
& + 2c(\Phi - \dot{\pi}) - 2\Psi(\Lambda - c) + (\dot{\Lambda} - \dot{c})\pi - \bar{m}_1^3 [\dot{\Phi} - \ddot{\pi} + 3H(\Phi - \dot{\pi})] - \partial_t(\bar{m}_1^3)(\Phi - \dot{\pi}) = \delta T_k^k / (3a^2) . \tag{B.9}
\end{aligned}$$

Again using the background equations of motion, we have

$$\begin{aligned}
& 2M_{\text{Pl}}^2 \left(\ddot{\Psi} + H\dot{\Phi} + 3H\dot{\Psi} + (3H^2 + 2\dot{H})\Phi + \partial^2(\Phi - \Psi)/(3a^2) \right) \\
& - \dot{\bar{p}}_D\pi + (\bar{\rho}_D + \bar{p}_D)(\Phi - \dot{\pi}) - \bar{m}_1^3 [\dot{\Phi} - \ddot{\pi} + 3H(\Phi - \dot{\pi})] - \partial_t(\bar{m}_1^3)(\Phi - \dot{\pi}) = \delta p_m . \tag{B.10}
\end{aligned}$$

The equations for the (ij) traceless components are

$$M_{\text{Pl}}^2 (\partial_i \partial_j - \frac{1}{3} \delta_{ij} \partial^2) (\Psi - \Phi) = \delta T_{ij} - \frac{1}{3} \delta_{ij} \delta T_k^k = 0 . \tag{B.11}$$

The equations for the $(0i)$ components are

$$2M_{\text{Pl}}^2 \partial_i (\dot{\Psi} + H\Phi) - (\bar{\rho}_D + \bar{p}_D) \partial_i \pi - 2\bar{m}_1^3 \partial_i (\Phi - \dot{\pi}) = \delta T_{i0} . \tag{B.12}$$

Notice that compared to [20], we have corrected a factor of two in Eq. (B.12) in front of $(\bar{\rho}_D + \bar{p}_D) \partial_i \pi$, a minus sign in front of $3\bar{m}_1^3 \dot{H}\pi$ in Eq. (B.8), and we have extra terms in (B.9) and (B.10) due to the time dependence of \bar{m}_1^3 in our system.

From the above action, we can read off the linear energy-momentum tensor of the dark energy as

$$\begin{aligned} \delta\rho_D &= 2c(t)(\dot{\pi} - 3H\pi - \Phi) + 4M_2^4(\dot{\pi} - \Phi) \\ &\quad + \bar{m}_1^3 \left[-3\dot{H}\pi - a^{-2}\partial^2\pi + 3H(\dot{\pi} - \Phi) - 3(\dot{\Psi} + H\Phi) \right], \end{aligned} \quad (\text{B.13})$$

$$\delta p_D = \dot{\bar{p}}_D\pi + 2c(t)(\dot{\pi} - \Phi) + \bar{m}_1^3[\dot{\Phi} - \ddot{\pi} + 3H(\Phi - \dot{\pi})] + \partial_t(\bar{m}_1^3)(\Phi - \dot{\pi}), \quad (\text{B.14})$$

$$\partial_i\delta q_D = -(\bar{\rho}_D + \bar{p}_D)\partial_i\pi + 2\bar{m}_1^3\partial_i(\dot{\pi} - \Phi), \quad (\text{B.15})$$

$$\pi_{ij}^D = 0, \quad (\text{B.16})$$

where $\delta\rho_D$ and δp_D are the energy and pressure density of dark energy, $\partial_i\delta q_D = \delta T_D^0{}_i$ is the momentum density and π_{ij}^D is the anisotropic stress.²⁷ The momentum density corresponding to the matter is also given as $\partial_i\delta q_m = \delta T^0{}_i$. As we see in the above, in the limits that we consider in this paper, the dark energy pressure density is very small and a relativistic correction comparing with its energy density.

Inserting the dark energy $T_{\mu\nu}$ in the linear Einstein equations, we find two constraints, the anisotropic stress equation

$$M_{\text{Pl}}^2\left(\partial_i\partial_j - \frac{1}{3}\delta_{ij}\partial^2\right)(\Psi - \Phi) = \pi_{ij}^D + \pi_{ij}^m, \quad (\text{B.17})$$

and (from the combination of Eq. (B.18) and Eq. (B.19)) the Poisson equation²⁸

$$\delta\rho_m - 3H\delta q_m + \delta\rho_D - 3H\delta q_D = 2M_{\text{Pl}}^2a^{-2}\partial^2\Psi. \quad (\text{B.21})$$

It is noteworthy to mention that in the above, the combination $\delta\rho_x - 3H\delta q_x$ is equal to the energy density perturbation on velocity orthogonal slicing, $\delta\rho^{(v.o.)}$ (see [85, 71]). Since the linear order anisotropic stress of our dark matter and dark energy are zero, the Bardeen potentials are equal here, $\Psi = \Phi$. The combination of dark matter continuity and Euler equations, linear equation of π and the above constraint equations fully determine our system at linear level.

B.1 Linear solution of π with $\bar{m}_1^3 = 0$

We are now ready to solve the linear equation of π in the clustering case ($c_s^2 \ll 1$) analytically. Recalling that $\frac{\partial_t M_2^4}{HM_2^4} = -3(1+w)$ and setting $\bar{m}_1^3 = 0$, we have the field equation of $\pi(a, \vec{x})$ in

²⁷The anisotropic stress is the trace-less spatial part of the energy-momentum tensor, $\pi_{ij} = T_{ij} - \frac{1}{3}g_{ij}T_k^k$.

²⁸For completeness and for future reference, the full linear G_{00} component of the Einstein equation including the relativistic corrections is

$$2M_{\text{Pl}}^2(a^{-2}\partial^2\Psi - 3H(\dot{\Psi} + H\Phi)) = \delta\rho_m + \delta\rho_D. \quad (\text{B.18})$$

while the G_{0i} is given as

$$2M_{\text{Pl}}^2\partial_i(\dot{\Psi} + H\Phi) + \partial_i\delta q_D = -\partial_i\delta q_m, \quad (\text{B.19})$$

and finally the trace of G_{ij} gives rise to

$$2M_{\text{Pl}}^2\left(\ddot{\Psi} + H\dot{\Psi} + 3H\dot{\Psi} + (3H^2 + 2\dot{H})\Phi + \partial^2(\Phi - \Psi)/(3a^2)\right) = \delta p_m + \delta p_D. \quad (\text{B.20})$$

Eq. (3.8) as

$$\ddot{\pi} - \dot{\Phi} - 3wH(\dot{\pi} - \dot{\Phi}) - \frac{c_s^2}{a^2}\partial^2\pi = 0. \quad (\text{B.22})$$

It is noteworthy to mention that the Newtonian potential, Φ , in the above equation is of the same order as the π terms and is *not* a relativistic correction in the field equation of π . As we see in Section 4, the system of equations for dark matter and dark energy reduce to one single second order differential equation for the total density contrast, $\delta_A(a, \vec{k}) = \delta_m(a, \vec{k}) + a^{-3w} \frac{\Omega_{D,0}}{\Omega_{m,0}} \frac{1+w}{c_s^2} (\dot{\pi} - \dot{\Phi})$. That equation has only one *growing* solution for δ_A which by the Poisson equation is directly related to the Newtonian potential, $\Phi = -\frac{3\Omega_{m,0}\mathcal{H}_0^2 a_0}{2ak^2} \delta_A$. Working out δ_A and therefore Φ in Section 4, we can determine π by solving Eq. (B.22) in which the Newtonian potential acts as the source term. In fact, the homogeneous part of the above equation has only decaying solutions and the inhomogeneous part, which is sourced by Φ , provides the growing mode.

In order to see the decaying nature of the homogeneous solution let us study its evolution during matter era. It is straightforward to see that it is damping during the dark-energy dominated era as well. In Fourier space, we can read off the homogeneous part of Eq. (B.22) in terms of the conformal time τ , as

$$\pi_{\tau\tau}^h - (1 + 3w)\mathcal{H}\pi_{\tau}^h + c_s^2 k^2 \pi^h = 0, \quad (\text{B.23})$$

where $\pi^h(\tau, \vec{k})$ is the homogeneous solution of π . The solution of $\pi^h(\tau, \vec{k})$ in the matter era, when $\mathcal{H} = 2/\tau$, can be expanded in terms of the Bessel J_ν and Y_ν functions as

$$\pi^h(\tau, \vec{k}) = \tau^{\frac{3}{2}(1+2w)} \left(c_1 J_\nu(c_s k \tau) + c_2 Y_\nu(c_s k \tau) \right) \quad \text{where} \quad \nu = \frac{3}{2}(1 + 2w), \quad (\text{B.24})$$

which using that $\tau \propto a^{\frac{1}{2}}$ implies that $\pi^h \propto a^{3(1+2w)}$ is always decaying and therefore negligible. As a result, only the particular solution of π , called π^P , which is sourced by Φ (and hence under the influence of dark matter) can be growing and important in structure formation. That is in agreement with the fluid picture observation that the energy contrast of dark energy, δ_D is proportional to δ_m during the matter era.

In order to determine the particular solution of Eq. (B.22), π^P , we use the following decomposition

$$\pi^P(a, \vec{x}) = \int^a d\tilde{a} \frac{\Phi(\tilde{a}, \vec{x})}{\mathcal{H}(\tilde{a})} + \tilde{\pi}(a, \vec{x}). \quad (\text{B.25})$$

where $\tilde{\pi}(a, \vec{x})$ satisfies²⁹

$$a^2 \mathcal{H}^2(a) \tilde{\pi}'' + a^{2+3w} \mathcal{H}(a) (\mathcal{H} a^{-3w})' \tilde{\pi}' = c_s^2 \int^a d\tilde{a} \frac{\partial^2 \Phi(\tilde{a}, \vec{x})}{\mathcal{H}(\tilde{a})}. \quad (\text{B.26})$$

The above equation has the following solution

$$\tilde{\pi}(a, \vec{x}) = \int^a da' \int^{a'} da'' K(a', a'') S_\Phi(a'', \vec{x}), \quad (\text{B.27})$$

²⁹Using the fact that the source term is proportional to c_s^2 and $c_s^2 k^2 \ll \mathcal{H}^2$, we dropped the spatial derivative of $\tilde{\pi}$ in (B.26).

where $S_\Phi(a, \vec{x})$ is the source term on the RHS of Eq. (B.26) and the kernel $K(a, a')$ is

$$K(a, a') = \frac{(a/a')^{3w}}{\mathcal{H}(a')\mathcal{H}(a)a'^2}. \quad (\text{B.28})$$

Finally, using Eq. (B.25) and Eq. (B.27), we obtain the linear order growing solution of $\pi(a, \vec{x})$ as

$$\pi(a, \vec{x}) = \int^a da' \frac{\Phi(a', \vec{x})}{\mathcal{H}(a')} + c_s^2 \int^a da' \int^{a'} da'' \int^{a''} da''' \frac{\partial^2 \Phi(a''', \vec{x})}{\mathcal{H}(a''')} K(a', a''), \quad (\text{B.29})$$

which is a function of the background and the Newtonian potential.

B.1.1 π during matter domination

Up to now, we worked out the $\pi(a, \vec{x})$ field in terms of the gravitational potential $\Phi(a, \vec{x})$. Now we turn to find the explicit form of $\pi(a, \vec{x})$ during matter era. In that regime, Φ is almost constant

$$\Phi(a, \vec{x}) \simeq \Phi(a_i, \vec{x}), \quad (\text{B.30})$$

and we have the Hubble parameter as $\mathcal{H}(a) \simeq a^{-\frac{1}{2}} \mathcal{H}_0$ where $\mathcal{H}_0 = H_0(\Omega_{m,0} a_0^3)^{\frac{1}{2}}$. Going to Fourier space and using the above in Eq. (B.29), we find the explicit form of the π field during the matter era

$$\pi(a, \vec{k}) \simeq \frac{2a}{3\mathcal{H}(a)} \Phi(a_i, \vec{k}) \left(1 - \frac{2}{5(1-3w)} \frac{c_s^2 k^2}{\mathcal{H}^2} \right). \quad (\text{B.31})$$

From this solution, we see that $\dot{\pi} - \Phi \sim c_s^2 H^{-2} \partial^2 \Phi$. Although this solution is only valid during matter domination, as shown in Eq. (B.29), the qualitative features and the scalings with c_s^2 are not different at other times.

Throughout this work, we choose the π language for describing the dynamics of the dark energy sector and its gravitational interactions with the dark matter. At this point, we determine the corresponding dark energy density contrast, δ_D , and velocity, θ_D , generated by π in the fluid picture. During the matter era, the dark energy has negligible contribution to the Poisson equation and we can read Φ as

$$-k^2 \Phi(a, \vec{k}) \simeq \frac{3}{2} \mathcal{H}^2 \delta_m(a, \vec{k}). \quad (\text{B.32})$$

Using the above in Eq. (B.31) and recalling that $\delta_m = -\theta_m/\mathcal{H}$, we find δ_D and Θ_D as

$$\delta_D(a, \vec{k}) = \frac{(1+w)}{c_s^2} (\dot{\pi} - \Phi) = \left(\frac{1+w}{1-3w} \right) \delta_m(a, \vec{k}), \quad (\text{B.33})$$

$$\theta_D(a, \vec{k}) = \frac{k^2}{a} \pi = \theta_m(a, \vec{k}). \quad (\text{B.34})$$

Moreover, the total density contrast δ_A in Eq. (3.13) is

$$\delta_A(a, \vec{k}) = \delta_m(a, \vec{k}) + a^{-3w} \frac{\Omega_{D,0}}{\Omega_{m,0}} \frac{1+w}{c_s^2} (\dot{\pi} - \Phi) = \left(1 + a^{-3w} \frac{\Omega_{D,0}}{\Omega_{m,0}} \frac{1+w}{1-3w} \right) \delta_m(a, \vec{k}). \quad (\text{B.35})$$

The above are the well-known linear relations in the fluid picture.

B.2 Linear solution of π , including \bar{m}_1^3

In this part, we consider $\bar{m}_1^3 \neq 0$ and solve the linear equation of π in the limit that $|c_s^2| \ll 1$. From (3.8), we find the speed of sound in the presence of \bar{m}_1^3 as

$$c_s^2 = \frac{c(t) + \frac{1}{2}a^{-1}\partial_t(a\bar{m}_1^3(t))}{2M_2^4(t) + c(t)}. \quad (\text{B.36})$$

Moreover, in the limit that $|c_s^2| \ll 1$, the field equation of π is given as

$$\frac{1}{a^3 M_2^4} \frac{d}{dt} \{a^3 M_2^4 (\dot{\pi} - \Phi)\} - c_s^2 a^{-2} \partial^2 \pi - c_s^2 \alpha_{\bar{m}} a^{-2} \frac{\partial^2 \Phi}{H} = 0, \quad (\text{B.37})$$

where $\alpha_{\bar{m}}$ is a dimensionless quantity of order one, given as

$$\alpha_{\bar{m}} \equiv \frac{H\bar{m}_1^3}{4M_2^4 c_s^2} \simeq \frac{H\bar{m}_1^3}{2c(t) + a^{-1}\partial_t(a\bar{m}_1^3)}, \quad (\text{B.38})$$

where in the last passage we used $|c_s^2| \ll 1$. From Eq. (B.37), we can easily see that in the $c_s^2 \rightarrow 0$ limit, we will again have the two species comoving, i.e. $\partial_i \pi = -av_m^i$ (as in Eq. (3.14)).

Next, we can use the Poisson equation Eq. (B.7) to get

$$\delta_A = \delta_m + \frac{4a^3 M_2^4}{a_0^3 \bar{\rho}_{m,0}} (\dot{\pi} - \Phi) - \frac{a^3 \bar{m}_1^3}{a_0^3 \bar{\rho}_{m,0}} a^{-2} \partial^2 \pi, \quad (\text{B.39})$$

in the non-relativistic limit. Taking the time derivative of this and using the equation of motion for π and the Euler equation for dark matter gives

$$\dot{\delta}_A = \dot{\delta}_m + \frac{4}{\bar{\rho}_{m,0}} \frac{d}{dt} (a^3 M_2^4 (\dot{\pi} - \Phi)) - \frac{1}{\bar{\rho}_{m,0}} \frac{d}{dt} (a\bar{m}_1^3) \partial^2 \pi - \frac{a\bar{m}_1^3}{\bar{\rho}_{m,0}} \partial^2 \dot{\pi} \quad (\text{B.40})$$

$$= \dot{\delta}_m + \frac{4a^3 M_2^4}{\bar{\rho}_{m,0}} \left(c_s^2 a^{-2} \partial^2 \pi + \frac{\bar{m}_1^3}{4M_2^4} a^{-2} \partial^2 \Phi \right) - \frac{1}{\bar{\rho}_{m,0}} \frac{d}{dt} (a\bar{m}_1^3) \partial^2 \pi - \frac{a\bar{m}_1^3}{\bar{\rho}_{m,0}} \partial^2 \dot{\pi} \quad (\text{B.41})$$

$$= \dot{\delta}_m + \frac{2ac}{\bar{\rho}_{m,0}} \partial^2 \pi + \frac{a\bar{m}_1^3}{\bar{\rho}_{m,0}} \partial^2 (\Phi - \dot{\pi}) \quad (\text{B.42})$$

$$= -\frac{1}{a} \theta_m - \frac{1}{a} \frac{2a^3 c}{\bar{\rho}_{m,0}} \theta_m = -\frac{1}{a} C(a) \theta_A, \quad (\text{B.43})$$

where we used $\partial^2(\dot{\pi} - \Phi) \propto c_s^2$, $\theta_A \equiv \theta_m$, and we have called $C(a) = 1 + \frac{2a^3 c}{\bar{\rho}_{m,0}} = 1 + (1+w) \frac{\Omega_{D,0}}{\Omega_{m,0}} a^{-3w}$. Thus, Eq. (B.43) along with the fact that the two species are comoving, $\partial_i \pi = -av_m^i$, means that the linear equations for δ_A are the same as in the $\bar{m}_1^3 = 0$ case studied in the main text, Eq. (3.17)

$$\dot{\delta}_A + \frac{1}{a} C(a) \theta_A = 0 \quad (\text{B.44})$$

$$\dot{\theta}_A + H\theta_A + \frac{3}{2} \frac{\Omega_{m,0} \mathcal{H}_0^2 a_0}{a^2} \delta_A = 0. \quad (\text{B.45})$$

As before, because the species are comoving, there is only one growing-mode degree of freedom. Thus, we can solve for δ_A in Eq. (B.44) and Eq. (B.45), and express Φ in terms of δ_A in the equation

of motion for π Eq. (B.37). Thus, we are able to treat Φ as a source in the equation of motion for π . Again we use the following decomposition

$$\pi^{\text{p}}(a, \vec{x}) = \int^a d \ln \tilde{a} \frac{\Phi(\tilde{a}, \vec{x})}{H(\tilde{a})} + \tilde{\pi}_{\bar{m}}(a, \vec{x}). \quad (\text{B.46})$$

where $\tilde{\pi}_{\bar{m}}(a, \vec{x})$ satisfies

$$a^2 \mathcal{H}^2(a) \tilde{\pi}_{\bar{m}}'' + a^{2+3w} \mathcal{H}(a) (\mathcal{H} a^{-3w})' \tilde{\pi}_{\bar{m}}' = c_s^2 \int^a d \ln \tilde{a} \frac{\partial^2 \Phi(\tilde{a}, \vec{x})}{H(\tilde{a})} + c_s^2 \alpha_{\bar{m}} \frac{\partial^2 \Phi}{H}. \quad (\text{B.47})$$

The above equation has the following solution

$$\tilde{\pi}_{\bar{m}}(a, \vec{x}) = \int^a da' \int^{a'} da'' K(a', a'') S_{\Phi}^{\bar{m}}(a'', \vec{x}), \quad (\text{B.48})$$

where $S_{\Phi}^{\bar{m}}(a, \vec{x})$ is the source term on the RHS of (B.47) and the kernel $K(a, a')$ is given in (B.28). Finally, using (B.46) and (B.48), we obtain the linear order growing solution of $\pi(a, \vec{x})$ as

$$\pi(a, \vec{x}) = \int^a da' \frac{\Phi(a', \vec{x})}{\mathcal{H}(a')} + c_s^2 \int^a da' \int^{a'} da'' \left(\alpha_{\bar{m}} \frac{\partial^2 \Phi(a'', \vec{x})}{H(a'')} + \int^{a''} da''' \frac{\partial^2 \Phi(a''', \vec{x})}{\mathcal{H}(a''')} \right) K(a', a''), \quad (\text{B.49})$$

which is a function of the background expansion rate and the Newtonian potential.

C The density and velocity Green's functions

The non-Linear continuity and Euler equations are two coupled inhomogeneous differential equations which can be solved analytically in terms of four Green's functions, two density Green's functions, G_1^δ , G_2^δ , and two velocity Green's functions, G_1^Θ and G_2^Θ . Therefore, at each perturbative order, $\delta_{\vec{k}}^{(n)}(a)$ and $\Theta_{\vec{k}}^{(n)}(a)$ are

$$\delta_{\vec{k}}^{(n)} = \int_0^1 d\tilde{a} \left(G_1^\delta(a, \tilde{a}) S_1^{(n)}(\tilde{a}, \vec{k}) + G_2^\delta(a, \tilde{a}) S_2^{(n)}(\tilde{a}, \vec{k}) \right), \quad (\text{C.1})$$

$$\Theta_{\vec{k}}^{(n)} = \int_0^1 d\tilde{a} \left(G_1^\Theta(a, \tilde{a}) S_1^{(n)}(\tilde{a}, \vec{k}) + G_2^\Theta(a, \tilde{a}) S_2^{(n)}(\tilde{a}, \vec{k}) \right), \quad (\text{C.2})$$

where $S_1^{(n)}(\tilde{a}, \vec{k})$ and $S_2^{(n)}(\tilde{a}, \vec{k})$ are the source terms of the continuity and Euler equations at the n -th order respectively

$$S_1^{(n)}(a, \vec{k}) = \frac{f_+(a)}{C(a)} \sum_{m=1}^{n-1} \int \frac{d^3 q}{(2\pi)^3} \alpha(\vec{q}, \vec{k} - \vec{q}) \Theta_{\vec{q}}^{(m)} \delta_{\vec{k}-\vec{q}}^{(n-m)}, \quad (\text{C.3})$$

$$S_2^{(n)}(a, \vec{k}) = \frac{f_+(a)}{C(a)} \sum_{m=1}^{n-1} \int \frac{d^3 q}{(2\pi)^3} \beta(\vec{q}, \vec{k} - \vec{q}) \Theta_{\vec{q}}^{(m)} \Theta_{\vec{k}-\vec{q}}^{(n-m)}. \quad (\text{C.4})$$

Using Eq. (4.16) in Eq. (4.4) and Eq. (4.5), we find that the four Green's functions are specified by the following equations

$$a \frac{dG_\sigma^\delta(a, \tilde{a})}{da} - f_+(a) G_\sigma^\Theta(a, \tilde{a}) = \lambda_\sigma \delta(a - \tilde{a}), \quad (\text{C.5})$$

$$a \frac{dG_\sigma^\Theta(a, \tilde{a})}{da} - f_+(a) G_\sigma^\Theta(a, \tilde{a}) - \frac{f_-(a)}{f_+(a)} \left(G_\sigma^\Theta(a, \tilde{a}) - G_\sigma^\delta(a, \tilde{a}) \right) = (1 - \lambda_\sigma) \delta(a - \tilde{a}), \quad (\text{C.6})$$

where λ_σ is given as

$$\lambda_1 = 1 \quad \text{and} \quad \lambda_2 = 0,$$

$\sigma = 1, 2$, and $\delta(a - \tilde{a})$ is the Dirac delta function. The retarded Green's functions satisfy the boundary conditions

$$G_\sigma^\delta(a, \tilde{a}) = 0 \quad \text{and} \quad G_\sigma^\Theta(a, \tilde{a}) = 0 \quad \text{for} \quad \tilde{a} > a, \quad (\text{C.7})$$

$$G_\sigma^\delta(\tilde{a}, \tilde{a}) = \frac{\lambda_\sigma}{\tilde{a}} \quad \text{and} \quad G_\sigma^\Theta(\tilde{a}, \tilde{a}) = \frac{(1 - \lambda_\sigma)}{\tilde{a}}. \quad (\text{C.8})$$

We can then construct the Green's functions in the usual way using the linear solutions and the Heaviside step function, $\text{H}(a - \tilde{a})$, and imposing the boundary conditions Eq. (C.7) and Eq. (C.8). This gives

$$G_1^\delta(a, \tilde{a}) = \frac{1}{\tilde{a}W(\tilde{a})} \left(\frac{dD_-(\tilde{a})}{d\tilde{a}} D_+(a) - \frac{dD_+(\tilde{a})}{d\tilde{a}} D_-(a) \right) \text{H}(a - \tilde{a}), \quad (\text{C.9})$$

$$G_2^\delta(a, \tilde{a}) = \frac{f_+(\tilde{a})/\tilde{a}^2}{W(\tilde{a})} \left(D_+(\tilde{a})D_-(a) - D_-(\tilde{a})D_+(a) \right) \text{H}(a - \tilde{a}), \quad (\text{C.10})$$

$$G_1^\Theta(a, \tilde{a}) = \frac{a/\tilde{a}}{f_+(a)W(\tilde{a})} \left(\frac{dD_-(\tilde{a})}{d\tilde{a}} \frac{dD_+(a)}{da} - \frac{dD_+(\tilde{a})}{d\tilde{a}} \frac{dD_-(a)}{da} \right) \text{H}(a - \tilde{a}), \quad (\text{C.11})$$

$$G_2^\Theta(a, \tilde{a}) = \frac{f_+(\tilde{a})a/\tilde{a}^2}{f_+(a)W(\tilde{a})} \left(D_+(\tilde{a}) \frac{dD_-(a)}{da} - D_-(\tilde{a}) \frac{dD_+(a)}{da} \right) \text{H}(a - \tilde{a}), \quad (\text{C.12})$$

where $W(\tilde{a})$ is the Wronskian of D_+ and D_-

$$W(\tilde{a}) = \frac{dD_-(\tilde{a})}{d\tilde{a}} D_+(\tilde{a}) - \frac{dD_+(\tilde{a})}{d\tilde{a}} D_-(\tilde{a}). \quad (\text{C.13})$$

Having the formal solutions Eq. (4.16) and the Green's functions in Eq. (C.9) - Eq. (C.12), we are ready to find the solutions of total δ and Θ at any perturbative order. For later convenience, it is useful to define the following independent combinations of the functions of momenta Eq. (2.33) and Eq. (2.34) as

$$\alpha^1(\vec{k}_1, \vec{k}_2, \vec{k}_3) \equiv \alpha(\vec{k}_1 - \vec{k}_2, \vec{k}_2) \alpha_s(\vec{k}_3, \vec{k}_2 - \vec{k}_3), \quad (\text{C.14})$$

$$\alpha^2(\vec{k}_1, \vec{k}_2, \vec{k}_3) \equiv \alpha(\vec{k}_1 - \vec{k}_2, \vec{k}_2) \beta(\vec{k}_3, \vec{k}_2 - \vec{k}_3), \quad (\text{C.15})$$

$$\beta^1(\vec{k}_1, \vec{k}_2, \vec{k}_3) \equiv 2\beta(\vec{k}_1 - \vec{k}_2, \vec{k}_2) \alpha_s(\vec{k}_3, \vec{k}_2 - \vec{k}_3), \quad (\text{C.16})$$

$$\beta^2(\vec{k}_1, \vec{k}_2, \vec{k}_3) \equiv 2\beta(\vec{k}_1 - \vec{k}_2, \vec{k}_2) \beta(\vec{k}_3, \vec{k}_2 - \vec{k}_3), \quad (\text{C.17})$$

$$\gamma^1(\vec{k}_1, \vec{k}_2, \vec{k}_3) \equiv \alpha(\vec{k}_2, \vec{k}_1 - \vec{k}_2) \alpha_s(\vec{k}_3, \vec{k}_2 - \vec{k}_3), \quad (\text{C.18})$$

$$\gamma^2(\vec{k}_1, \vec{k}_2, \vec{k}_3) \equiv \alpha(\vec{k}_2, \vec{k}_1 - \vec{k}_2) \beta(\vec{k}_3, \vec{k}_2 - \vec{k}_3). \quad (\text{C.19})$$

The form of the source terms at third order can be most simplified in terms of the above functions of momenta. In particular, the source terms at third order are given as

$$S_1^{(3)}(a, \vec{k}) = \frac{f_+(a)D_+(a)}{C(a)D_+(a_i)} \int \frac{d^3p}{(2\pi)^3} \left(\alpha(\vec{k} - \vec{p}, \vec{p}) \delta_{\vec{p}}^{(2)}(a) + \alpha(\vec{p}, \vec{k} - \vec{p}) \Theta_{\vec{p}}^{(2)}(a) \right) \delta_{\vec{k}-\vec{p}}^{\text{in}}, \quad (\text{C.20})$$

$$S_2^{(3)}(a, \vec{k}) = \frac{f_+(a)D_+(a)}{C(a)D_+(a_i)} \int \frac{d^3p}{(2\pi)^3} 2\beta(\vec{k} - \vec{p}, \vec{p}) \Theta_{\vec{p}}^{(2)} \delta_{\vec{k}-\vec{p}}^{\text{in}}, \quad (\text{C.21})$$

which after using Eq. (4.20) and Eq. (4.21) and in terms of Eq. (C.14) - Eq. (C.19)

$$\begin{aligned}
S_1^{(3)}(a, \vec{k}) &= \frac{f_+(a)D_+(a)}{C(a)D_+(a_i)} \iint \frac{d^3p}{(2\pi)^3} \frac{d^3q}{(2\pi)^3} \left(\alpha^\sigma(\vec{k}, \vec{p}, \vec{q}) \mathcal{G}_\sigma^\delta(a) + \gamma^\sigma(\vec{k}, \vec{p}, \vec{q}) \mathcal{G}_\sigma^\ominus(a) \right) \delta_{\vec{k}-\vec{p}}^{\text{in}} \delta_{\vec{p}-\vec{q}}^{\text{in}} \delta_{\vec{q}}^{\text{in}}, \\
S_2^{(3)}(a, \vec{k}) &= \frac{f_+(a)D_+(a)}{C(a)D_+(a_i)} \iint \frac{d^3p}{(2\pi)^3} \frac{d^3q}{(2\pi)^3} \beta^\sigma(\vec{k}, \vec{p}, \vec{q}) \mathcal{G}_\sigma^\ominus(a) \delta_{\vec{k}-\vec{p}}^{\text{in}} \delta_{\vec{p}-\vec{q}}^{\text{in}} \delta_{\vec{q}}^{\text{in}}, \tag{C.22}
\end{aligned}$$

where summation over upper and lower indices is assumed.

D Non-linear evolution with smooth dark energy

In this section, we briefly discuss dark matter evolution in the presence of a smooth dark energy with $c_s^2 = 1$, typically called w CDM, which is a model that provides a familiar and simple example against which to compare our results. Because it has been thoroughly discussed in the literature (see for example [72, 86, 10]), we only give a brief explanation here. The linear equation of a dark energy density with an arbitrary speed of sound, c_s^2 , and equation of state w , is given as (neglecting relativistic corrections)

$$\partial_\tau^2 \delta_D + (1 - 3w)\mathcal{H}\partial_\tau \delta_D + c_s^2 k^2 \delta_D + 3(c_s^2 - w) \left(\partial_\tau \mathcal{H} + (1 - 3c_s^2)\mathcal{H}^2 \right) \delta_D = -(1 + w)k^2 \Phi, \tag{D.1}$$

where the conformal time τ is given by $d\tau = da/(a\mathcal{H})$. As we see, the sound speed introduces another natural momentum scale in the theory, the sound horizon \mathcal{H}/c_s , besides the cosmological horizon, \mathcal{H} :

- Deep inside the sound horizon where $\frac{c_s k}{\mathcal{H}} \gg 1$, the density contrast has a damped oscillatory behavior and there is no growing solution. In this regime, sometimes called smooth dark energy, we can neglect δ_D compared to dark matter clustering.
- At super sound horizon scales $\frac{c_s k}{\mathcal{H}} \ll 1$, however, the dark energy is in the clustering regime and δ_D has growing solutions. Since we are in the Newtonian regime in which $\frac{k}{\mathcal{H}} \gg 1$, dark energy clustering can only happen in the interval $1 \ll \frac{k}{\mathcal{H}} \ll \frac{1}{c_s^2}$ which requires a very small sound speed. This is the regime that we exhaustively studied in the previous section.

In the limit that $c_s^2 \sim 1$, the sound horizon is very close to the cosmological horizon and the dark energy is spatially smooth. In this regime, dark energy only affects gravitational growth of structure through changing the expansion rate (up to relativistic corrections). In the other limit with $|c_s^2| \ll 1$, dark energy perturbations can cluster and contribute to the Poisson equation as well. In Figure 6, we present the time evolution of dark energy, δ_D , in the clustering and smooth limits at linear level. This confirms that dark-energy fluctuations can be ignored, and that dark energy only affects the dark-matter clustering through changing the expansion rate.

In w CDM, we have $\delta_A \approx \delta_m$, so that the equation of motion of the adiabatic mode is simply the

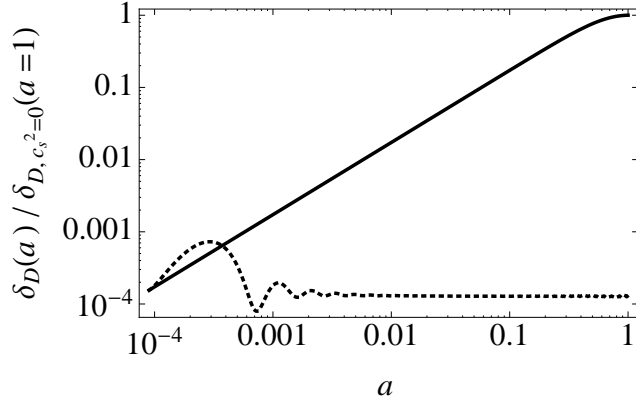


Figure 6: In this plot, we show the growing modes for the dark-energy linear density contrast as a function of scale factor for two models, one with $c_s^2 = 0$ (clustering quintessence, the solid black curve), and the other with $c_s^2 = 1$ (smooth dark energy, the dotted black line), normalized to the value of the clustering density at the current time $a = 1$. The density contrast in the clustering case grows as $a \rightarrow 1$, while in the smooth case any initial fluctuations oscillate and are quickly damped. In order to compare the growing modes, we assume that the two modes have the same size fluctuations at $a = 0.9 \times 10^{-4}$. This time was chosen because, for a typical mode of interest for large scale structure, $k = 0.05 h\text{Mpc}^{-1}$, we have $k\tau \approx 5$ (where τ is conformal time), which means that we are justified in dropping relativistic effects.

standard one for dark matter (writing the adiabatic mode in $w\text{CDM}$ as δ_w)

$$a\mathcal{H}\delta_w(a, \vec{k})' + \theta_w(a, \vec{k}) = - \int \frac{d^3q}{(2\pi)^3} \alpha(\vec{q}, \vec{k} - \vec{q}) \theta_w(a, \vec{q}) \delta_w(a, \vec{k} - \vec{q}) \quad (\text{D.2})$$

$$a\mathcal{H}\theta_w(a, \vec{k})' + \mathcal{H}\theta_w(a, \vec{k}) + \frac{3}{2} \frac{\Omega_{m,0} \mathcal{H}_0^2 a_0}{a} \delta_w(a, \vec{k}) = 9(2\pi) c_{s,w}^2(a) H(a)^2 \frac{k^2}{k_{\text{NL}}^2} \delta_w(a, \vec{k}) - \int \frac{d^3q}{(2\pi)^3} \beta(\vec{q}, \vec{k} - \vec{q}) \theta_w(a, \vec{k} - \vec{q}) \theta_w(a, \vec{q}). \quad (\text{D.3})$$

The most important difference at late times between this model and ΛCDM is that $H(a)$, and therefore the linear growth rate D_w , has $w \neq -1$. The equation for the growth factor is

$$\frac{d^2}{d \ln a^2} \left(\frac{D_w}{H} \right) + \left(2 + 3 \frac{d \ln H}{d \ln a} \right) \frac{d}{d \ln a} \left(\frac{D_w}{H} \right) + \frac{d \ln H}{d \ln a} \left(\frac{d \ln C}{d \ln a} - 1 + \frac{1}{C} \right) \frac{D_w}{H} = 0, \quad (\text{D.4})$$

whose numerical solution can be obtained by either using CAMB or your favorite numerical solver. Loops can then be computed in the same way as in the dark-matter case. For the plots in Section 6, we use the EdS approximation, which is as valid as it is in the dark-matter case: for example, with $w = -0.9$, $(\Omega_{m,0} \mathcal{H}_0^2 a_0 / (a \mathcal{H}^2)) / (a D_w' / D_w)^2$ is unity at early times and is around 1.17 near $a = 1$.

References

- [1] **Supernova Search Team** Collaboration, A. G. Riess et al., *Observational evidence from supernovae for an accelerating universe and a cosmological constant*, *Astron. J.* **116** (1998) 1009–1038, [[astro-ph/9805201](#)].

- [2] **Supernova Cosmology Project** Collaboration, S. Perlmutter et al., *Measurements of Omega and Lambda from 42 high redshift supernovae*, *Astrophys. J.* **517** (1999) 565–586, [[astro-ph/9812133](#)].
- [3] A. G. Riess et al., *BV RI light curves for 22 type Ia supernovae*, *Astron. J.* **117** (1999) 707–724, [[astro-ph/9810291](#)].
- [4] **SDSS** Collaboration, M. Tegmark et al., *Cosmological parameters from SDSS and WMAP*, *Phys. Rev.* **D69** (2004) 103501, [[astro-ph/0310723](#)].
- [5] **SDSS** Collaboration, M. Tegmark et al., *Cosmological Constraints from the SDSS Luminous Red Galaxies*, *Phys. Rev.* **D74** (2006) 123507, [[astro-ph/0608632](#)].
- [6] **WMAP** Collaboration, D. N. Spergel et al., *First year Wilkinson Microwave Anisotropy Probe (WMAP) observations: Determination of cosmological parameters*, *Astrophys. J. Suppl.* **148** (2003) 175–194, [[astro-ph/0302209](#)].
- [7] **Planck** Collaboration, P. A. R. Ade et al., *Planck 2015 results. XIV. Dark energy and modified gravity*, *Astron. Astrophys.* **594** (2016) A14, [[arXiv:1502.01590](#)].
- [8] W. J. Percival, S. Cole, D. J. Eisenstein, R. C. Nichol, J. A. Peacock, A. C. Pope, and A. S. Szalay, *Measuring the Baryon Acoustic Oscillation scale using the SDSS and 2dFGRS*, *Mon. Not. Roy. Astron. Soc.* **381** (2007) 1053–1066, [[arXiv:0705.3323](#)].
- [9] E. Aubourg et al., *Cosmological implications of baryon acoustic oscillation measurements*, *Phys. Rev.* **D92** (2015), no. 12 123516, [[arXiv:1411.1074](#)].
- [10] L. Amendola et al., *Cosmology and Fundamental Physics with the Euclid Satellite*, [arXiv:1606.00180](#).
- [11] D. Spergel et al., *Wide-Field InfrarRed Survey Telescope-Astrophysics Focused Telescope Assets WFIRST-AFTA 2015 Report*, [arXiv:1503.03757](#).
- [12] S. Das et al., *The Atacama Cosmology Telescope: temperature and gravitational lensing power spectrum measurements from three seasons of data*, *JCAP* **1404** (2014) 014, [[arXiv:1301.1037](#)].
- [13] A. van Engelen et al., *A measurement of gravitational lensing of the microwave background using South Pole Telescope data*, *Astrophys. J.* **756** (2012) 142, [[arXiv:1202.0546](#)].
- [14] D. H. Weinberg, M. J. Mortonson, D. J. Eisenstein, C. Hirata, A. G. Riess, and E. Rozo, *Observational Probes of Cosmic Acceleration*, *Phys. Rept.* **530** (2013) 87–255, [[arXiv:1201.2434](#)].
- [15] A. Joyce, L. Lombriser, and F. Schmidt, *Dark Energy vs. Modified Gravity*, [arXiv:1601.06133](#).
- [16] S. Weinberg, *Anthropic Bound on the Cosmological Constant*, *Phys. Rev. Lett.* **59** (1987) 2607.
- [17] P. Creminelli, M. A. Luty, A. Nicolis, and L. Senatore, *Starting the Universe: Stable Violation of the Null Energy Condition and Non-standard Cosmologies*, *JHEP* **12** (2006) 080, [[hep-th/0606090](#)].
- [18] C. Cheung, P. Creminelli, A. L. Fitzpatrick, J. Kaplan, and L. Senatore, *The Effective Field Theory of Inflation*, *JHEP* **03** (2008) 014, [[arXiv:0709.0293](#)].
- [19] P. Creminelli, G. D’Amico, J. Norena, and F. Vernizzi, *The Effective Theory of Quintessence: the $w < -1$ Side Unveiled*, *JCAP* **0902** (2009) 018, [[arXiv:0811.0827](#)].
- [20] G. Gubitosi, F. Piazza, and F. Vernizzi, *The Effective Field Theory of Dark Energy*, *JCAP* **1302** (2013) 032, [[arXiv:1210.0201](#)]. [[JCAP1302,032\(2013\)](#)].
- [21] J. Gleyzes, D. Langlois, F. Piazza, and F. Vernizzi, *Essential Building Blocks of Dark Energy*, *JCAP* **1308** (2013) 025, [[arXiv:1304.4840](#)].
- [22] J. K. Bloomfield, E. E. Flanagan, M. Park, and S. Watson, *Dark energy or modified gravity? An effective field theory approach*, *JCAP* **1308** (2013) 010, [[arXiv:1211.7054](#)].

- [23] J. Gleyzes, D. Langlois, and F. Vernizzi, *A unifying description of dark energy*, *Int. J. Mod. Phys.* **D23** (2015), no. 13 1443010, [[arXiv:1411.3712](#)].
- [24] J. Gleyzes, D. Langlois, F. Piazza, and F. Vernizzi, *Exploring gravitational theories beyond Horndeski*, *JCAP* **1502** (2015) 018, [[arXiv:1408.1952](#)].
- [25] B. Hu, M. Raveri, N. Frusciante, and A. Silvestri, *Effective Field Theory of Cosmic Acceleration: an implementation in CAMB*, *Phys. Rev.* **D89** (2014), no. 10 103530, [[arXiv:1312.5742](#)].
- [26] A. Silvestri, L. Pogosian, and R. V. Buniy, *Practical approach to cosmological perturbations in modified gravity*, *Phys. Rev.* **D87** (2013), no. 10 104015, [[arXiv:1302.1193](#)].
- [27] F. Piazza, H. Steigerwald, and C. Marinoni, *Phenomenology of dark energy: exploring the space of theories with future redshift surveys*, *JCAP* **1405** (2014) 043, [[arXiv:1312.6111](#)].
- [28] L. Perenon, F. Piazza, C. Marinoni, and L. Hui, *Phenomenology of dark energy: general features of large-scale perturbations*, *JCAP* **1511** (2015), no. 11 029, [[arXiv:1506.03047](#)].
- [29] N. Frusciante, G. Papadomanolakis, and A. Silvestri, *An Extended action for the effective field theory of dark energy: a stability analysis and a complete guide to the mapping at the basis of EFTCAMB*, *JCAP* **1607** (2016), no. 07 018, [[arXiv:1601.04064](#)].
- [30] A. Adams, N. Arkani-Hamed, S. Dubovsky, A. Nicolis, and R. Rattazzi, *Causality, analyticity and an IR obstruction to UV completion*, *JHEP* **10** (2006) 014, [[hep-th/0602178](#)].
- [31] D. Baumann, A. Nicolis, L. Senatore, and M. Zaldarriaga, *Cosmological Non-Linearities as an Effective Fluid*, *JCAP* **1207** (2012) 051, [[arXiv:1004.2488](#)].
- [32] J. J. M. Carrasco, M. P. Hertzberg, and L. Senatore, *The Effective Field Theory of Cosmological Large Scale Structures*, *JHEP* **09** (2012) 082, [[arXiv:1206.2926](#)].
- [33] R. A. Porto, L. Senatore, and M. Zaldarriaga, *The Lagrangian-space Effective Field Theory of Large Scale Structures*, *JCAP* **1405** (2014) 022, [[arXiv:1311.2168](#)].
- [34] L. Senatore and M. Zaldarriaga, *The IR-resummed Effective Field Theory of Large Scale Structures*, *JCAP* **1502** (2015) 013, [[arXiv:1404.5954](#)].
- [35] J. J. M. Carrasco, S. Foreman, D. Green, and L. Senatore, *The 2-loop matter power spectrum and the IR-safe integrand*, *JCAP* **1407** (2014) 056, [[arXiv:1304.4946](#)].
- [36] J. J. M. Carrasco, S. Foreman, D. Green, and L. Senatore, *The Effective Field Theory of Large Scale Structures at Two Loops*, *JCAP* **1407** (2014) 057, [[arXiv:1310.0464](#)].
- [37] E. Pajer and M. Zaldarriaga, *On the Renormalization of the Effective Field Theory of Large Scale Structures*, *JCAP* **1308** (2013) 037, [[arXiv:1301.7182](#)].
- [38] S. M. Carroll, S. Leichenauer, and J. Pollack, *Consistent effective theory of long-wavelength cosmological perturbations*, *Phys. Rev.* **D90** (2014), no. 2 023518, [[arXiv:1310.2920](#)].
- [39] L. Mercolli and E. Pajer, *On the velocity in the Effective Field Theory of Large Scale Structures*, *JCAP* **1403** (2014) 006, [[arXiv:1307.3220](#)].
- [40] R. E. Angulo, S. Foreman, M. Schmittfull, and L. Senatore, *The One-Loop Matter Bispectrum in the Effective Field Theory of Large Scale Structures*, *JCAP* **1510** (2015) 039, [[arXiv:1406.4143](#)].
- [41] T. Baldauf, L. Mercolli, M. Mirbabayi, and E. Pajer, *The Bispectrum in the Effective Field Theory of Large Scale Structure*, *JCAP* **1505** (2015), no. 05 007, [[arXiv:1406.4135](#)].
- [42] L. Senatore, *Bias in the Effective Field Theory of Large Scale Structures*, *JCAP* **1511** (2015), no. 11 007, [[arXiv:1406.7843](#)].

- [43] L. Senatore and M. Zaldarriaga, *Redshift Space Distortions in the Effective Field Theory of Large Scale Structures*, [arXiv:1409.1225](#).
- [44] M. Lewandowski, A. Perko, and L. Senatore, *Analytic Prediction of Baryonic Effects from the EFT of Large Scale Structures*, *JCAP* **1505** (2015) 019, [[arXiv:1412.5049](#)].
- [45] M. Mirbabayi, F. Schmidt, and M. Zaldarriaga, *Biased Tracers and Time Evolution*, *JCAP* **1507** (2015), no. 07 030, [[arXiv:1412.5169](#)].
- [46] S. Foreman and L. Senatore, *The EFT of Large Scale Structures at All Redshifts: Analytical Predictions for Lensing*, *JCAP* **1604** (2016) 033, [[arXiv:1503.01775](#)].
- [47] R. Angulo, M. Fasiello, L. Senatore, and Z. Vlah, *On the Statistics of Biased Tracers in the Effective Field Theory of Large Scale Structures*, *JCAP* **1509** (2015) 029, [[arXiv:1503.08826](#)].
- [48] M. McQuinn and M. White, *Cosmological perturbation theory in 1+1 dimensions*, *JCAP* **1601** (2016), no. 01 043, [[arXiv:1502.07389](#)].
- [49] V. Assassi, D. Baumann, E. Pajer, Y. Welling, and D. van der Woude, *Effective theory of large-scale structure with primordial non-Gaussianity*, *JCAP* **1511** (2015) 024, [[arXiv:1505.06668](#)].
- [50] T. Baldauf, E. Schaan, and M. Zaldarriaga, *On the reach of perturbative descriptions for dark matter displacement fields*, *JCAP* **1603** (2016), no. 03 017, [[arXiv:1505.07098](#)].
- [51] T. Baldauf, M. Mirbabayi, M. Simonović, and M. Zaldarriaga, *Equivalence Principle and the Baryon Acoustic Peak*, *Phys. Rev.* **D92** (2015), no. 4 043514, [[arXiv:1504.04366](#)].
- [52] S. Foreman, H. Perrier, and L. Senatore, *Precision Comparison of the Power Spectrum in the EFTofLSS with Simulations*, *JCAP* **1605** (2016) 027, [[arXiv:1507.05326](#)].
- [53] T. Baldauf, L. Mercolli, and M. Zaldarriaga, *Effective field theory of large scale structure at two loops: The apparent scale dependence of the speed of sound*, *Phys. Rev.* **D92** (2015), no. 12 123007, [[arXiv:1507.02256](#)].
- [54] T. Baldauf, E. Schaan, and M. Zaldarriaga, *On the reach of perturbative methods for dark matter density fields*, *JCAP* **1603** (2016), no. 03 007, [[arXiv:1507.02255](#)].
- [55] D. Bertolini, K. Schutz, M. P. Solon, J. R. Walsh, and K. M. Zurek, *Non-Gaussian Covariance of the Matter Power Spectrum in the Effective Field Theory of Large Scale Structure*, [arXiv:1512.07630](#).
- [56] D. Bertolini, K. Schutz, M. P. Solon, and K. M. Zurek, *The Trispectrum in the Effective Field Theory of Large Scale Structure*, [arXiv:1604.01770](#).
- [57] V. Assassi, D. Baumann, and F. Schmidt, *Galaxy Bias and Primordial Non-Gaussianity*, *JCAP* **1512** (2015), no. 12 043, [[arXiv:1510.03723](#)].
- [58] M. Lewandowski, L. Senatore, F. Prada, C. Zhao, and C.-H. Chuang, *On the EFT of Large Scale Structures in Redshift Space*, [arXiv:1512.06831](#).
- [59] M. Cataneo, S. Foreman, and L. Senatore, *Efficient exploration of cosmology dependence in the EFT of LSS*, [arXiv:1606.03633](#).
- [60] D. Bertolini and M. P. Solon, *Principal Shapes and Squeezed Limits in the Effective Field Theory of Large Scale Structure*, [arXiv:1608.01310](#).
- [61] T. Fujita, V. Mauerhofer, L. Senatore, Z. Vlah, and R. Angulo, *Very Massive Tracers and Higher Derivative Biases*, [arXiv:1609.00717](#).
- [62] A. Perko, L. Senatore, E. Jennings, and R. H. Wechsler, *Biased Tracers in Redshift Space in the EFT of Large-Scale Structure*, [arXiv:1610.09321](#).

- [63] L. Senatore and M. Zaldarriaga, *The Effective Field Theory of Multifield Inflation*, *JHEP* **04** (2012) 024, [[arXiv:1009.2093](https://arxiv.org/abs/1009.2093)].
- [64] S. Schlamminger, K. Y. Choi, T. A. Wagner, J. H. Gundlach, and E. G. Adelberger, *Test of the equivalence principle using a rotating torsion balance*, *Phys. Rev. Lett.* **100** (2008) 041101, [[arXiv:0712.0607](https://arxiv.org/abs/0712.0607)].
- [65] C. Cheung, A. L. Fitzpatrick, J. Kaplan, and L. Senatore, *On the consistency relation of the 3-point function in single field inflation*, *JCAP* **0802** (2008) 021, [[arXiv:0709.0295](https://arxiv.org/abs/0709.0295)].
- [66] O. Hahn, R. E. Angulo, and T. Abel, *The Properties of Cosmic Velocity Fields*, *Mon. Not. Roy. Astron. Soc.* **454** (2015), no. 4 3920–3937, [[arXiv:1404.2280](https://arxiv.org/abs/1404.2280)].
- [67] T. Baldauf, U. Seljak, L. Senatore, and M. Zaldarriaga, *Galaxy Bias and non-Linear Structure Formation in General Relativity*, *JCAP* **1110** (2011) 031, [[arXiv:1106.5507](https://arxiv.org/abs/1106.5507)].
- [68] T. Baldauf, U. Seljak, L. Senatore, and M. Zaldarriaga, *Linear response to long wavelength fluctuations using curvature simulations*, *JCAP* **1609** (2016), no. 09 007, [[arXiv:1511.01465](https://arxiv.org/abs/1511.01465)].
- [69] T. Lazeyras, C. Wagner, T. Baldauf, and F. Schmidt, *Precision measurement of the local bias of dark matter halos*, *JCAP* **1602** (2016), no. 02 018, [[arXiv:1511.01096](https://arxiv.org/abs/1511.01096)].
- [70] A. Lewis, A. Challinor, and A. Lasenby, *Efficient computation of CMB anisotropies in closed FRW models*, *Astrophys. J.* **538** (2000) 473–476, [[astro-ph/9911177](https://arxiv.org/abs/astro-ph/9911177)].
- [71] P. Creminelli, G. D’Amico, J. Norena, L. Senatore, and F. Vernizzi, *Spherical collapse in quintessence models with zero speed of sound*, *JCAP* **1003** (2010) 027, [[arXiv:0911.2701](https://arxiv.org/abs/0911.2701)].
- [72] E. Sefusatti and F. Vernizzi, *Cosmological structure formation with clustering quintessence*, *JCAP* **1103** (2011) 047, [[arXiv:1101.1026](https://arxiv.org/abs/1101.1026)].
- [73] G. D’Amico and E. Sefusatti, *The nonlinear power spectrum in clustering quintessence cosmologies*, *JCAP* **1111** (2011) 013, [[arXiv:1106.0314](https://arxiv.org/abs/1106.0314)].
- [74] S. Anselmi, G. Ballesteros, and M. Pietroni, *Non-linear dark energy clustering*, *JCAP* **1111** (2011) 014, [[arXiv:1106.0834](https://arxiv.org/abs/1106.0834)].
- [75] S. Anselmi, D. López Nacir, and E. Sefusatti, *Nonlinear effects of dark energy clustering beyond the acoustic scales*, *JCAP* **1407** (2014) 013, [[arXiv:1402.4269](https://arxiv.org/abs/1402.4269)].
- [76] N. Arkani-Hamed, H.-C. Cheng, M. A. Luty, and S. Mukohyama, *Ghost condensation and a consistent infrared modification of gravity*, *JHEP* **05** (2004) 074, [[hep-th/0312099](https://arxiv.org/abs/hep-th/0312099)].
- [77] A. L. Fitzpatrick, L. Senatore, and M. Zaldarriaga, *Contributions to the Dark Matter 3-Pt Function from the Radiation Era*, *JCAP* **1005** (2010) 004, [[arXiv:0902.2814](https://arxiv.org/abs/0902.2814)].
- [78] M. Zumalacárregui, E. Bellini, I. Sawicki, and J. Lesgourgues, *hi_class: Horndeski in the Cosmic Linear Anisotropy Solving System*, [arXiv:1605.06102](https://arxiv.org/abs/1605.06102).
- [79] Z. Huang, “COOP: first release; EFTDE/XFASTER/CPLDE.” <http://dx.doi.org/10.5281/zenodo.61166>, 2016.
- [80] D. Lopez Nacir, R. A. Porto, L. Senatore, and M. Zaldarriaga, *Dissipative effects in the Effective Field Theory of Inflation*, *JHEP* **01** (2012) 075, [[arXiv:1109.4192](https://arxiv.org/abs/1109.4192)].
- [81] L. Senatore and M. Zaldarriaga, *A Naturally Large Four-Point Function in Single Field Inflation*, *JCAP* **1101** (2011) 003, [[arXiv:1004.1201](https://arxiv.org/abs/1004.1201)].
- [82] P. McDonald and A. Roy, *Clustering of dark matter tracers: generalizing bias for the coming era of precision LSS*, *JCAP* **0908** (2009) 020, [[arXiv:0902.0991](https://arxiv.org/abs/0902.0991)].

- [83] E. Poisson, *A Relativists Toolkit: the Mathematics of Black-Hole Mechanics*. 2004.
- [84] R. M. Wald, *General Relativity*. 1984.
- [85] H. Kodama and M. Sasaki, *Cosmological Perturbation Theory*, *Prog. Theor. Phys. Suppl.* **78** (1984) 1–166.
- [86] D. Sapone, M. Kunz, and M. Kunz, *Fingerprinting Dark Energy*, *Phys. Rev.* **D80** (2009) 083519, [[arXiv:0909.0007](https://arxiv.org/abs/0909.0007)].